CHARACTERIZATION OF SORBENT PRODUCED FROM CHICKEN FEATHER-KAOLIN COMPOSITE AND ITS APPLICATION FOR REMOVAL OF SELECTED HEAVY METALS FROM WASTEWATER

BY

Isiaka SULEIMAN

DEPARTMENT OF CHEMISTRY,
FACULTY OF PHYSICAL SCIENCES,
AHMADU BELLO UNIVERSITY,

ZARIA, NIGERIA

FEBRUARY, 2021

CHARACTERIZATION OF SORBENT PRODUCED FROM CHICKEN FEATHER-KAOLIN COMPOSITE AND ITS APPLICATION FOR REMOVAL OF SELECTED HEAVY METALS FROM WASTEWATER

BY

Isiaka SULEIMAN

BSc. (CHEMISTRY, ABU, 2012)
P15SCCH8016

A THESIS SUBMITTED TO THE SCHOOL OF POSTGRADUATE STUDIES, AHMADU BELLO UNIVERSITY, ZARIA IN PARTIAL FULFILLMENT OF THE REQUIREMENTS FOR THE AWARD OF MASTER DEGREE IN ANALYTICAL CHEMISTRY

DEPARTMENT OF CHEMISTRY,
FACULTY OF PHYSICAL SCIENCES,
AHMADU BELLO UNIVERSITY,

ZARIA, NIGERIA

FEBRUARY, 2021

DECLARATION

I declare that the work in this dissertation entitled CHARACTERIZATION OF SORBENT PRODUCED FROM CHICKEN FEATHER-KAOLIN COMPOSITE AND ITS APPLICATION FOR REMOVAL OF SELECTED HEAVY METALS FROM WASTEWATERhas been performed by me in the Department of Chemistry. The information derived from the literature has been duly acknowledged in the text and a list of references provided. No part of this dissertation was previously presented for another degree or diploma at this or any other institution.

Isiaka Suleiman	_____	_____
Student	**Signature**	**Date**

CERTIFICATION

This dissertation entitled CHARACTERIZATION OF SORBENT PRODUCED FROM CHICKEN FEATHER-KAOLIN COMPOSITE AND ITS APPLICATION FOR REMOVAL OF SELECTED HEAVY METALS FROM WASTEWATERby Isiaka SULEIMAN meets the regulations governing the award of the degree of Master of Science in Analytical Chemistry of the Ahmadu Bello University, and is approved for its contribution to knowledge and literary presentation.

Dr K. I. Omoniyi	_____	_____
(Chairman, Supervisory Committee)	Signature	Date
Dr Z.I. Yashim	_____	_____
(Member, Supervisory Committee)	Signature	Date
Prof. G.I. Ndukwe	_____	_____
(Head of Department)	Signature	Date
Professor S. A. Abdullahi	_____	_____
(Dean, Postgraduate School)	Signature	Date

ACKNOWLEDGMENT

No word can aptly capture the depth of my sincere gratitude to God Almighty for His divine grace and profound mercy upon me all through the period of this research work.

I wish to express my profound gratitude to my supervisors: Dr K. I. Omoniyi, Dr Z.I Yashim of Department of Chemistry, Ahmadu Bello University, Zaria and Dr A. O. Lawal of Department of Applied Science, Kaduna Polytechnic, Kaduna, for their guidance, motivation and amazing intellectual contributions towards the success of this work.

My warm appreciation also goes to the Head of Chemistry Department and to the entire members of staff of the department and those of all the laboratories where this work was conducted.

Furthermore, to my dear parents: Alhaji Suleiman Onyukwu and Asmau Idakpo, and to all my beloved and awesome siblings and relatives, I ask Allah to increase them profusely in firm faith, lawful wealth and sound health. I also wish them all forms of goodness in this world and in the hereafter.

Lastly, my profound gratitude goes to all my good friends, teaching and non- teaching staff, colleagues and students of Chemistry Department ABU Zaria. I ask Allah to bless and elevate you all.

DEDICATION

This work is dedicated to almighty God and all those great, noble and faithful people around me who always assist me immensely and tirelessly and have guided me aright on my sojourn so far through this thorny and fiercely challenging world.

ABSTRACT

The study presents the characterization and adsorption studies of chicken feather-kaolin composite (CFK) produced using chicken feather (CF) and kaolin (K) and used for removal of Pb^{2+}, Cu^{2+} and Ni^{2+} from aqueous medium. The FTIR result of the CFK reveals the appearance of bands at 3690.1 cm^{-1} and 3265.1 cm^{-1} that indicate the –OH group of kaolin and the –NH group of the protein keratin in the chicken feather. And there was also the appearance of new adsorption bands at 3649.10 cm^{-1}, 3619.20 cm^{-1} and 3425.40 cm^{-1} which were assigned to O-H and N-H inter hydrogen bonds' vibration between the kaolin and the chicken feather as well as reduction in pick intensity which signifies that there was interaction between the kaolin(K) and chicken feather (CF) in formation of CFK composite. SEM result reveals that, the K particles are packed in the form of agglomerates while CF contains protein fibres with barbs and barbules. It also shows that chicken feather (CF)had kaolin (K) particles adhering to the surface of chicken feather (CF) thereby providing an efficient and strong support for K in forming CFK composite, therefore, the intercalation via guest displacement reaction between the CF and K using sodium acetate as the intercalating agent to pack CF between the lamella spacing of K in the composite failed to occur, rather, it obeys the surface interaction through hydrogen bonding between the O-H group of K and NH_2 and COO^- groups of the protein keratin fibre of CF.BET indicates an increase in the surface area of K from 352.5 m^2/g to 424.8m^2/g in CFK, and pore volume from 0.148 cc/g to 0.164 cc/g in CFK composite.XRD difactograms show well defined peaks of Kaolinite in K, peaks due to the protein keratin in CF indicating semi-crystalline nature of CF and an increased crystallinity due to the appearance of more peaks in CFK, and a reduction in peak intensity indicating interaction between CF and K in the formation of CFK composite. The CFK composite had adsorption affinity for the metals in the order Pb^{2+}> Cu^{2+}> Ni^{2+}.Adsorption for all the metals follow the pseudo-second order kinetic model.The intra-particle diffusion

model reveals that the adsorption process was both by boundary layer and intra-particle diffusion. Adsorption of Pb^{2+} and Cu^{2+} follow the Freundlich model while Ni^{2+} fits better into the Langmuir isotherm. The Dubini-Radushkevich isotherm shows that the adsorption process was by physisorption and the thermodynamic study reveals that the adsorption was spontaneous, feasible, endothermic and was accompanied by an increase in entropy.

The full factorial design and response surface methodology for the optimization gives the maximum percentage adsorbed for Pb^{2+} as 97.03%, 75.50% for Cu^{2+} and 66.26% for Ni^{2+} at 147.19 ppm, 75^{o}C and 10 minute.Therefore, CFK composite can be used as an effective low-cost adsorbent for removal of heavy metals from wastewater.

Table of Contents

List of Figures

List of Tables

List of Appendices

CHAPTER ONE

1.0INTRODUCTION

Every sector of the society makes use of minerals and mineral resources on a daily basis. For instance, the roads people ride on, the buildings used for habitation or use for other purposes contain minerals.Such minerals include metallic and non-metallic minerals. An example of such minerals is clay (kaolin) used as absorbent and filtering materials, construction materials and cosmetics. The name kaolin is derived from Chinese and means 'high ridge' which refers to the hill in South-eastern China where the clay was originally discovered and used. The Chinese first used kaolin to make porcelain in the 7^{th} and 8^{th} centuries. It was many centuries later that other areas of the world were able to do same (Ismadji *et al*., 2015).

Kaolin is nearly white in colour with the ability to disperse in water, thus making it an ideal pigment. It is a hydrated aluminium silicate that occurs naturally as a clay and is prepared for pharmaceutical purposes by washing with water to remove sand and other impurities. The mineral kaolinite is the major constituent in kaolin, formed by the decomposition of minerals such as feldspar. Kaolinite has two-layers (sheet structures composed of units of one layer of silica tetrahedrons and one layer of alumina octahedrons) (Ismadji *et al*., 2015). This kaolinite group has the molecular formula $Al_2Si_2O_5(OH)_4$. The chemical composition of the kaolinite group is majorly SiO_2, Al_2O_3, H_2O and minor amounts of Mg, K, Fe, Ti (Murray, 2007).

In recent years, there is an increasing interest in utilizing clay minerals such as bentonite, kaolinite and diatomite as adsorbents to remove either inorganic or organic molecules. The adsorption capacity of clays generally is due to itshigh potential for ion-exchange, net negative charge on its surface minerals, being mechanically and chemically stable and having high surface

area. The negative charge gives clay the capability to adsorb positively charged species (Gupta and Suhas, 2009).

Chicken feather is one of the epidermal growth that forms the outer covering on birds. They are considered the most complex integumentary structures found in vertebrates and indeed a premier example of a complex evolutionary novelty. Chicken feather comprises mainly about 90% keratin protein and 10% water (Prum and Brush, 2002). Since almost two decades ago,chicken feather began to find increasing application in combating water pollution with highly toxic heavy metals that are released to the environment through industrial effluents (De la Rosa *et al*., 2008).

Pollution is the introduction of contaminants into the environment which lead to harm or discomfort to man and other living things and in the process damage the environment. It can be in the form of chemical substances or energy such as heat, light and noise.

Environmental pollution is therefore the contamination of the earth's or atmosphere's physical or biological components. One of such earth's environments that can be polluted is water.

Water pollution is defined as the introduction of any substance or energy into water body at a rate faster than what it can accommodate, or simply put as any human activity that impairs the use of water as a resource.

In recent years, water pollution with heavy metals has become an important environmental threat mainly because of the numerous industrial effluents containing them and other pollutants (Davydova, 2005). Hence methods for treating water contaminated with heavy metals should be developed; using cheap and ecofriendly materials.

1.1 Statement of Problem

In recent times, researchers have focused their efforts in the production of composite materials made of natural fibres such as wood, flax, hemp, jute or bamboo (Ashori 2008, Cheung *et al*., 2009) for treating wastewater of heavy metals. However, cellulose fibres, which are the most typical natural fibres, also show some technical disadvantages. One of such crucial issues is their incompatibility with hydrophobic polymer (Martínez *et al*., 2007). In addition, the use of farmland for the cultivation of such fibres, which can compete with food production, is of serious public concern (Van-Dam and Bos, 2004).

Aluigui *et al*. (2008), conducted a research on the use of chicken keratin/poly ethylene oxide composite as an adsorbent, but concluded that the practical uses of the keratin/poly ethylene oxide nanofibrous materials, were ultimately limited by their water instability and poor mechanical properties.

According to Ojo (2016) "Nigeria is one of the worst in the world with household water access and features third in the world on the list of top ten countries with the greatest number of people living without access to safe water". Also, among all environmental pollutions, water pollution by industrial waste which consists of toxic heavy metals such as nickel, copper, arsenic, lead, aluminium etc. is serious, complex and really disturbing (Ratna and Sobha, 2015).

Through extraction from ores and further processing into different uses, heavy metals have been released into the environment over many years. They are not biodegradable, so they accumulate to the extent that they become harmful. Some heavy metals are carcinogenic, while others cause neurological and behavioural changes mostly in children. Heavy metals, especially lead, arsenic, nickel, cadmium, mercury, copper and antimony are highly toxic and tend to cause several diseases and health disorders in humans, and other living organisms(Hazrat *et al*., 2013 and

Wang and Bjorn 2014). Nigeria is one of the worst hit countries with these problems due to lack of efficient water treatment system. Therefore, it is necessary to treat metal-contaminated water prior to its discharge to the environment or water bodies.

Various kind of absorbents such as agricultural wastes and industrial byproducts have been explored for the removal of heavy metals from wastewater and the results indicate that they may serve as an alternative to the costlier materials, such as commercial activated carbons or synthetic ion exchange resins. Even though these alternative adsorbents are abundantly available and cheap, the major drawback these adsorbents are their poor adsorption capacity (Ratna and Sobha, 2015).

1.2 Justifications

Due to its suitability and versatility, activated carbon is widely employed in water and wastewater treatment. However, the operating cost of activated carbon adsorption is high. Also due to their low mechanic intensity, limited reusability and relative low adsorption capacity, there is a shift from expensive commercial activated carbon to low cost ecofriendly and readily available adsorbent (Yan and Viraraghavan, 2001). Problems of regeneration and difficulty in separation from the wastewater after use are the two major concerns of using this material (Trevino *et al*., 2013).

Adsorption methods using low-cost adsorbent materials to purify water contaminated with metals were found to be more effective and attractive due to its lower costs and the higher efficiency of removing heavy metal ions from wastewater even at very low concentrations (Hui *et al.*, 2005).

It is in this regard that research is being undertaken to develop a novel composite made up of low cost and readily available materials for heavy metal removal from industrial wastewater.

Kaolinite is a clay mineral that can be used as an adsorbent, but its adsorption capacity remains low in comparison to other adsorbents. (Jiang *et al*., 2011). It is therefore believed that by combining kaolin clay with chicken feather which has good adsorption or sorption property, the overall sorption characteristics of the resulting composite will be greatly improved.

The poultry industry generates large amount of feathers as a byproduct, which is perceived as a waste, therefore, much effort is needed to address its disposal. Hence dumping it in the landfill or any other open space is the order of the day for most poultry industries of developing countries like Nigeria. Moreover, abundant feather debris is considered detrimental to human health (Leeson and Walsh, 2004). Nigeria has the highest poultry farms as well as highest participation of people in poultry industry in Africa. Nigeria presently produces above 550,000 metric tonnes of poultry meat per annum and 700,000 metric tonnes of eggs according to (FAO, 2010). Nigeria currently produce far more than this, consequently, generating large amount of chicken feathers. In 2014, 8.5 billion broilers were produced in the U.S. alone, generating approximately 7.8 million metric tonnes of chicken litter (USDA, 2014). Therefore, chicken feathers are available in abundance.

Since the production of chicken feather is abundant and most of the feathers are disposed as waste, the application of these keratin fibres for purification of industrial wastewater and drinking water is very economical and using it is equivalent to the use of one waste for clean-up of another (Pandima and Muthukumaran, 2013). Clays are readily available, cheap and environment friendly with high specific surface area, chemical and mechanical stability. They

have been found to be very effective, economical, versatile and simple for the purpose of metal adsorption from wastewater (Ijagbemi *et al*., 2009, Zaini *et al*., 2010).

Therefore, the use of common chicken feather wastes and kaolin in this research to produce a composite will not only serve as an efficient alternative adsorbent to the costlier ones but will also remove the competition for land to be used for planting food crops and that which will be used for planting crops for use as adsorbents for treating wastewater of heavy metals.

Also, there are no reports concerning the use of chicken feather-kaolin composite as an adsorbent for heavy metal removal from wastewater yet, this study therefore employs chicken feather to form a composite with kaolin clay in order to enhance its capacity to adsorb heavy metal from wastewater.

Aims and Objectives

1.3 Aim

The aim of this study is to produce and characterize chicken feather-kaolin composite and study the kinetics of its application for removal of selected heavy metals from wastewater.

The specific objectives for achieving this aim are to:

i. obtain chicken feather, kaolin and produce chicken feather-kaolin composite adsorbents;

ii. characterize the chicken feather, kaolin as well as their composite;

iii. determine the optimum conditions for the adsorption of the selected heavy metals using full factorial design and Response Surface Methodology (RSM);

iv. study the kinetic, isotherm and thermodynamics of the adsorption process;

v. use the kaolin (K), chicken feather (CF) and their composite (CFK) to remove selected heavy metals (Ni^{2+}, $Pb^{2+}$and Cu^{2+}) from wastewater and compare their adsorption capacities;

CHAPTER TWO

2.0LITERATURE REVIEW

2.1 Kaolin Clay

Several studies on soil chemistry have revealed the ability of clays and oxides to adsorb metal ions. It has also been shown that kaolinite clay is a potential and low cost adsorbent for Pb^{2+} ions from aqueous solutions (Waid and Hossam, 2007). In the past decades, research has focused on using low-cost, solid extractors for adsorption and removal of pollutants and the adsorbents used were clay minerals (Ma'rquez *et al*., 2004; Ijagbemi *et al*., 2009), agricultural by-products (Šćiban *et al*., 2008), some aquatic plants (Keskinkan *et al*., 2004) and microorganisms (Li *et al*., 2004).

Also, a number of studies considered kaolinite clay to remove heavy metals from aqueous solutions (Arias *et al*., 2002; Adebowale *et al*., 2005; Bhattacharyya and Gupta, 2011, Jiang *et al*., 2011). The kinetics and dynamics of nickel ion adsorption on calcined kaolinite clay has also been studied (Lawrence *et al*., 2013). In addition, removal of lead from water by adsorption on a kaolinite clay has been investigated (Orumwense, 1996).

Clays and modified clays have been discovered to be very useful for heavy metal adsorption. They have been found to be excellent adsorbents of metals such as As, Cd, Cr, Co, Cu, Fe, Pb, Mn, Ni, and Zn in their ionic forms from aqueous medium. The capacity to adsorb differs from one metal to another and also depends on the clay type employed (Bhattacharyya, 2008).

More recently, several ways of modifying clay minerals to obtain specific chemical, surface, and structural properties for various applications via pretreatment with chemicals or combined treatment such as heating and chemical attacks have been reported (San *et al*., 2009; Ijagbemi *et al*., 2010; Auta and Hameed, 2012; Yavuz and Saka, 2013; Adeyemo *et al*., 2015; Gao *et al*.,

2015). As a result, there are now different composite materials made of clay and other adsorbent materials to enhance its adsorption capacity.

Furthermore, the development and characterization of nanostructured polymer-clay composites have been given special attention, because of their advantages in comparison to the traditional polymer composites. Minimal additions of nanoclay enhances mechanical, thermal, and dimensional and barrier performance properties significantly because of the large contact area between polymer and clay on a nanoscale (Rajani, 2011). In the last few years, polymer-clay nanocomposites have received a great deal of attention, including studies on developing the composites as sorbents for nonionic and anionic pollutants (Churchman, 2002).

Oliveira *et al*. (2003) prepared clay iron oxide composite for adsorption of metal ions Ni^{2+}, Cu^{2+}, Cd^{2+}, and Zn^{2+} from aqueous solution. It was shown that advances in application of natural Clay and its composites in removal of biological, organic and inorganic contaminants from drinking water has been studied (Rajani, 2011).

The removal of Cd (II) from aqueous solution by kaolinite, montmorillonite and their poly (oxo zirconium) and tetrabutylammonium derivatives has been studied (Gupta and Bhattacharyya, 2006).

In the light of the ability of kaolin clay to form composites with other materials so as to improve its adsorption capacity, it serves as a potential component to form composite with chicken feathers among others for heavy metal removal from wastewater.

2.1.1 Applications of kaolinclay

Kaolin is used in the industry mainly in paper making as the coating and paper filler. When used as filler, it is mixed with the cellulose fibers in wood pulp while as a coating it is mixed with water, adhesives, and various additives and coated onto the surface of the paper (Murray, 2007).

Kaolin is also applied extensively as filler in the plastics industry as a result of its inert chemical nature and its unique size, shape and structure. Due to its white colour, fine particle size and plate-like structure, kaolin is suitably employed as the pigment for paint, ceramic raw material, functional filler, extender, cosmetic, food additive, adhesives, Portland cement, sealant, etc. It has also been used as an important start up material (raw material) in refractory applications, catalysts, concrete, fiberglass, and can be employed as the adsorbent for removal of organic compounds and heavy metals (Ismadji *et al*., 2015).

2.2 Chicken Feathers

Feathers serve as covering for birds. They are non-abrasive, have low density and good mechanical properties, insoluble in water and organic solvents at ambient temperatures (Ratna and Sobha, 2015). Feather is one of the most important features in bird's anatomy and they are fundamentally specific to birds. They contain basically an insoluble keratin protein. Keratin protein can also be found in mammalian hair, hoofs, horns, wool and reptilian scales (Leeson and Walsh, 2004).

The continuous and sustainable growth of the poultry industry and an ever increasing demand for poultry consumption is leading to an over-supply of the byproducts (mainly chicken feather waste). The efficient utilization of chicken feather is a challenge, but one which should be

surmountedespecially being a worldwide industrial waste. It is estimated that over 65 million tonnes of feather waste are produced worldwide (Poole *et al*., 2009; Ullah *et al*., 2011; Wu and Ullah, 2013).

Chicken feathers which represents about 6.0% of the total weight of a mature chicken become a huge environmental problem as waste by-product at commercial poultry plants. Chicken feather,a bio source, hasbeen very effective in removal of precious metals like gold (Suyam *et al*., 1996) and has also been reported for binding of copper, iron and chromium (Schmidt *et al*., 1997).

The suitability of chicken feathers for the removal of acid brown 348 dye from its aqueous solution was studied. Its keratin fibre has properties such as tensile strength and water insolubility, making it more attractive for bio sorption (Pandima, and Muthukumaran, 2013).

In a study by Al-Asheh *et al*.(2002) to investigate the adsorption of copper, zinc and nickel ions from single and binary metal ion mixtures onto chicken feathers, it was found that in the binary mixtures, the presence of one metal affects the uptake of the other, by the chicken feather. Further, the adsorption of erythrosine, a hazardous dye onto chicken feather was reported (Gupta *et al*., 2006). Also, the adsorption kinetics of the removal of a toxic dye, Malachite green from wastewater using chicken feather was studied by Mittal, 2006a; Mittal, 2006b.

Several studies have employed chicken feather to remove organic dyes and heavy metal ions from wastewater on account of their high surface area and several reactive functional groups (McGovern, 2000; Al-Asheh *et al*., 2003; Gupta *et al*., 2006). Amongst several waste materials used as adsorbents for removal of dyes, metal and other pollutants from industrial effluents, chicken feathers have shown good potential (Al-Asheh *et al*., 2003). The efficacy of chicken

litter and wood biochars and their activated counterparts in heavy metal clean up from wastewater was studied (Isabel *et al*., 2015). Chicken feather has also been employed as sequestrant for lead ions in aqueous solution (Egwuatu *et al*., 2014).

Chicken feathers have also been shown to be very effective in the formation of composites. In view of this, the use of chicken feather wastes for the fabrication of composite materials and its life cycle assessment was studied (Carrillo *et al*., 2012; Molins *et al*., 2012). Tesfaye *et al*. (2017) stated that "chicken feather barb fibre has low density, high flexibility, good spinning length and a hollow honeycomb structure and suitable for the manufacture of composite materials".Chemical modification, characterization, and application of chicken feathers as novel biosorbents for arsenic removal from water has been reported (Khosa *et al*., 2013).

The wastewater of a synthesized dye prepared with acid blue-A dye was treated with chicken feather keratin-based composite decolourant (keratin agent), using batch decoloration technique. A modified keratin agent was also developed to improve the decolouration efficiency (Bi *et al*., 2016). Scientists have been using biodegradable natural fibre to develop environment-friendly polymer matrix composites (Das and Mondal, 2011). There is plethora of reports on the use of chicken feather barbs as "feather fibers" for composites and non-woven applications (Barone and Schmidt, 2005; Cheung *et al*., 2009).

2.2.1 Uses of feathers

Feathers have a number of utilitarian, cultural and religious uses. They are both soft and excellent at trapping heat; thus, they are sometimes used in high-class bedding, especially pillows, blankets, and mattresses. They are also used as filling for winter clothing, such as quilted coats and sleeping bags; goose and eider down have great loft, the ability to expand from

a compressed, stored state to trap large amounts of compartmentalized, insulating air. Apart from domestic poultry, feather plays the critical role of enabling birds to fly. Feathers are also indicative of the welfare status of birds, or oppositely, of physiological stress, like molting (Leeson and Walsh, 2004).

Interestingly, chicken feather has been introduced in almost two decades ago for combating water pollution, removing highly toxic heavy metals that are released to the environment through industrial effluents (De la Rosa *et al*., 2008).

2.3 Heavy Metals

The use of heavy metals increased rapidly due to industrial revolution. Heavy metals cause direct toxicity to humans and other living beings due to their presence in aquatic environment beyond the permissible limits (Rajesh Kanjan, 2014). Heavy metals have the ability to dissolve in wastewater and when such water is discharged into surface water, they enter into the food chain and can be ingested and become accumulatedin human body thereby causing harm to them. Dissolved heavy metals can also sink into groundwater, leading to the contamination of drinking and irrigation water. Large quantities of heavy metals in wastewater pose great risks to the environment, animals as well as humans.

For example, lead is toxic and essentially has no nutritional value to human life, but it is rapidly absorbed into the bloodstream and is believed to have adverse effects on the cardiovascular system, kidneys, the immune system and cause brain disorder and brings about damages to nervous connections especially in young children (Bergeson, 2008). In pregnant women, high levels of exposure to lead may cause miscarriage. Chronic high-level exposure has been shown to reduce fertility in men (Golub, 2005). Also, cases of lead poisoning leading to death of people and animals were reported in Zamfara State, Nigeria (Sadeeq 2010; Isah, 2010).

Nickel and arsenic compounds are also extremely fatal and carcinogenic to all living organisms. Arsenic in exceeding amounts, once ingested, can cause severe nausea and gastrointestinal symptoms (Hughes, 2002 and Muhammad *et al.*, 2013).

Copper is an essential metal in a number of enzymes for all forms of life. However, its accumulation in the human body causes brain, skin, pancreas, and heart diseases, stomach and lung ulcers and central nervous system disorder (Dalida *et al*., 2011).

Sources of heavy metal pollution include exhaust fumes from automobiles, wastewater from battery manufacturing, metallurgical, electroplating, metal-finishing and other chemical industries such as textiles industries, crude oil exploration and refining operations, mining operations, etc as well as natural processes such as volcanic eruption, weathering of rocks. Therefore, it is necessary to treat heavy metal-contaminated water before its discharge to the environment or water bodies.

There are many conventional processes for the removal of heavy metals from industrial wastewater or streams. These includeprecipitation, coagulation, ion exchange etc. (Nilsson, 1971). These processes have many disadvantages such as incomplete removal, high energy requirement, high reagent cost, disposal of toxic sludge and their suitability only for solution of high metal concentrations**.** Hence, the sorption method of water treatment has been employed in several studies having the pollutants in low concentration.

2.4 Sorption

Sorption is the taking up and holding of one substance by another. Sorption is used especially as a general term for absorption and adsorption. The material that is used for sorption is called a

sorbent. Sorbents are insoluble materials or mixtures of materials used to recover liquids through the mechanism of absorption, or adsorption, or both (Králik, 2014).

2.4.1 Adsorption

The process of adsorption arises due to presence of unbalanced or residual forces at the surface of liquid or solid phase. These unbalanced residual forces have the tendency to attract and retain molecular species that comes in contact with its surface. Adsorption is essentially a surface phenomenon. Adsorption process involves two components, adsorbent and adsorbate. Adsorbent is the substance on the surface of which adsorption takes place (Králik, 2014). Adsorbate is the substance which is being adsorbed on the surface of the adsorbent. Adsorption can be physical (physisorption) or chemical (chemisorption).

2.4.2Physisorption

When the force of attraction existing between adsorbate and adsorbent are weak Vander waal forces of attraction, the process is called physical adsorption or physisorption. Physical adsorption takes place with formation of multilayer of adsorbate on adsorbent. It has low enthalpy of adsorption, that is, ΔH is 10-40kJ/mol. It takes place at low temperature below boiling point of adsorbate. As the temperature increases, process of physisorption decreases (Králik, 2014).

2.4.3Chemisorption

When the force of attraction existing between adsorbate and adsorbent are chemical forces of attraction or chemical bond, the process is called chemical adsorption or chemisorption.

Chemisorption takes place with formation of unilayer of adsorbate on adsorbent. It has high enthalpy of adsorption, that is, ΔH is 20-400kJ/mol. With the increases in temperature, chemisorption first increases and then decreases (Králik, 2014).

2.4.4Adsorbents

Adsorbents are materials that pick up and retain liquid causing the material to swell (50 percent or more). Adsorbents are insoluble materials that are coated by a liquid on its surface. There are many types of adsorbents; earth's forests and plants, ocean and freshwater plankton, algae and fish, all living creatures, including animals are all "biomass adsorbents". There are various types of adsorbents used in electroplating industry for removal of heavy metals according to requirement and availability. Basically, there are two types of adsorbents which are inorganic and organic adsorbents (Králik, 2014).

2.4.5Inorganic adsorbents

They may be natural minerals, ores, clay and waste materials from various industries like fly ash, metallurgical solid wastes like bauxite red muds etc. Kaolinite has been used to accumulate Zn^{2+} (Singh *et al*., 1988), Illite to remove Pb^{2+} (Chantawong *et al*., 2001), Bentonite was used to adsorb Cr(VI) (Khan *et al*., 1995), activated red mud was used to trap Ni^{2+} and Cr^{2+} (Zouboulis and Kydros, 1993).

2.4.6Organic adsorbents

A large number of waste materials of organic origin like dead leaves of trees, bark, roots, seed shells, oil cakes and saw dust from various plants in the form of powder have been utilized for

the removal of heavy metals, and their adsorption properties have been explored. In addition to these adsorbents, wool, albumin, feathers, waste rubber, hair, used tea leaves, bagasse, rice husk etc. have also been used as organic non- conventional adsorbents (Rai *et al*., 1998). Exhausted coffee was used to remove Cd^{2+} and Cr(VI) (Orhan and Buyukgungor, 1993), formaldehyde-polymerized peanut skin was used to remove Cd^{2+} and Pb^{2+} (Randall *et al*., 1978), untreated sawdust was used to remove Cr(VI) from tannery effluents (Zarraa, 1995), leaf mould was used to remove Cr (VI) (Sharma, and Foster, 1994). Activated carbon from hazelnut shells was used for the adsorption of Co^{2+} from aqueous solution (Demirbas, 2003). Activated carbon from coconut coir pith was used for the removal of Cd^{2+} from aqueous solution (Kadirvelu and Namasivayam, 2000).

2.5 Composites

Composites can be defined as natural or synthesized materials made from two or more materials with varying physical and chemical properties which remain separate and distinct at the microscopic or macroscopic scale within the material (Rajani, 2011). Composites are synthesized to combine the desired properties of the materials in the composite.

In nanocomposite, nanoparticles (clay, metal, carbon nanotubes, etc.) act as fillers in a matrix. Nanoparticles are particles of less than 100nm in diameter that exhibit new or enhanced size dependent properties compared with larger particles of the same material. Clay composite or nanocomposites are the materials in which the major component is clay in combination with other materials like metals, polymer (Rajani, 2011).

2.5.1 Need for an alternative adsorbent

Sequel to the various setbacks associated with the existing methods of water treatment, the need therefore arises for the development of new and better alternatives. Several technologies for heavy metal removal from wastewater have been developed. Some of such technologies commonly employed for heavy metal removal are chemical precipitation and filtration, chemical oxidation, electrochemical treatment, reverse osmosis, evaporation, ion-exchange, flocculation and coagulation. However, these processes have numerous economic and technical setbacks, such as selective or partial metal removal, high capital and operational cost, high sensitivity to operational conditions, significant energy consumption with increased disposal of residual metal sludge, making them unsuitable and unsustainable for small scale industries and even purification of water for township supplies.Hence, it is necessary to develop effective, low-cost, and environment friendly methods with readily available raw materials for water treatment (Ratna and Sobha, 2015).

2.6 Conceptual Framework for Chicken Feather- Kaolin Composite

A conceptual framework is a researcher's understanding of how the particular variables in a study connects with each other. McGaghie *et al*. (2001) defines conceptual framework as what sets the stage for the presentation of the particular research question that derives the investigation being reported based on the problem statement. The problem statement of a thesis presents the context, and the issues that caused the researcher to conduct the study. Regarding this work, the following framework will be utilized.

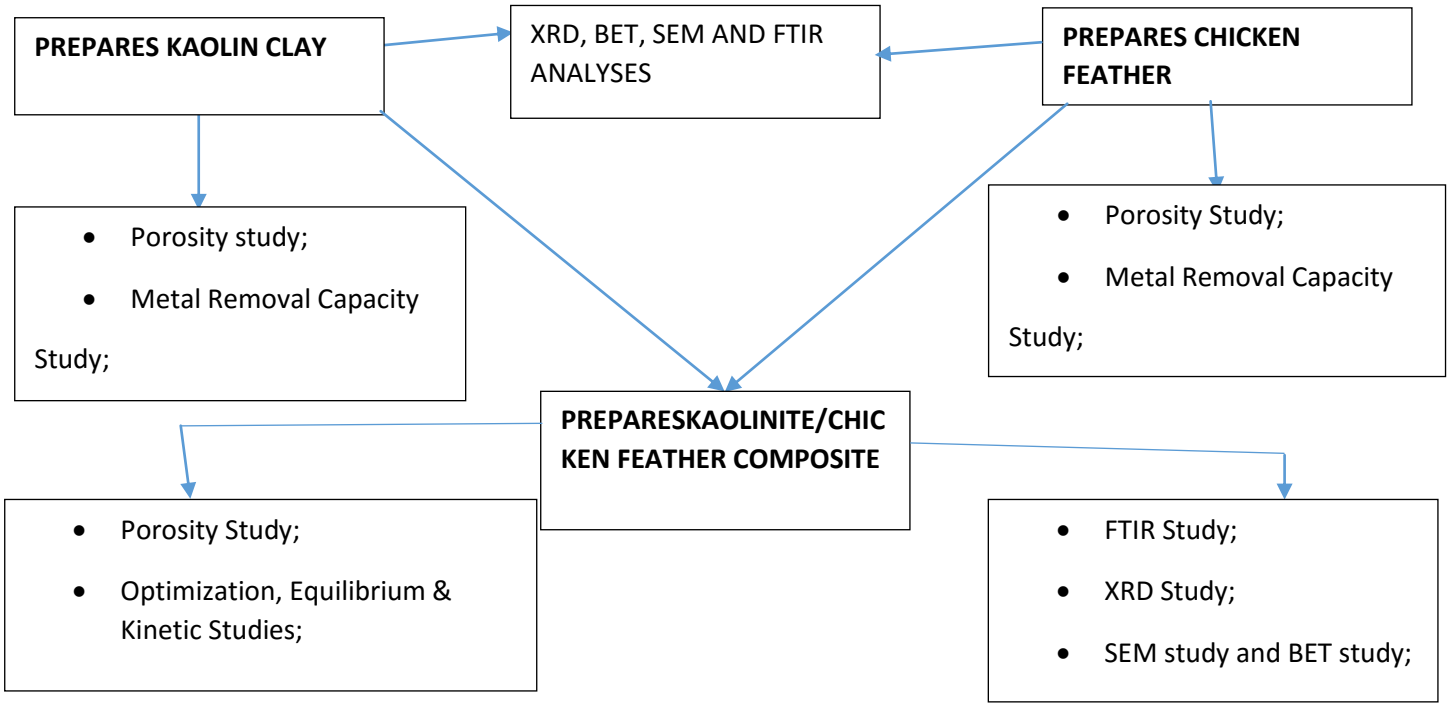

Figure 2.1: Conceptual framework diagram

Based on literature and the gaps noticed with using chicken feather only or kaolin only respectively as adsorbents for water treatment, it is anticipated that the following qualities of chicken feather and kaolin will give avenue for the two to form a more potential adsorbent with improved characteristics for heavy metal removal from wastewater. The adsorption suitability of clays generally results from abundance, high potential for ion exchange, net negative charge on the structure of the minerals, mechanical and chemical stability, low permeability, swelling ability, and high surface area. The negative charge gives clay the capability to adsorb positively charged species (Gupta and Suhas, 2009).

Feather has the advantage of abundance, high tensile strength, water insolubility, stability over a wide range of pH and structural toughness (Kar and Misra, 2004; De la Rosa*et al*., 2008).The pH of the solution is a crucial factor in the adsorption of heavy metals onto clay minerals, the surface layer charge of the clay minerals varies with pH and the exchange capacity is also a function of pH. Values of pH significantly influence the solution chemistry of heavy metals (precipitation,

hydrolysis, complexation, redox reaction, etc.). In a certain range of pH, the uptake of heavy metal by clay minerals increases with increase in pH to a certain value and then followed by a reduction in the uptake amount as the pH increases further (Dos-Santos*et al*., 2015). Hence clay is suitable within a narrow pH range.

Efficient and effective water treatment process must resist pHchange; thus it is expected that the chicken feather will contribute its property of stability over a wide range of pH to this composite to ensure a stable process. Chicken feather is also hoped to contribute its characteristics of high structural toughness, high tensile strength and low density to enhance the overall performance of the composite for heavy metal removal from wastewater. Another important point of consideration in the formation of this composite is that, both of them are very cheap and readily available.

As a result of large surface area between nanoclay and other composite materials, little additions of nanoclay to them has been found to improve mechanical, thermal, and dimensional and barrier performance properties of the resulting composites significantly (Ara'Ujo *et al*., 2004; Ekici *et al*., 2006; Li *et al*., 2007; Wang *et al*., 2008; Pandey and Misra, 2011). These features contributed by kaolin to chicken feather/kaolin composites will enhance the performance.

Both chicken feather and kaolin have negatively charged surface that aid their individual adsorption capacity which in turn depends on the strength of the negative charge. Hence combining them will improve the overall negative charge on the surface of the composite, and thus its ion exchange capacity.

In general, chicken feather/kaolin composite may offer combined properties and represent an improvement upon thermal, mechanical and porosity properties compared with the homogenous characteristics of the bare individual chicken feather and kaolin components.

2.7 Theoretical Framework

The theoretical framework is the researcher's presentation of a theory that explains a particular problem. It is the summary of the researcher's theory regarding a particular research question that is developed through a review of previous research on the variables involved. It therefore identifies a plan for investigation and interpretation of findings and help readers to understand and assess the researcher's perspective.

The followings therefore are some of the theories from literature upon which this work is based and from which the theory for this research was formulated and developed.

Clays have been good adsorbents because of the existence of several types of active sites on the surface, which include Bronsted and Lewis acid sites and ion exchange sites. The edge hydroxyl groups have been particularly active for various types of interactions (Van, 1977; Bhattacharyya, 2008). With the chemical composition of ($Si_2Al_2O_5(OH)_4$) (Hydrated aluminosilicate), kaolinite is a 1:1 phyllosilicate layers in which each layer in the structure is comprised of two sub layers. One layer of the mineral consists of an alumina octahedral sheet (Al_2 (OH) $_4)^{2+}$ and the second layer is a silica tetrahedral sheet $[Si_2O_5]^{2-}$(Elbokl and Detellier, 2006; Zhang *et al*., 2007; Zhang and Xu, 2007). Thus kaolinite can interact with other species via its outer or edge hydroxyl groups.

Another very important characteristics of Kaolinite is its asymmetric structure which creates large superposed dipoles in the lamellar structure and allows the formation of hydrogen bonds

between consecutive layers, resulting in a large cohesive energy (Elbokl and Detellier, 2006; Zhang *et al*., 2007; Zhang and Xu, 2007). Thus clay minerals can be modified by inserting an inorganic and/or organic guest species into the inter-lamellar region (Meziane *et al*., 2017) because the kaolinite interlayer region can react with a small group of organic and/or inorganic materials via a process called intercalation. This implies that some types of molecules can insert between the kaolinite layers and react chemically with the inner-surfaces leading to the expansion of the kaolinite layers (intercalation reaction) (Kelleher *et al*., 2002).

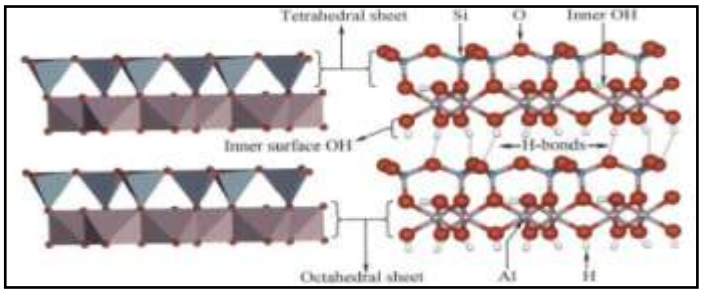

Figure 2.2: Structural models of kaolinite (Deng *et al*., 2002)

2.8 Intercalation Reaction of Kaolin Clay

The Intercalation is a chemical process of modifying kaolinite inner surfaces, resulting in significant changes in the kaolinite surface properties. For example, intercalation can cause significant disordering of the kaolinites, increased surface areas and provide surfaces, which are more readily available for chemical reactions. The mechanism of intercalation reaction depends on the disruption of the hydrogen bonding between the kaolinite layers and the formation of new hydrogen bonds with the inserting molecule (Rintoul *et al*., 2000; Frost *et al*., 2001; Asmatulu, 2002).

Oxygen atoms and hydroxyl ions between the layers are paired with hydrogen bonding in clay. This interaction is expected to occur between the oxygen and hydroxyl groups of kaolinite and

that of chicken feathers thereby binding them together. Intercalating compounds also have a certain hydrogen bonding capacity. Formamide, dimethyl-sulfoxide (DMSO), and N-methyl formamide (NMF) are known to directly intercalate, resulting in an increase of the interlayer spacing within the kaolinite. This increase depends on the size and arrangement of the guest species. Hence, should the CF size or particle arrangement prevent it from being inserted into the kaolinite, it can still combine with it at the surface. Although not many compounds have the ability to intercalate, the number may be extended by the so-called "displacement method" (Kelleher *et al*., 2002).

2.8.1 Guest displacement reaction

In recent years, intercalation reactions of kaolinite have been extended to include guest displacement method in which new guest species can be intercalated by displacing previous species (Zhang *et al*., 2007; Jia *et al*., 2008). Guest displacement reaction is one of the various techniques which were developed in order to facilitate the process of intercalation of the organic compounds between the lamellar layers of kaolinite. Displacement involves the replacement of a directly intercalated species (e.g., NMF or potassium acetate) by a second organic molecule. The use of a directly intercalating compound which expand the inter- lamella space in kaolinite as an intermediate for the intercalation of other polar organic compounds opens up new areas for basic, strategic, and applied research (Komori and Koroda, 2000; Kelleher *et al*., 2002; Elbokl and Detellier, 2006; Zhang *et al*., 2007; Jia *et al*., 2008; Kowshik *et al.*, 2017).

This method is considered the most effective and the most used to obtain nanocomposites polymer/kaolin, either by reaction of polymerization or direct intercalation of polymers to the

melt in the inter-foliar space of kaolinite (Komori and Koroda, 2000; Itagaki *et al*., 2001; Elbokl and Detellier, 2006; Zhang *et al*., 2007; Jia *et al*., 2008; Kowshik *et al.,* 2017).

Various work used this method for the intercalation of kaolinite, such as the work by Olejnik *et al*. (1970) in which complexes of kaolinite/amides (formamide, N-methylformamide (NMF), dimethylformamide (DMF), acetamide, N-methylacetamide, dimethylacetamide and pyridine) were formed. Also, using the complex kaolinite/dimethyl sulfoxide (DMSO) as precursor, vinyl acetate and styrene were polymerized between the layers of kaolinite(Elbokl and Detellier, 2006; Jia *et al*., 2008). This process is as illustrated in Figure 2.3

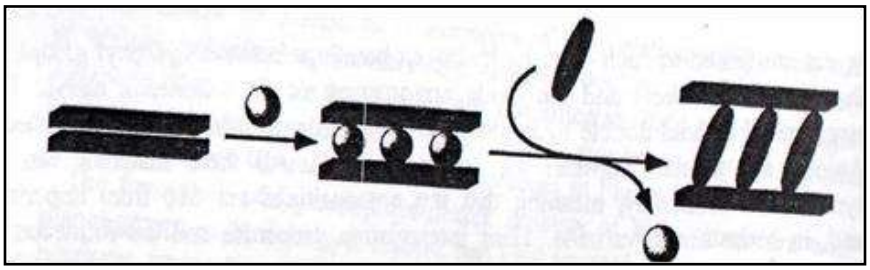

Figure 2.3: Method of Guest Displacement reaction (Mezian*et al.,* 2014)

Chicken feathers and all feathers are mainly composed of 91% protein (keratin) (Thyagarajan *et al*., 2013). Keratins are long chains of amino acids constituting cysteine, hydrophobic residues and β-sheet conformations (Onifade *et al*., 1998; Guhados *et al*., 2005). Based on the side chain of an amino acid, it can be classified as hydrophobic, polar or charged. The polar amino acids side chains are hydrocarbons containing atom(s) that can form hydrogen bond and has more carbon, which means more capacity to adsorb. Several functional groups present in keratin protein, especially peptide backbone, such as disulfide (-S-S), amino ($-NH_2$) and carboxylic acid (-COOH), makes it chemically reactive under conducive reaction conditions (Khosa and Ulla, 2013).

Figure 2.4: General keratin protein structure

Also, the β conformation of feather makes it have large surface area, a look under a microscope shows that there are lot of empty space in quill, shaft, rami and barbules of feather. The large surface area makes it possible for the trapping, entanglement and occlusion of adsobates within the feather void. This in combination with the above characteristics of the clay kaolinite is also expected to boost the adsorption capacity of the composite (Khosa and Ullah, 2013).

With the possibility of interactions such as hydrogen bonding on the surfaces of kaolin and chicken feather due to the presence of OH and NH_2 and other active groups, it can be inferred that, during the process of intercalation, CF can either be inserted in the inter- lamella spacing in K or have K particles trapped on its surface or entanglement via hydrogen bondingto form the composite.

CHAPTER THREE

3.0MATERIALS AND METHODS

3.1Materials and Chemicals

All chemical reagents used in this study are of analytical grades (Sigma Chemical Company), bought from Hadi chemical company, Samaru Zaria. The chemicals used in this work are listed in Appendix I, while the apparatuses and equipment used in this study are listed in Appendix II.

3.2 Methods

3.2.1Collection of kaolin and chicken feather

The Kaolin clay ($Al_2Si_2O_5(OH)_4$) was obtained from Kankara in Katsina State, Nigeria, November, 2017, and ground to pass 90 µm sieve (Salwa *et al*., 2015). The chicken feather was collected from the poultry slaughter house in Karu Modern Market Abuja, Nigeria, November, 2017.

3.2.2Purification of kaolin

This was done using the method employed by Meziane *et al*. (2017).A 40 g of kaolin was suspended in one litre of distilled water. The suspension was then agitated for 30 minutes and decanted. This operation was repeated six successive times in order to eliminate all the impurities. After each washing, the suspension was centrifugedat 200rpm for 10 minutes using a centrifuge machine(Autobench centrifuge mark IV,Baird & Tatlock, London), then at the end, the kaolin obtainedwas dried in an oven (Gallenkamp Hot Box Oven, England) at 150°C for 24 hour and pounded using mortar and pestle.

3.3.3Purification of chicken feather

This was carried out according to the method used by Kelle and Udeozo.(2015),with slight modification toget it in powdered form.The chicken feather was washed several times with tap water and highly dilutedliquid detergent, andwas then rinsed with much distilled water before being left to sun-dry for two weeks. Thereafter, the chicken feather was dried for 2 days in an oven (Gallenkamp Hot Box Oven, England) at 70ºC to ensure complete dryness. Then, a mortar and pestle was first used to pound the chicken feather to disintegrate it and then ground using a mechanical blender to powdered form, it was then sieved using a 90µm sieve.

3.3.4Sodium acetate (Naac) treatment (intercalation reaction)

Intercalationis a chemical process used for modifying kaolinite inner surfaces, resulting in significant changes in the kaolinite surface properties (Rintoul *et al*., 2000; Frost *et al*., 2001; Asmatulu, 2002).

For the Naac treatment, the method of Asmatulu.(2002), was employed with modification with respect to the weight of the kaolin and Naac. A mixture of 70 g of dry Kaolin clay with 45 g of dry Naac was kept in an oven (Gallenkamp Hot Box Oven, England) at 110^{o}C overnight. This was then hand-ground using a mortar and pestle for 10 min. Half of the mixture was then transferred to a suitable screw-cap centrifuge tube and 2.5cm^{3} of 8M Naac was added. This was also done to the other half and were then mixed up to get a homogeneous mixture. The sample was then covered, shaken and allowed to stand for 2 days at room temperature. This was then used for preparing the composite via guest displacement reaction.

3.3.4 Preparation of kaolin-chicken feather composite via guest displacement reaction

The experimental method used for chicken feather intercalation into kaolinite clay to form the composite via guest displacement reaction was carried out according to the procedures described by Hussein *et al*. (2015) with slight modification with regard to the weight of samples used.

The kaolin/sodium acetate intercalate previously prepared which contained 70 g kaolin and 45g sodium acetate was placed in a beaker (500cm^3). A 70 g of ground chicken feather was weighed and added to the kaolin/sodium acetate intercalates in the beaker. The mixture was then mixed manually in a mixer in its dry form. Then 250 cm^3 of water was added to the mixture while stirring continuously with a stirrer to get a kaolin-chicken feather solution. It was then washed thoroughly

with 150 cm^3 distilled water twice and decanted to remove any sodium acetate left. The mixture was thereafter spread on a porcelain crucible and heated in an oven at 150^{0}C till dryness.

The product was then ground through a ball milling process (using Welay milling machine) and a mortar and pestle for a period of 1.30 hour, followed bygrinding for 15 minute using a mechanical grinder. It was then sieved using a 90 µm sieve.

3.4Instrumentation

3.4.1 Fourier transform infrared spectrophotometer (FTIR)

Characterization of the adsorbents was carried out by Fourier transform infrared spectrophotometer (CARY 630 FTIR, Agilent Technologies, US). This was employed to get insight into interactions between the kaolinite and chicken feather and to identify the functional groups present in each sample. FTIR (CARY 630 FTIR, Agilent Technologies, US)

spectrophotometer was used to determine the functional groups in the samples responsible for metal adsorption. The FTIR studies was done in the range of 4000–650 nm region at a resolution of $8cm^{-1}$ with sample scan of 30 and back ground scan of 16 for the tested solid samples of the kaolin, chicken feather and the composite. This was carried out at the Multi-user Research Laboratory, Ahmadu Bello University, Zaria, in December, 2018.

3.4.2 Scanning electron microscope (SEM)

Scanning electron microscope (SEM 800-07334, Phenomworld, Nertherlands)was used to assess the surface morphology of the adsorbents at a magnification of between 300-4000 at Umar Musa Yar'adua University, Katsina State, Nigeria, in September, 2018.

3.4.3X-ray diffraction spectrophotometer (XRD)

The XRD study of the kaolin, chicken feather and chicken feather-kaolin composite was done at Umar Musa Yar'adua University, Katsina State, Nigeria, in September, 2018. XRD was used to study the raw kaolin, ground chicken feather and the chicken feather-kaolin composite using diffractometer equipped with Cu-kα radiation (λ=1.154nm) at room temperature (25^oC). A dried sample of the produced materials was ground using a mortar and pestle and tested at 40KV and 40mA. The scans were a 2 theta type and taken in a range from 5.000 to 70.000° at a step size of 0.030°, integration time of 0.150 second and scan rate of 12^o/min.

3.4.4 Brunauer-Emette-Teller (BET)

The BET analysis of the samples of kaolin, chicken feather and chicken feather-kaolin composite was done at Federal University of Technology, Minna, Niger State, Nigeria, in October, 2018. A

0.12 g amount of the composite was poured into a fabricated crucible and then charged into an electric furnace. It was then heated to a temperature of 250°C and outgassed at this temperature for 3.0 hours. The surface area and volume of pores and micro-pores were obtained by nitrogen adsorption isotherms (BET method) at 77.350K at an analysis time of 93.9 min. These analysis was performed using Nova station A instrument for BET method. The analysis was also carried out on raw chicken feather and kaolin. Surface area measurements were obtained at 77K using a Nova 2000 Surface Area Analyzer (Quantachrome Instrument Version 11.03).

3.4.5Atomic absorption spectrophotometer (AAS)

Atomic adsorption spectrophotometer (AA-480 FS, Agilent Technologies, US) was used for determination of the Pb^{2+}, Cu^{2+} and Ni^{2+} contents in the standard and treatedsolutions. This was carried out at the Multi-user Research Laboratory, Ahmadu Bello University, Zaria, in September, 2018.

3.5 Preparation of Metal Solution and Determination of its Concentration

This was undertaken using the procedure of Mekonnen *et al*, (2015) with some modifications to suit a multi-component system. A 1000ppm stock solution containing Pb^{2+}, Cu^{2+} and Ni^{2+} was prepared by dissolving 1.615 g of $Pb(NO_3)_2$, 3.819 g of $Cu(NO_3)_2.3H_2O$ and 2.230 g of $NiCl_2.6H_2O$ in 100cm^3distilled water contained in three different 250 cm^3 volumetric flasks respectively as presented in Appendix III. Each flask was then thoroughly shaken for 5 minutes to dissolve the salts. The content of each flask was then emptied into a single 1000 cm^3 volumetric flask. The solution was thoroughly mixed and then made up to the mark to prepare a multi-elemental stock solution of the three metal ions (1000ppm). The different concentrations

used in the adsorption experiments were 100 cm^3 of 50ppm, 100ppm, 150ppm, 200ppm and 250ppm and each was prepared by serial dilution method from the stock solution using the formula:

$$C_1V_1 = C_2V_2(1)$$

where C_1= initial concentration, V_1 initial volume, C_2 = final concentration, V_2 = final volume

All the adsorption studies were carried out in tubes of 120 cm^3 at a constant shaking of 200rpm at the required temperature and time given in their procedures using a water bath shaker. At the end of each study, the K, CF and CFK suspensions were filtered using a Whatman filter paper and the supernatant solutions were subjected to heavy metals analysesusing AAS. The amount of the metal ions adsorbed by the adsorbents were calculated from the difference between the initial concentration and the equilibrium concentration. All assays were carried out in triplicate and only mean values are presented. A constant adsorbent dose of 0.5 g was used for the entire study.

3.6 Kinetic Studies Experiment

Batch kinetic studies were performed using a mixture of 150ppm Pb^{2+}, Cu^{2+} and Ni^{2+} metal solution and 0.5 g of the adsorbent. Keeping other parameters constant, samples were drawn at intervals of 3, 6, 9, 12 and 15min and analyzed. The kinetics of Pb^{2+}, Cu^{2+} and Ni^{2+} adsorption onto CFK composite was studied using pseudo-first-order (Lagergren, 1916) model, pseudo-second-order model and intra-particle diffusion (Weber and Morris, 1963) model. The agreement between the experimental and theoretical values was expressed by the correlation coefficient, R^2.

3.6.1 Lagergren model

The pseudo-first-order kinetic model was proposed by Lagergren and was extensively studied. Its linearized form can be expressed as follows:

$$\ln(Q_{e(expt)} - \mathrm{qt}) = \ln Q_{e(cal)} - \mathrm{K_1 t} \qquad (2)$$

Where $Q_{e(expt)}$ and $Q_{e(cal)}$ are the experimental and theoretical equilibrium adsorption and qt is experimental amount of metal ion adsorbed (mg/g of adsorbent) at any time t(min) and K_1 is Langmuir constant. By applying this linear equation and plotting $\ln(Q_{e(expt)} - \mathrm{qt})$ against t, the slope of K_1 and intercept of $\ln Q_{e(cal)}$ are obtained. The amount of metal adsorbed per unit mass of adsorbent was calculated by applying the following equation:

$$Q_e = (C_o - C_e)\mathrm{V} / \mathrm{W} \quad (3)$$

Where Qe is the amount of metal adsorbed on the adsorbent in (mg/g), Co (mg/ml) is the initial concentration of metal, Ce (mg/ml) is the equilibrium concentration of the metal or final concentration, V (ml) is the volume of metal solution in litre, and W is the mass of adsorbent used in gramme. The percentage removal efficiency of the metal was calculated using the following:

$$\text{Percentage Sorption} = (C_o - C_e/C_o) * 100 \quad (4)$$

Co and Ce are initial concentration of metal in solution before treatment with adsorbent and final concentration of metal in the solution after treatment with adsorbent.

3.6.2 Pseudo-second-order model

The pseudo-second-order model estimates the behaviour over the whole range of adsorption. This model is also based on the adsorption capacity of the solid phase.

The kinetics of adsorption process as described by the pseudo-second-order rate equation is expressed by (Ho and McKay, 1999) as

$$\frac{t}{qt} = \frac{1}{K_2 Q_{cal}{}^2} + t/Q_{cal} \quad (5)$$

A plot of t/qt versus t gives a slope and an intercept, from which the values of Q_{cal} in mg/g which is the calculated equilibrium concentration and the pseudo- second order rate constant k_2 in gm/gmincan be calculated respectively.

3.6.3 Intra-particle diffusion model

In a solid-liquid adsorption process, the transfer of the adsorbate is controlled by either boundary layer diffusion (external mass transfer) or intra-particle diffusion (mass transfer through the pores), or by both (Dąbrowski, 2001).

The intra-particle diffusion model is based on the theory proposed by Weber and Morris (Weber and Morris, 1963).

According to this theory, $q_t = K_d t^{1/2} + l$ (6)

Where l is the intercept, qt is adsorption capacity at time t, K_d is intra-particle diffusion rate constant in mg/g/min$^{1/2}$. This model shows whether the rate determining step is by the boundary film diffusion or by intra-particle diffusion. If the plot of q_t against $t^{1/2}$ is linear and passes through the origin, then, the intra-particle diffusion is the sole rate controlling step but where there is a deviation from this, then other surface phenomena are involved.

3.7 Equilibrium Studies Experiment

A 100 cm^3 of varying concentrations (50ppm, 100ppm, 150ppm, 200ppm and 250ppm) of the Pb^{2+}, Cu^{2+} and Ni^{2+} solution was put into 120 cm^3 tubes containing 0.5 g of the adsorbent. These were agitated at 200rpm for 1.30hour to equilibrate them in a mechanical shaker during which, other parameters such as temperature were kept constant at 25^0C. The composite samples were collected from the mixture and the supernatant analyzed for metal ions using AAS. The data obtained from the experiment were then fitted in thethree different isotherms of Langmuir, Freundlich and Dubilin-Raduskevich models. The correlation coefficient, R^2 was used to determine the best fit isotherm model.

3.7.1 Langmuir isotherm model

Langmuir isotherm which applies to equilibrium monolayer adsorption onto a surface with a finite number of identical sites (Langmuir, 1916) is represented by the linearized equation:

$$\frac{1}{q} = \frac{1}{q_{max}\ K_1 C_e} + 1/q_{max} \quad (7a)$$

Where q is the amount of adsorbed metal in mg/g, q_{max} is the maximum sorption capacity in mg/g, K_l is the Langmuir constant, Ce is equilibrium concentration of metal. A plot of 1/q against 1/Ce allows for the determination of q_{max} and k_l. The essential characteristics and the feasibility of the Langmuir isotherm is expressed in terms of a dimensionless constant known as separation factor or equilibrium parameter SF, which is defined as:

$$SF = {}^{1}/_{1 + K_1 C_o} \quad (7b)$$

Where C_o (mg/l) is initial metal ion concentration.The SFvalues indicate the shape of the isotherm and are significant because they give the type of isotherm.

SF> 1 is unfavorable, SF = 1is Linear, 0< SF< 1 is Favorable, SF = 0 is Irreversible

3.7.2 Freundlich isotherm model

The Freundlichisotherm for the adsorption of the selected heavy metals onto CFK composite gives the relationship between equilibrium liquid and solid phase capacity based on the multilayer adsorption (heterogeneous surface). This isotherm is derived from the assumption that the adsorption sites are distributed exponentially with respect to the heat of adsorption (Freundlich, 1906). The Freundlich isotherm is empirical and is best suited for adsorption on heterogeneous surfaces (Freundlich, 1906). The equation in linearized form is given as:

$$lnq = lnK_f + {}^{1}/_{n}\, lnC_e \quad (8)$$

Where K_f and n are Freundlich constants. A plot of lnq versus lnCe is used to determine k_F and n.

3.7.3 Dubinin–Radushkevich isotherm (D-R) model

This isotherm postulates that the characteristics of the sorption curve are related to the porosity of the biosorbents (Abdelwahab, 2007).

This model was also used to evaluate the mean energy of sorption of the selected heavy metals onto CFK composite. It is represented in the linear form by the equation (Dubinin, 1960).

$$lnq = lnQ_{DR} - \beta\varepsilon^2 \quad (9a)$$

Where

$$\varepsilon = RTln(1 + 1/C_e) \quad (9b)$$

where q is amount adsorbed per gram of the adsorbent (mg/g), Q_{DR} is equilibrium adsorption capacity (mg/g) using model, β is Polanyi potential, ε is activity coefficient, Ce is concentration in mg/l of metal ion in solution at equilibrium, R is universal gas constant (8.314J/K/mol) and T is temperature in Kelvin. The values of β and Q_{DR} are evaluated from the slope and intercept of the graph of lnq versus ε^2. The mean energy of sorption E (kJ mol^{-1}) is calculated from the relation; $E = 1/\sqrt{2\beta}$(9c)

3.8 Thermodynamic Studies

The thermodynamic study was done using the van't Hoff thermodynamic plot to evaluate the spontaneity of the process.With all other parameter kept constant, adsorption experiments were carried out at temperatures of 25, 50 and 75^{o}C in a water bath. Thermodynamic parameters such as Gibb's free energy changes (ΔG), enthalpy change (ΔH), and entropy change (ΔS) were determined. Gibb's free energy of adsorption was computed from the equation (Ada *et al.*, 2009):

$\Delta G = -RT\ln K_c$(10)

Where ΔG is standard free energy change, R is universal gas constant (8.314 J/mol/ K), T is absolute temperature in K, and K_C is the equilibrium constant. The apparent equilibrium constant, K_C, is defined as (Yu *et al.*, 2001):

$Kc = q/C$(11)

Where q is the concentration of adsorbed metal in ppm, C is concentration in ppm of solution after adsorption. The values of ΔH and ΔS were estimated from the relationships

$\Delta G = \Delta H - \Delta S$(12)

3.9 Optimization and Statistical Analysis

Optimization and statistical analyses were carried out using Design Expert version 7.0. For the optimization studies, the effect of different operating parameters (concentration, temperature and time) on the adsorption efficiency of the composite (CFK) was investigated using a three-level three-factor full factorial and response surface methodology in order to identify the optimum conditions for heavy metal removal. The list of the independent variables (A, B, C) with their coded and actual levels are presented in Table 3.1.

Table 3.1: Variables and levels for the three-level and three-factor full factorial design and response surface methodology

Variables	Symbols	Low Level (-1)	Middle Level (0)	High Level (+1)
Concentration (ppm)	A	100	150	200
Temperature (^{o}C)	B	25	50	75
Time (min)	C	10	35	60

CHAPTER FOUR

4.0 RESULTS

4.1 Characterization of Kaolin, Chicken Feather and Chicken Feather-Kaolin Composite

Figure 4.1 shows the FTIR spectra of Kaolin (K). The spectra analysis was run between the 650-4000 cm^{-1} region of the FTIR spectrophotometer. Kaolin shows bands at 3,690.10 $cm^{-1}$and 3,623.0 cm^{-1} due to stretching vibrations of hydroxyl groups.

Figure 4.2 shows the FTIR spectra of chicken feather (CF) with a peak at 3690.10 cm^{-1} indicating O-H group from water of the feather fibre and another peak at 3265.10 cm^{-1} which is due to N–H (amine) group from an amino acid present in the chicken feather (CF).

Figure 4.3 shows the FTIR spectra of chicken feather-kaolin composite (CFK). After the formation of the composite, sharp band at 3690.1 cm^{-1} in the chicken feather spectra has shifted to 3734.8 cm^{-1} indicating an interaction between CF and K. New absorption bands which appeared at wavenumbers 3649.1 cm^{-1}, 3619.2 cm^{-1} and 3425.4 cm^{-1} are due to O-H and N-H; inter hydrogen bond's vibration between CF and K. The band at 3265.1 cm^{-1} in the CF spectra which shifted to 3291.2 cm^{-1} in the CFK composite also suggested an interaction between CF and K.

Figure 4.4 shows the SEM micrograph of kaolin which reveals the presence of large particles that appeared to have been formed by very small particles stacked together in the form of agglomerates.

Figure 4.5 shows the SEM micrograph of chicken feather (CF). The feathers have long shafts with barbs and barbules attached to it. It can be deduced that the chicken feather has a crystalline microfibril embedded in a fibrous protein matrix, thus making it amorphous in structure.

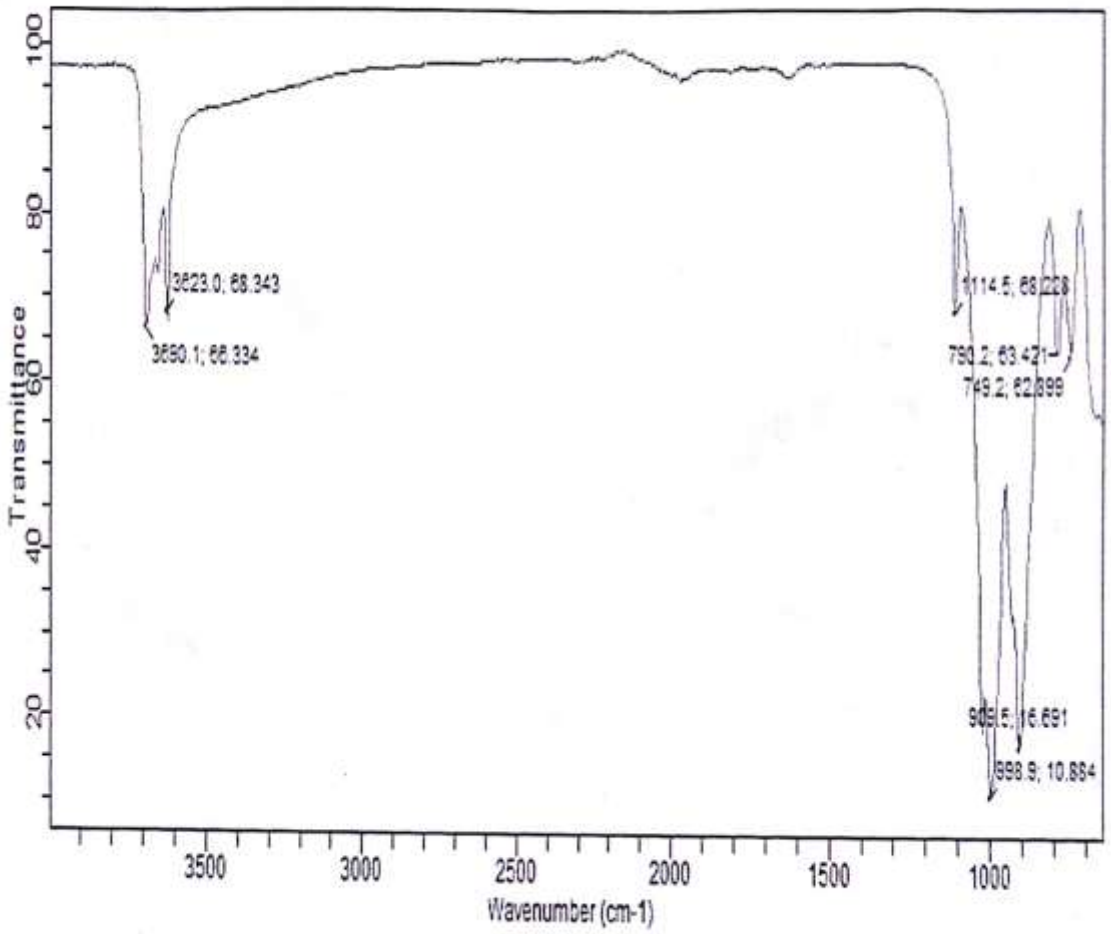

Figure 4.1: FTIR of Kaolin (K)

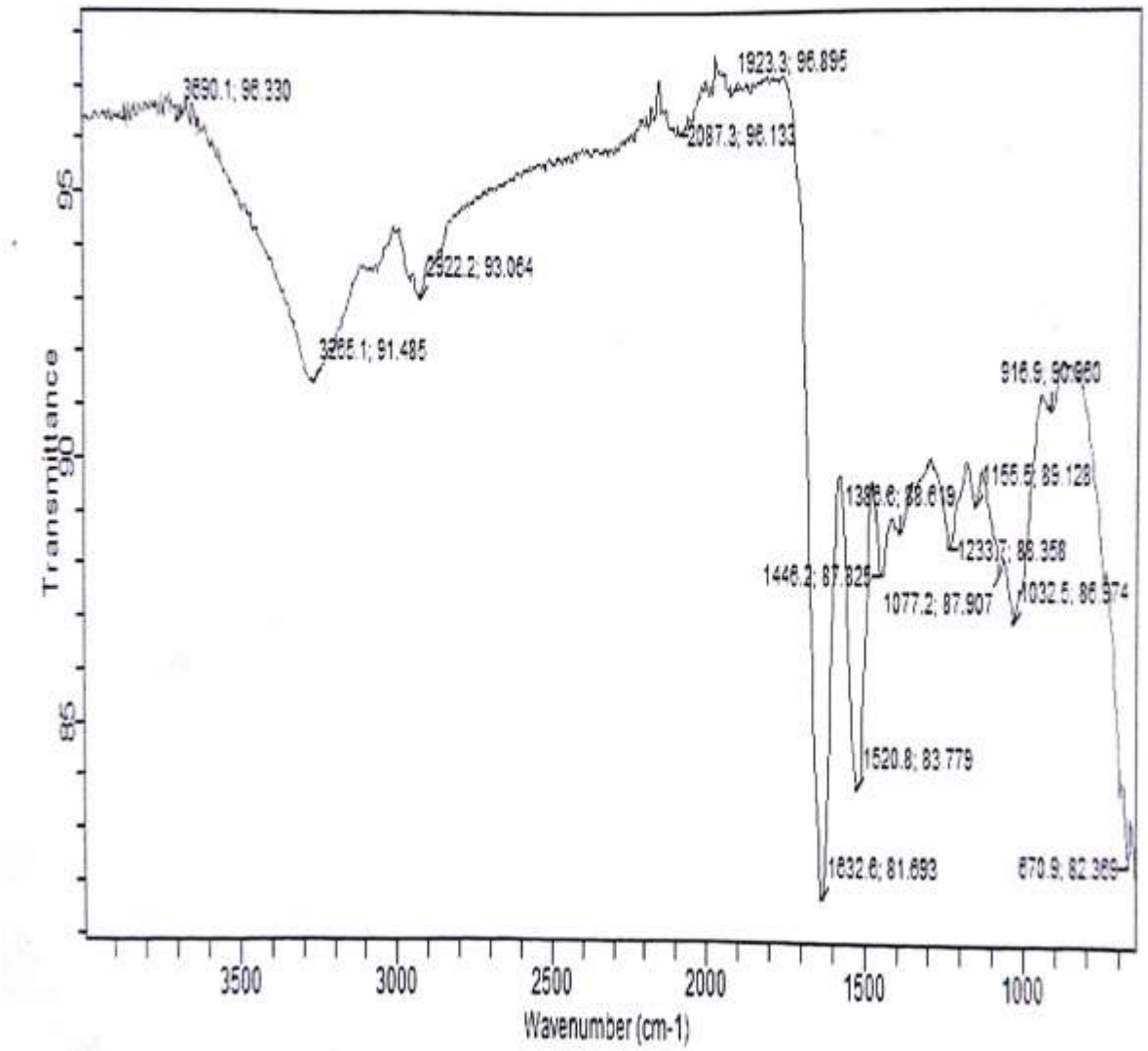

Figure 4.2: FTIR of Chicken Feather (CF)

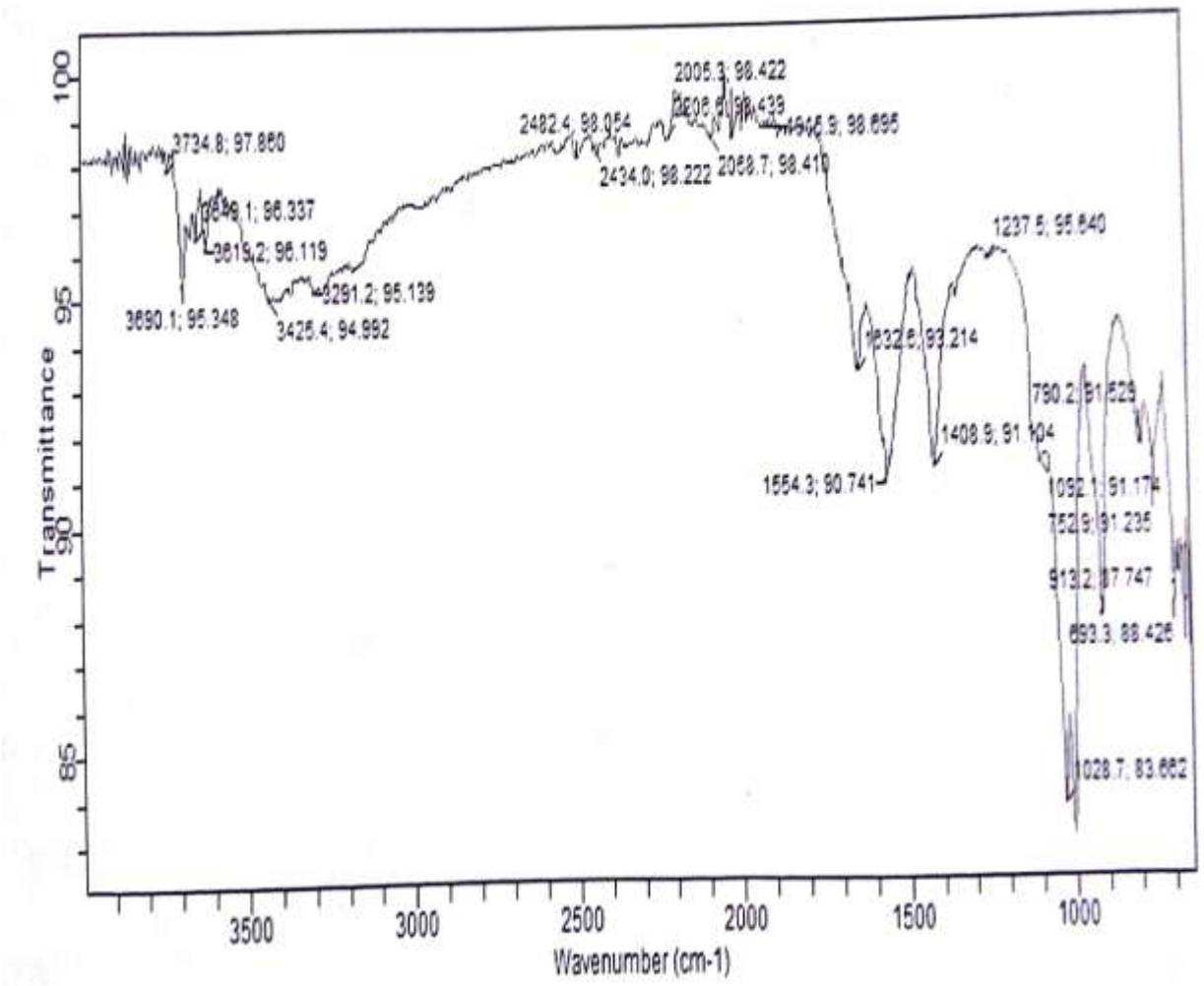

Figure 4.3: FTIR of Chicken Feather-Kaolin Composite (CFK)

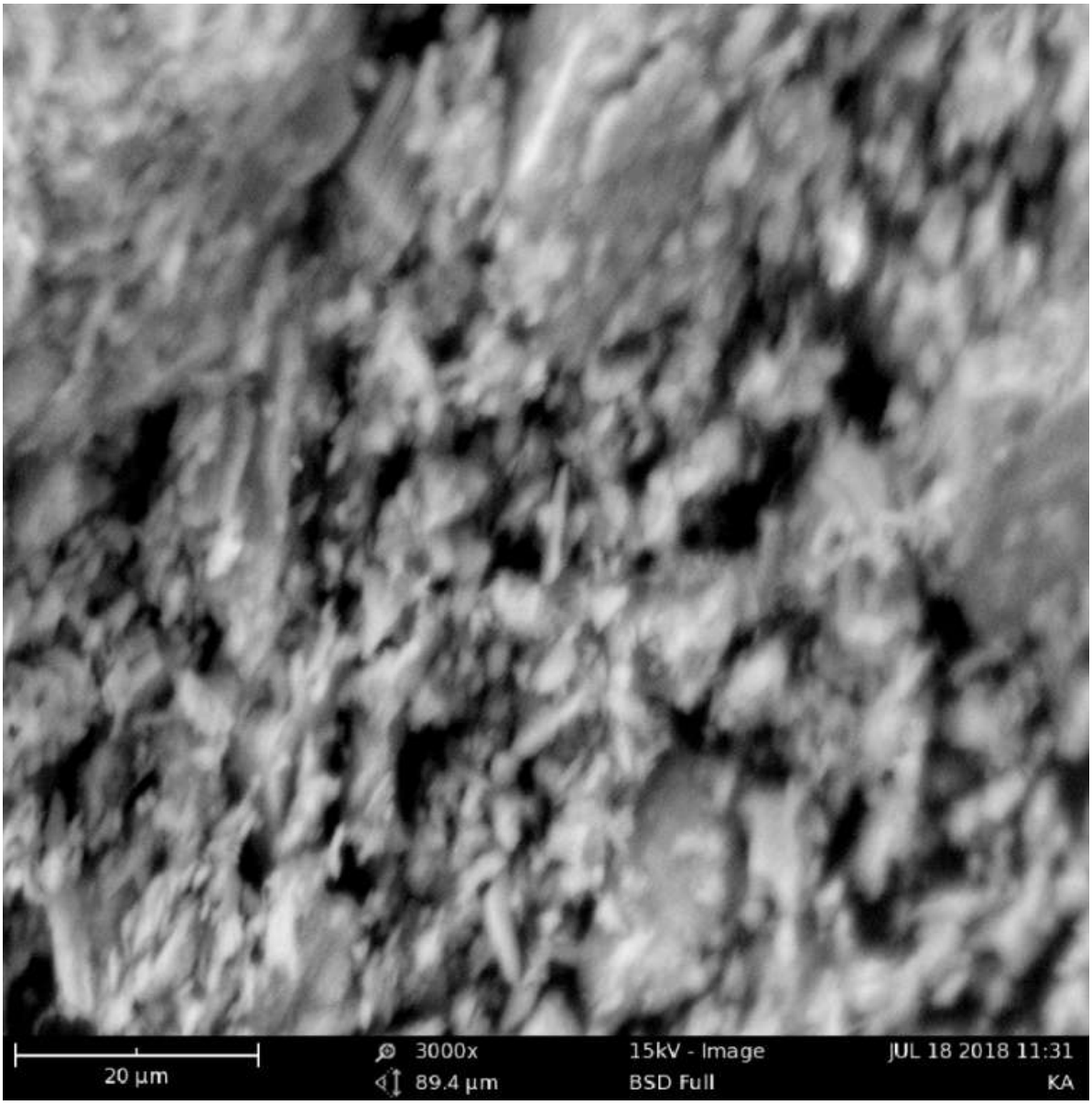

Figure 4.4: SEM Micrograph of Kaolin (K)

Figure 4.5: SEM Micrograph of Chicken Feather (CF)

Figure 4.6 shows the SEM micrograph of chicken feather-kaolin composite (CFK) revealing that the K particles were found attached to the surface of the CF fibre along the barbs and the barbules in the matrix possibly through a certain degree of hydrogen bonding.

Figure 4.7 shows the X-ray diffractogram of kaolin revealing well defined reflections at 2θ value of 12.41◦ corresponding to the d values of 7.13 Å and to the reflections from [001], which are typical characteristic peaks of kaolinite.

Figure 4.8 shows the X-ray diffractogram of chicken feather (CF) showing very broad peaks at 8.49^0, 19.28^0 and 20.59^0 which specifically corresponds to the b-sheet structure.The X-ray diffractogram also revealed amorphous nature of the CF, with peaks at 2θ positions of 17.78^0, 21.14^0, 23.90^0, 28.68^0, 35.31^0, 41.19^0 and 43.69^0 and the corresponding d-spacing of $4.93A^0$, $4.20A^0$, $3.72A^0$, $3.11A^0$, $2.54A^0$, $2.19A^0$ and $2.07A^0$.

Figure 4.9 shows the X-ray diffractogram of chicken feather-kaolin composite (CFK) revealing new peaks at 11.63^0 d-spacing of $7.6A^0$ with 003 reflections and 13.74^0, d-spacing of $6.44A^0$ with 110 reflections and shows that an interaction has occurred between the CF and K. There was no observable change in the intensity and the interplanar spacing of the kaolinite peak at 12.41◦ corresponding to the d values of 7.13 Å, indicating that the CF particles did not pack between the lamella spacing of K, but rather particles of K are attached to the surface of CF particles in the composite.

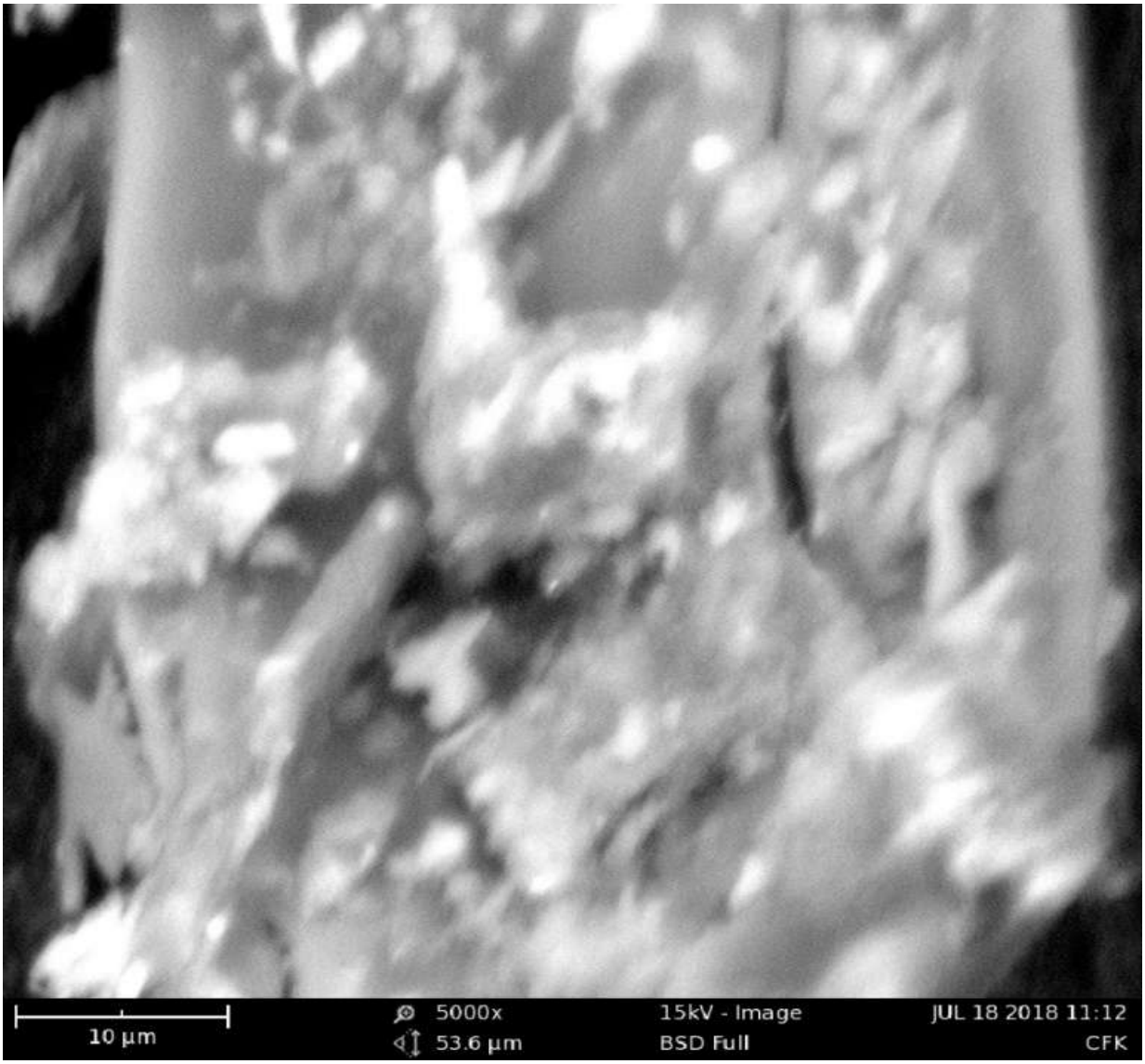

Figure 4.6: SEM Micrograph of Chicken Feather- Kaolin Composite (CFK)

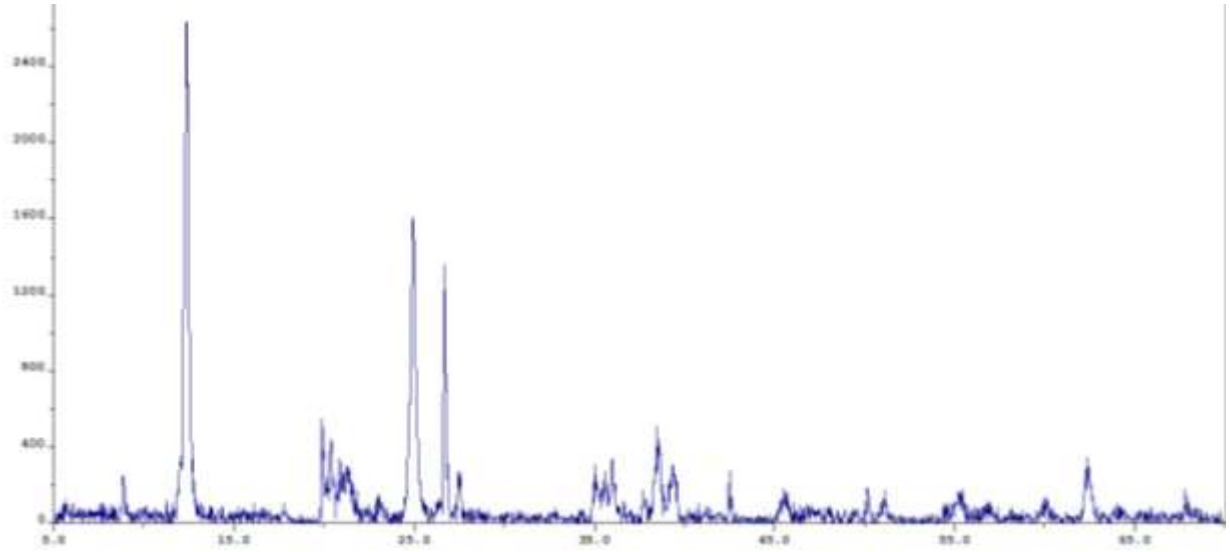

Figure 4.7: X-ray Diffractogram of Kaolin (K)

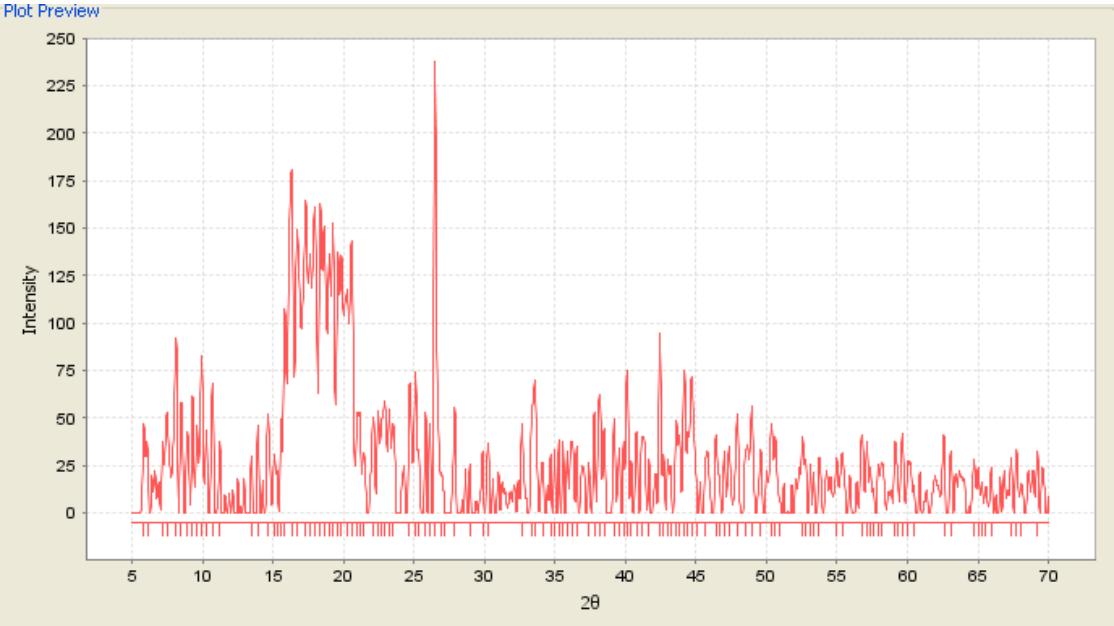

Figure 4.8: X-ray Diffractogram of Chicken Feather (CF)

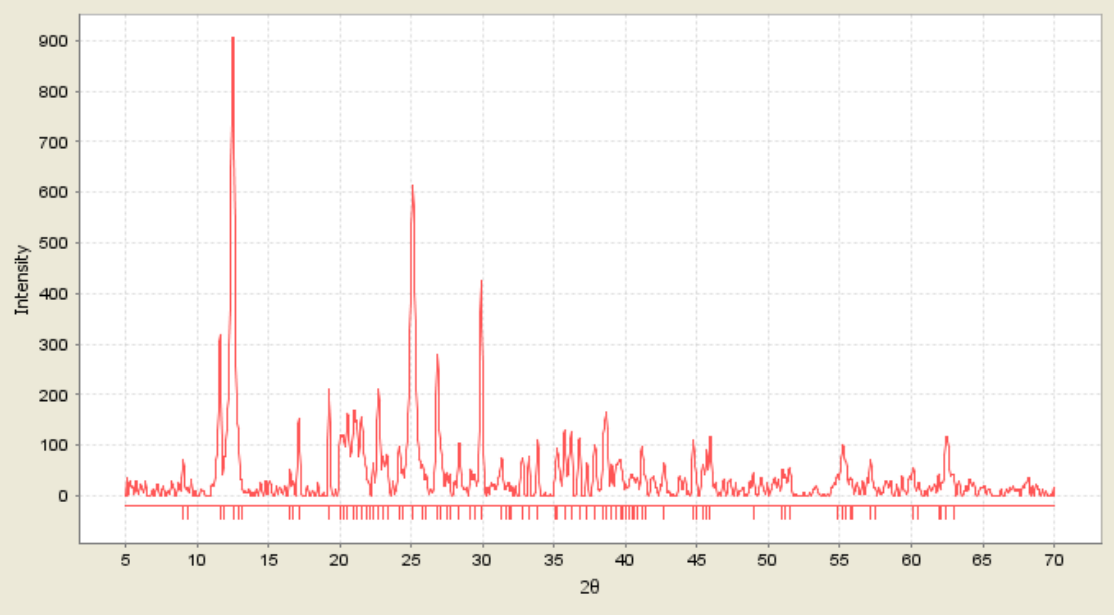

Figure 4.9: X-ray Diffractogram of Chicken Feather-Kaolin Composite (CFK)

4.2 Kinetic, Equilibrium and Thermodynamic Studies of the Adsorption of Selected Heavy Metals onto the CFK Composite

Figures 4.10a-c show the pseudo-first order kinetic model plots for the adsorption of Pb^{2+}, Cu^{2+} and Ni^{2+} onto CFK composite. The results did not give perfect straight lines for any of the three metals indicating that the adsorption of the three metals did not fit into the pseudo-first order kinetic model.

Figures 4.11a-c show the pseudo- second order kinetic model plots for the adsorption of Pb^{2+}, Cu^{2+} and Ni^{2+} onto CFK composite. The results give perfect straight lines passing through the origin for all the three metals indicating that the adsorption of the three metals fit perfectly well into the pseudo-second order kinetic model.

Figures 4.12a-c show the intra- particle diffusion plots for theadsorption of Pb^{2+}, Cu^{2+} and Ni^{2+} onto CFK composite.From the figures, the linear plots for all the three metals did not pass through the origin. This implies that intra-particle diffusion was not the only rate controlling step but other surface phenomena were actively involved and that there were differences in the rate of mass transfer in the initial and final stages in the sorption process.

The Langmuir isotherm plots of (1/qe) against (1/Ce) for the adsorption of Pb^{2+}, $Cu^{2+}$and Ni^{2+}onto CFK composite are shown in Figures 4.13a- 4.13c. Figures 4.13b and 4.13c which are for $Cu^{2+}$and Ni^{2+}indicate better fit to Langmuir model than Figure 4.13a which is for Pb^{2+}, because they give better straight lines and have higher R^2 values of 0.9205 and 0.9089 as against 0.6544 for Pb^{2+}.

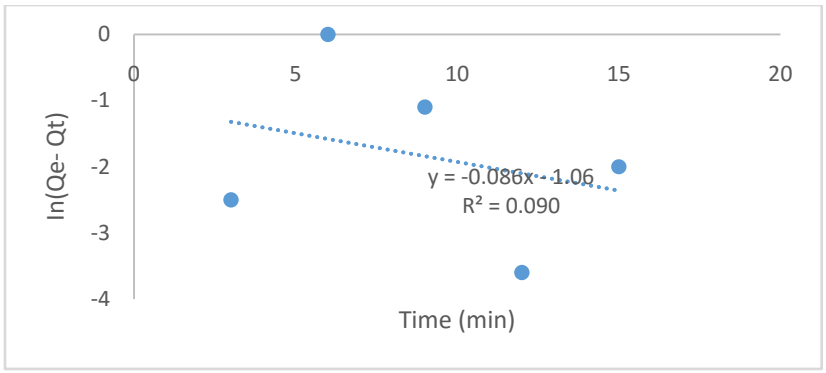

Figure 4.10a: Pseudo-First Order Kinetic Model for the Sorption of Pb^{2+} onto CFK Composite

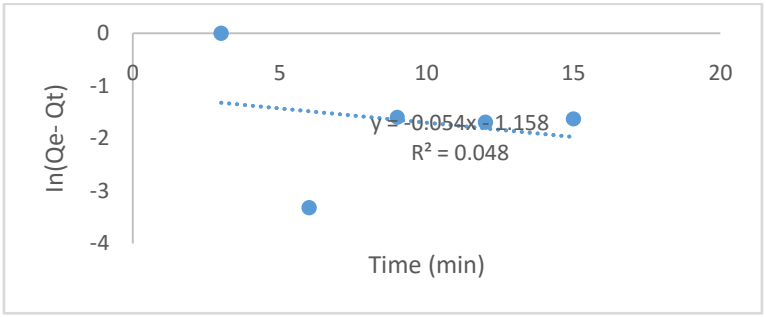

Figure 4.10b: Pseudo-First Order Kinetic Model for the Sorption of Cu^{2+} onto CFK Composite

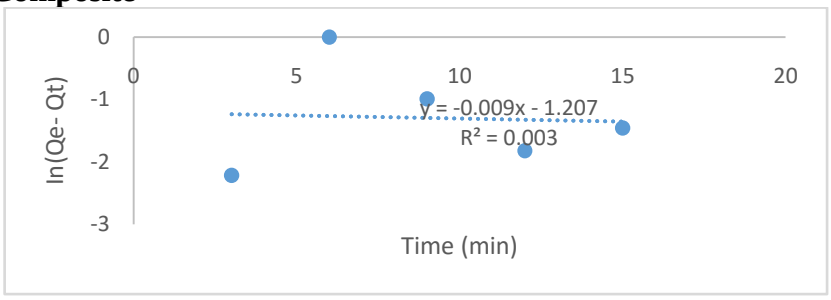

Figure 4.10c: Pseudo-First Order Kinetic Model for the Sorption of Ni^{2+} onto CFK Composite

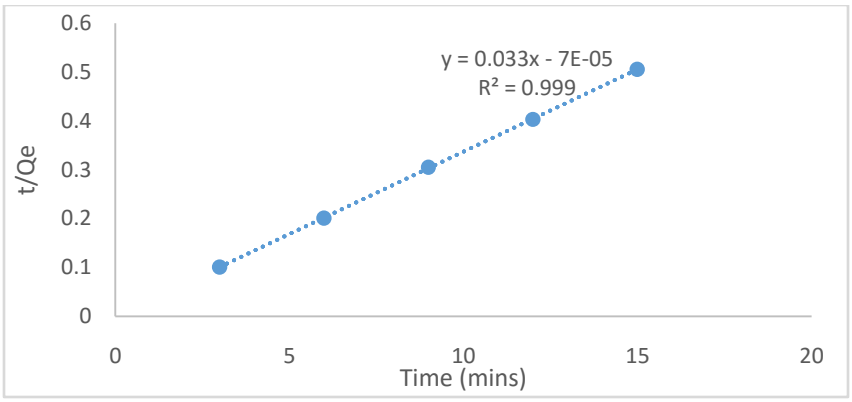

Figure 4.11a: Pseudo-Second Order Kinetic Model for the Sorption of Pb^{2+} onto CFK Composite

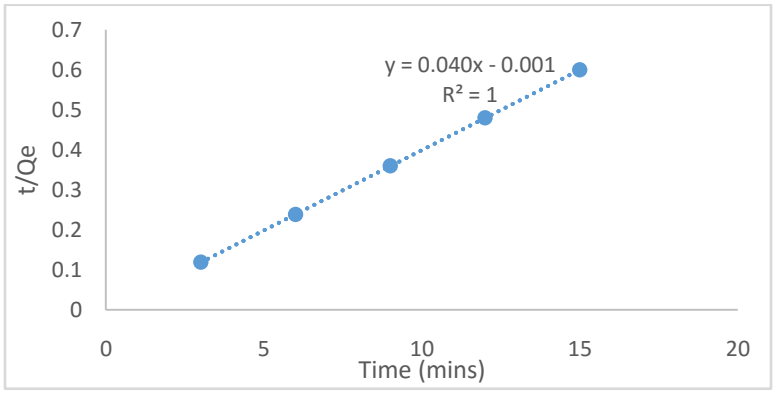

Figure 4.11b: Pseudo-Second Order Kinetic Model for the Sorption of Cu^{2+} onto CFK Composite

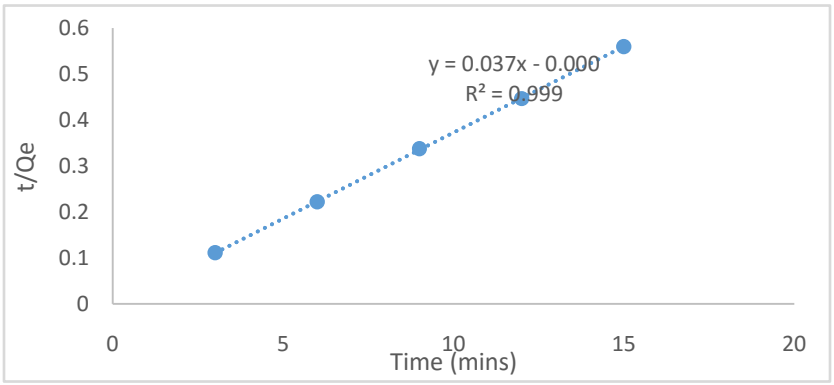

Figure 4.11c: Pseudo-Second Order Kinetic Model for the Sorption of Ni^{2+} onto CFK Composite

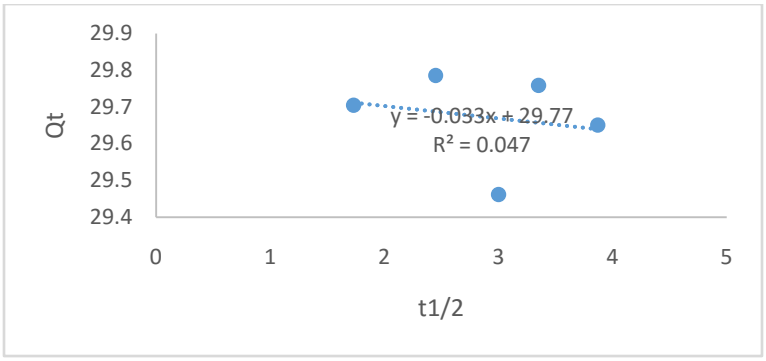

Figure 4.12a: Intra-Particle Diffusion Plot for Sorption of Pb^{2+} onto CFK Composite

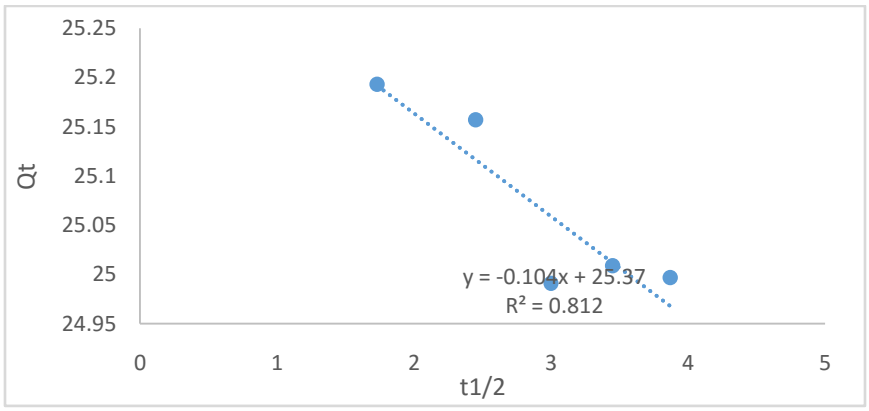

Figure 4.12b: Intra-Particle Diffusion Plot for Sorption of Cu^{2+} onto CFK Composite

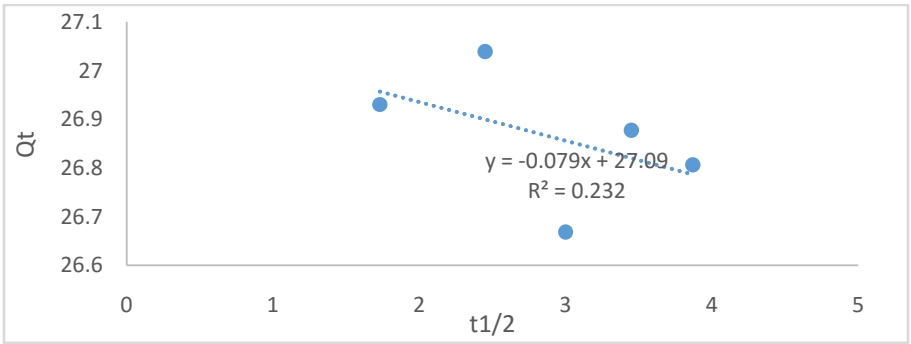

Figure 4.12c: Intra-Particle Diffusion Plot for Sorption of Ni^{2+}onto CFK Composite

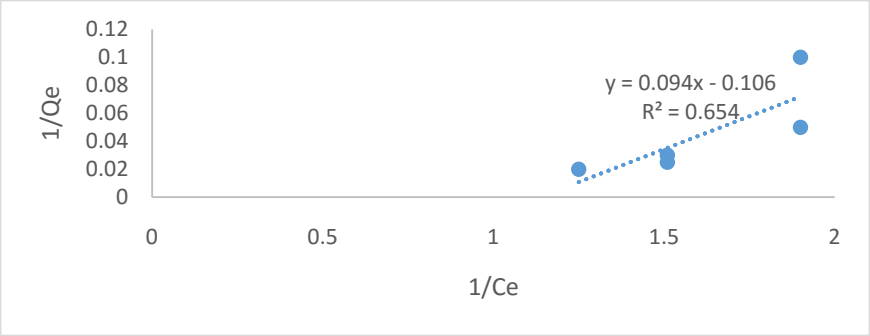

Figure 4.13a: Langmuir Equilibrium Isotherm Plot for the Sorption of Pb^{2+} onto CFK Composite

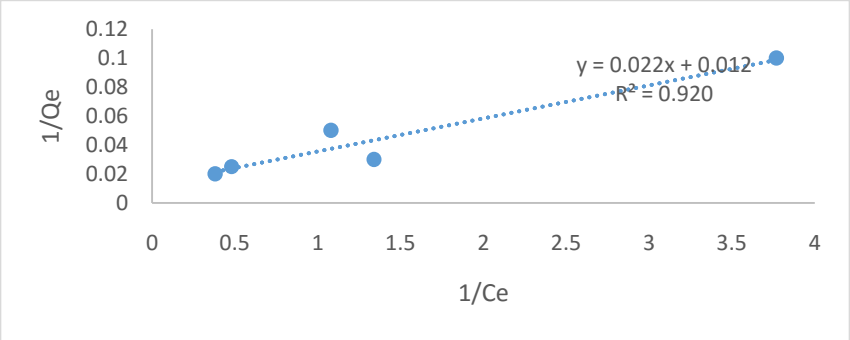

Figure 4.13b: Langmuir Equilibrium Isotherm Plot for the Sorption of Cu^{2+} onto CFK Composite

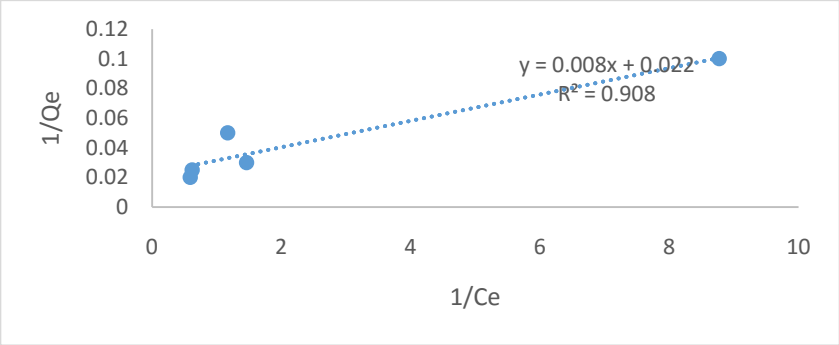

Figure 4.13c: Langmuir Equilibrium Isotherm Plot for the Sorption of Ni^{2+} onto CFK Composite

Figures 4.14a-c show the Freudlich equilibrium isotherm plots for the sorption of Pb^{2+}, Cu^{2+} and Ni^{2+} onto chicken feather-kaolin (CFK) composite. The plots gave a straight line for all the three metals. However, the R^2 value of 0.9212 for Cu^{2+} in Freundlich plot which is slightly higher than 0.9205 in Langmuir shows that the Freundlich model provides better fit for Cu^{2+} adsorption in this work. Also, Pb^{2+} R^2 value of 0.8002 in Freundlich isotherm which is higher than 0.6544 in Langmuir model signifies that Pb^{2+} adsorption follows the Freundlich model. On the other hand, the 0.9089 R^2 value for Ni^{2+} in Langmuir model as against 0.8779 in Freundlich isotherm indicates that the Langmuir model explains Ni^{2+} adsorption better than the Freundlich model in this work.

The plots of the Dubinin-Radushkevich isotherm for Pb^{2+}, $Cu^{2+}$and Ni^{2+} sorption onto CFK composite are shown in Figures 4.15a-4.15c. As indicated in the R^2 values of the metals of 0.9946 for Pb^{2+}, 0.9508 for $Cu^{2+}$and 0.9691 for Ni^{2+}, the Dubinin-Radushkevich model also provides a good fit for the adsorption of the metals.

The thermodynamic plot of ΔG versus temperature for the sorption of Pb^{2+}, Cu^{2+} and Ni^{2+} onto CFK composite (Figures 4.16a-4.16c) are found to be linear indicating good fit. The ΔG values for all three metals at the different temperatures investigated (Table 8) are all negative showing that the adsorption process is feasible and spontaneous. The ΔH values are all positive signifying that the adsorption process for the metals is endothermic.

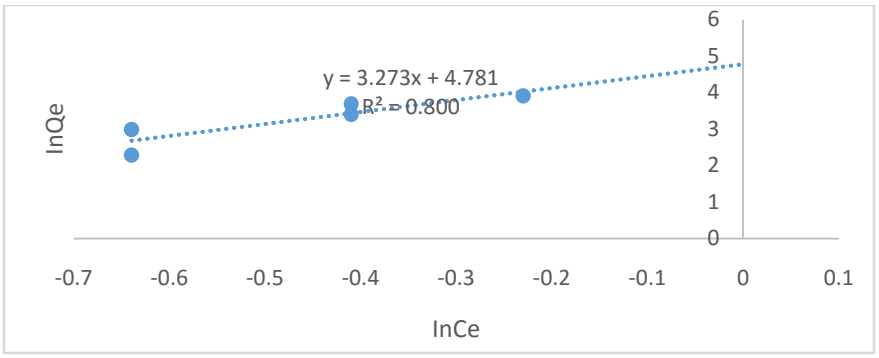

Figure 4.14a: Freundlich Equilibrium Isotherm Plot for the Sorption of Pb^{2+} onto CFK Composite

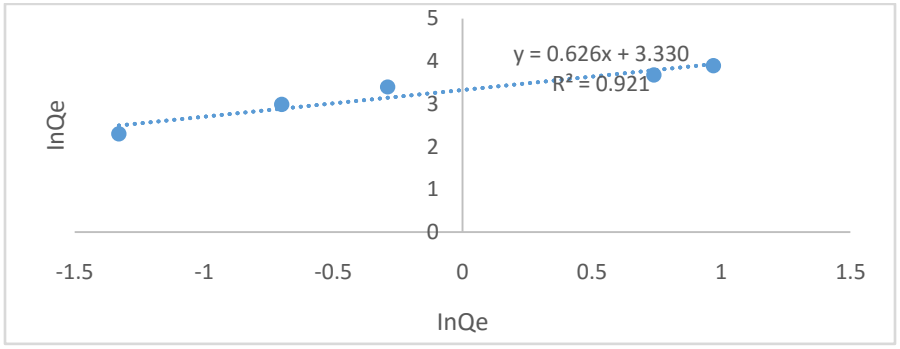

Figure 4.14b: Freundlich Equilibrium Isotherm Plot for the Sorption of Cu^{2+} onto CFK Composite

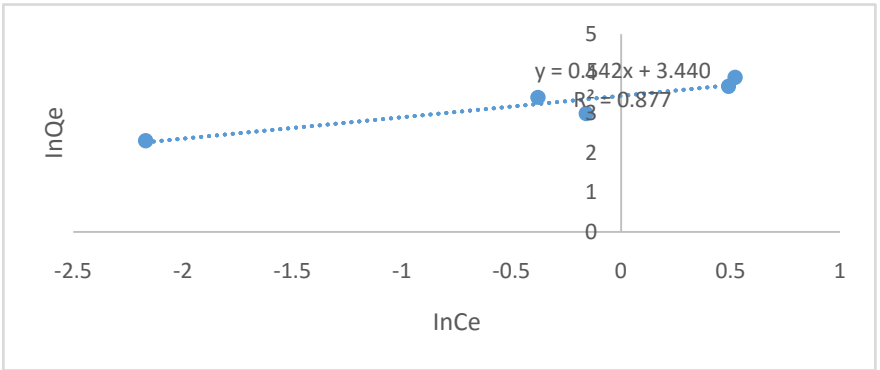

Figure 4.14c: Freundlich Equilibrium Isotherm Plot for the Sorption of Ni^{2+} onto CFK Composite

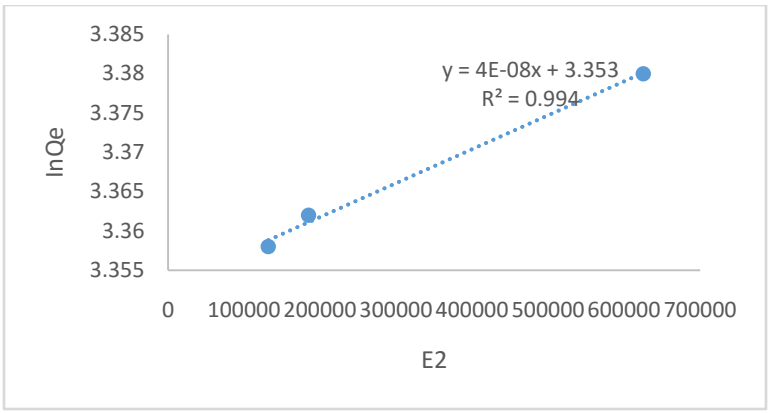

Figure 4.15a: Dubinin-Radushkevich Isotherm Plot for Pb^{2+} Sorption onto CFK Composite

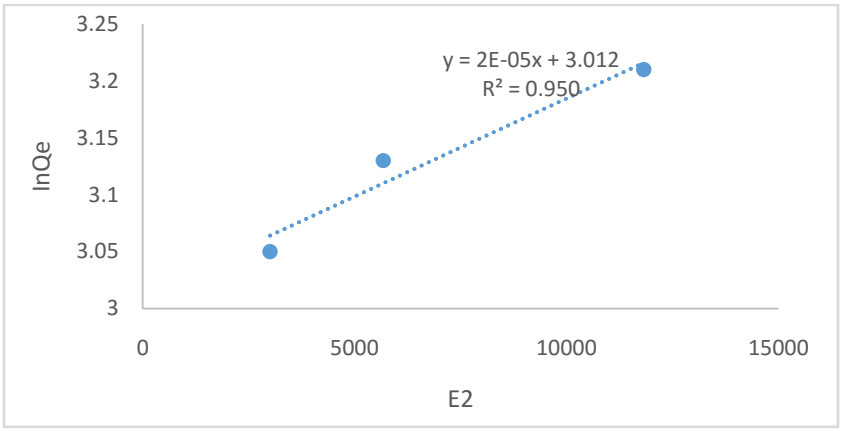

Figure 4.15b: Dubinin-Radushkevich Isotherm Plot for Cu^{2+} Sorption onto CFK Composite

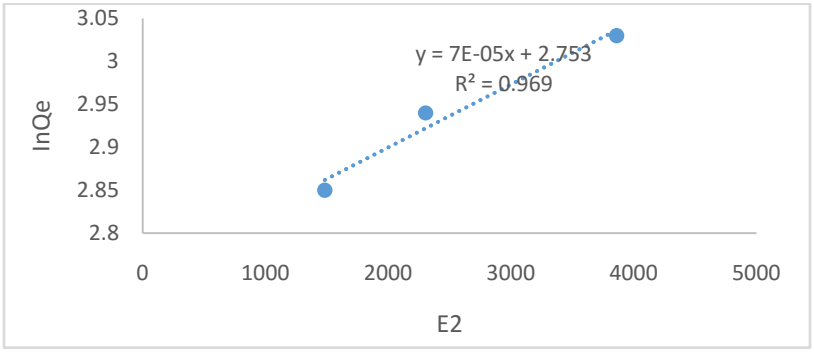

Figure 4.15c: Dubinin-Radushkevich Isotherm Plot for Ni^{2+} Sorption onto CFK Composite

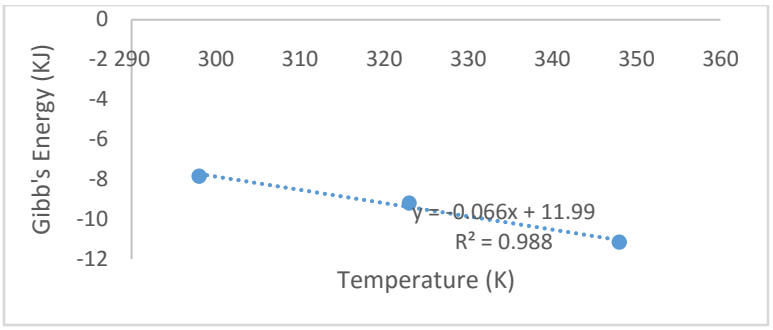

Figure 4.16a: Thermodynamic Plot for Sorption of Pb^{2+} onto CFK Composite

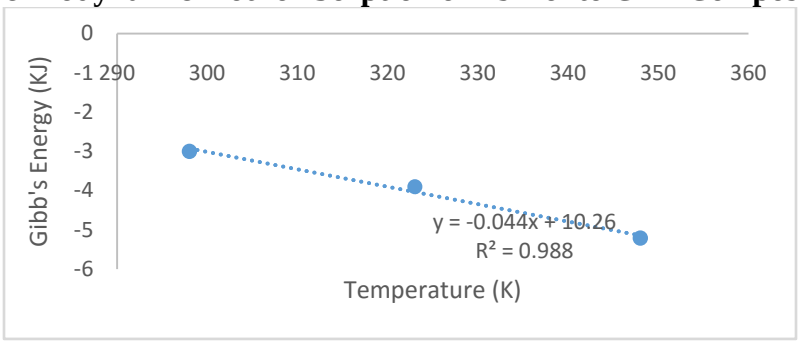

Figure 4.16b: Thermodynamic Plot for Sorption of Cu^{2+} onto CFK Composite

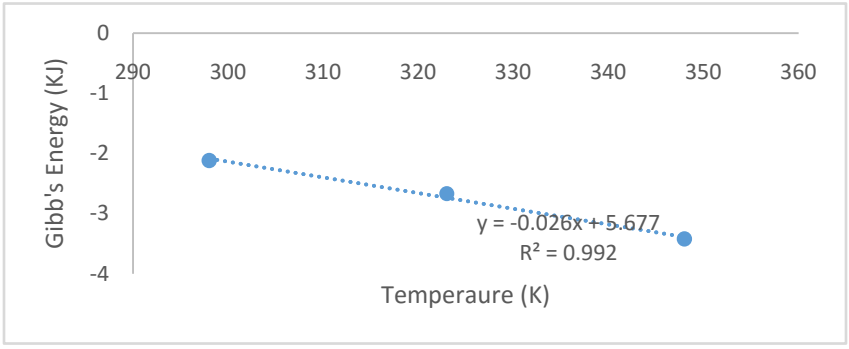

Figure 4.16c: Thermodynamic Plot for Sorption of Ni^{2+} onto CFK Composite

Table 4.1 shows BET results for CF, K and CFK composite. It reveals that CF with a value of 711.9 has the highest surface area, followed by CFK with 424.8 and then K with a surface Area of 352.5.

Likewise, Table 4.2a shows the result of the pseudo-first order parameters for Pb^{2+}, Cu^{2+} and Ni^{2+}sorption with R^2 values of 0.0902, 0.0483 and 0.0030 respectively. The R^2 values for all three metals are far from unity, indicating the pseudo-first order model could not explain the mechanism of adsorption of the metals.

But Table 4.2b which shows the result of the pseudo-second order parameters for Pb^{2+}, Cu^{2+} and Ni^{2+}sorption reveals very high R^2values of 0.9999, 1 and 0.9999 respectively for all the metals, signifying the pseudo-second order model is the appropriate mechanism for the sorption of the three metals onto CFK composite.

Also, Table 4.3 shows the result of intra-particle diffusion isotherm parameters for Pb^{2+}, Cu^{2+} and Ni^{2+}sorption. The low intra-particle diffusion constants (K_d) values of -0.0398, -0.1045and -0.0795 respectively for the metals indicates that intra-particle diffusion is not the only rate determining step but that other surface phenomena such as external mass transfer or boundary surface diffusion are involved.

Furthermore, Table 4.4 shows the result of the Langmuir isotherm parameters for Pb^{2+}, $Cu^{2+}$and Ni^{2+}sorption. The table indicates very good fit for Cu^{2+} and Ni^{2+} but poor fit for Pb^{2+} sorption base on their R^2 values of 0.6544 for Pb^{2+}, 0.9205 for Cu^{2+} and 0.9089 for Ni^{2+}.

Table 4.1: BET Results for Kaolin (K), Chicken Feather (CF) and Chicken Feather-Kaolin Composite (CFK)

Samples	BET surface Area (m^2/g)	Pore Volume(cc/g)	Pore Size (nm)
K	352.5	14.75	5.749
CFK	424.8	16.36	6.243
CF	711.9	25.40	6.503

Table 4.2a: Pseudo-First Order Parameters for Pb^{2+}, Cu^{2+} and Ni^{2+}Sorption onto CFK Composite

Heavy Metal Ions	Q_{exp} (mg/g)	Q_{cal} (mg/g)	K_1(g/mg.min)	R^2
Pb^{2+}	29.4622	0.346	0.0867	0.0902
Cu^{2+}	24.9906	0.314	0.0544	0.0483
Ni^{2+}	26.6676	0.299	0.0099	0.003

Table 4.2b: Pseudo-Second Order Parameters for Pb^{2+}, Cu^{2+} and Ni^{2+}Sorption onto CFK Composite

Heavy Metal Ions	Q_{exp} (mg/g)	Q_{cal} (mg/g)	K_2 (g/mg.min)	h (mg/g.min)	R^2
Pb^{2+}	29.46	29.67	-16.224	14080.67	0.9999
Cu^{2+}	24.99	24.94	-1.072	669.46	1
Ni^{2+}	26.67	26.74	-1.554	1105.34	0.9999

Table 4.3: Intra-Particle Diffusion Isotherm Parameters for the Sorption of Pb^{2+}, Cu^{2+} and Ni^{2+} onto CFK Composite

Heavy Metal Ions	I	$K_{d\ (mg/g.min)}$	R^2
Pb^{2+}	29.77	-0.0398	0.047
Cu^{2+}	25.373	-0.1045	0.8128
Ni^{2+}	27.095	-0.0795	0.2323

Table 4.4: Langmuir Isotherm Parameters for Pb^{2+}, $Cu^{2+}$and Ni^{2+}Sorption onto CFK Composite

Metal ions	Q_{max}(mg/g)	K_l(l/g)	R^2
Pb^{2+}	-9.35	-1.14	0.6544
Cu^{2+}	78.13	0.56	0.9205
Ni^{2+}	44.25	2.54	0.9089

The result of Langmuir isotherm separation factor (SF) for adsorption of Pb^{2+}, Cu^{2+} and Ni^{2+}onto CFK composite is depicted in Table 4.5. The lower the SF value, the easier the interaction between the adsorbent and the adsorbate. The SF values of -0.02, 0.034 and 0.008 respectively for all three metals are low indicating the adsorbent and the metals interacted well.

Additionally, Table 4.6 shows the result of Freundlich isotherm parameters for sorption of Pb^{2+}, Cu^{2+} and Ni^{2+}. The R^2 values of 0.8002,0.9212 and 0.8779respectively for the metals are closed to unity implying that the Freundlich isotherm explains well the adsorption of all the three metals onto the CFK composite.

Additionally, Table 4.7 shows the result of Dubinin-Radushkevich (D-R) isotherm parameters. The result indicates the sorption process is well explained by the D-R model andgiving its high R^2 values of 0.9946 for Pb^{2+}, 0.9508 for Cu^{2+} and 0.9691 for Ni^{2+}.

4.3 Thermodynamics of the Adsorption of Selected Heavy Metals onto the CFK Composite

Table 4.8 depicts the result of the thermodynamic ΔG values for Pb^{2+}, Cu^{2+} and Ni^{2+}. The negative values of ΔG for all the metals indicates a spontaneous process.

Also, Table 4.9 shows the result of the thermodynamic entropy and enthalpy values Pb^{2+}, Cu^{2+} and Ni^{2+}. The positive ΔH values shows the process is endothermic while the positive ΔS values indicates an increase in entropy during the adsorption process.

Table 4.10 shows the result of the comparison of the adsorption of Pb^{2+}, Cu^{2+} and Ni^{2+} onto CFK. at an initial concentration of 100 ppm, temperature of 75^{o}c and time of 10min for single and multi- component system.

Table 4.5: Langmuir Isotherm Separation Factor (SF) for of Pb^{2+}, Cu^{2+} and Ni^{2+}Sorption onto CFK Composite

Metal ion	Low initial concentration (50 ppm)	High initial Concentration (250 ppm)
Pb^{2+}	-0.02	-0.004
Cu^{2+}	0.034	0.007
Ni^{2+}	0.008	0.002

Table 4.6:Freundlich Isotherm Parameters for Sorption of Pb^{2+}, Cu^{2+} and Ni^{2+} onto CFK Composite

Metal ions	1/n	K_f(l/g)	R^2
Pb^{2+}	0.47	115.58	0.8002
Cu^{2+}	0.1	42.52	0.9212
Ni^{2+}	0.04	32.79	0.8779

Table 4.7: Dubinin-Radushkevich (D-R) Isotherm Parameters for Pb^{2+}, Cu^{2+} and Ni^{2+} Sorption onto CFK Composite

Metal Ions	$Q_{DR(mmol/g)}$	B (mol^2/kJ^2)	E (kJ/mol)	R^2
Pb^{2+}	28.591	$4X\ 10^{-8}$	3.536	0.9946
Cu^{2+}	20.332	$2X\ 10^{-5}$	0.158	0.9508
Ni^{2+}	15.691	$7x\ 10^{-5}$	0.085	0.9691

Table 4.8: Thermodynamic ΔG values for Pb^{2+}, Cu^{2+} and Ni^{2+} Sorption onto CFK Composite

Temperature (K)	ΔG for Pb^{2+} (kJ/mol)	ΔG for Cu^{2+} (kJ/mol)	ΔG for Ni^{2+} (kJ/mol)
298	-7.730	-2.117	-0.743
323	-9.099	-3.182	-1.425
348	-11.086	-4.685	-2.359

Table 4.9: Thermodynamic Entropy and Enthalpy values Pb^{2+}, Cu^{2+} and Ni^{2+} Sorption onto CFK Composite

Metal Ions	ΔH (kJ/mol)	ΔS (kJ/mol)
Pb^{2+}	11.995	0.0662
Cu^{2+}	10.261	0.0443
Ni^{2+}	5.6778	0.026

Table 4.10: Comparison of the Sorption of Pb^{2+}, Cu^{2+} and Ni^{2+} onto CFK Composite for Single and Multi-Component System

Heavy Metal Ions	Percentage (%) Sorption (single system)	Percentage (%) Sorption (Multi-component system)
Pb^{2+}	99.88	98.86
Cu^{2+}	99.78	83.61
Ni^{2+}	86.43	68.49

4.4 Optimization of the Adsorption Process and Statistical Analysis

Table 4.11 presents the result of the comparison of the adsorption of Pb^{2+}, Cu^{2+} and Ni^{2+} onto chicken feather-kaolin composite (CFK), kaolin (K) and chicken feather (CF) at an initial concentration of 100 ppm, temperature of 75^{o}c and time of 10min for multi-component system.

Likewise, Table 4.12 shows the result of the analysis of variance (ANOVA) of response surface quadratic model for Pb^{2+} sorption. It indicates that the model is significant with F-value of 74.5.

Also, Table 4.13 shows the result of the quadratic model statistical values for Pb^{2+} sorption. The R^2 value of 0.9037 indicates a good model fit.

Table 4.14 shows the result of the coefficient estimates and parameter interactions of the empirical model for Pb^{2+} sorption. The concentration coefficient of -1.21 is the highest and shows that it has the highest impact on sorption more than temperature and time.

Likewise, Table 4.15 presents the result of the analysis of variance (ANOVA) for response surface quadratic model for Cu^{2+} sorption. The table shows that the model is significant with high F-value of 360.95.

Futhermore, Table 4.16 shows the result of the quadratic model statistical values for $Cu^{2+.}$ With R^2 value of 0.9786, it can be inferred that the model is fit for Cu^{2+} sorption.

Also, Table 4.17 shows the result of the coefficient estimates and parameter interactions of the empirical models for Cu^{2+} sorption. The concentration coefficient of -12.01 was the highest and as such has higher negative influence on Cu^{2+} sorption than temperature and time.

Table 4.11: Comparison of the Sorption of Pb^{2+}, Cu^{2+} and Ni^{2+} onto Chicken Feather-Kaolin Composite, Kaolin and Chicken Feather for Multi-Component System

Metal Ions	Sorption of CFK (%)	Sorption of K (%)	Sorption of CF (%)
Pb^{2+}	98.86	69.90	80.35
Cu^{2+}	83.61	73.48	75.00
Ni^{2+}	68.49	65.46	67.39

Table 4.12: Analysis of Variance (ANOVA) for Response Surface QuadraticModelfor Pb^{2+}Sorption onto CFK Composite

Source	Sum of Squares	Degree of Freedom(df)	Mean Square	F- Value	P- Value Prob > **F**	Inference
Model	183.05	9	20.34	74.5	<0.0001	Significant
A-Concentration	79.40	1	79.40	289.06	<0.0001	
B-temperature	7.25	1	7.25	26.40	<0.0001	
C-time	11.45	1	11.45	41.70	<0.0001	
AB	13.40	1	13.40	48.77	<0.0001	
AC	0.34	1	0.34	1.24	0.2695	Not Significant
BC	51.29	1	51.29	186.72	<0.0001	
A^2	3.63	1	3.63	13.23	0.0005	
B^2	8.37	1	8.37	30.48	<0.0001	
C^2	7.92	1	7.92	28.82	<0.0001	

Table 4.13:Quadratic Model Statistical Values for Pb^{2+}Sorption onto CFK Composite

Std. Dev	0.52
Mean	95.79
R-Square	0.9037
Adj. R-Square	0.8915
Pred. R-Square	0.8758
C. V %	0.55
Press	25.17
Adeq Precision	37.760

Table 4.14: Coefficient Estimates and Parameter Interactions of the EmpiricalModels for Pb^{2+} Sorption onto CFK Composite

Factor	Coefficient Estimate	Degree of Freedom(df)	Standard Error	95%Cl Low	95% Cl High	VIF
Intercept	96.98	1	0.15	96.68	97.29	
A-Concentration	-1.21	1	0.071	1.357	1.00	
B-temperature	-0.37	1	0.071	0.51	0.22	1.00
C-time	-0.46	1	0.071	-0.60	0.32	1.00
AB	-0.61	1	0.087	-0.78	-0.44	1.00
AC	-0.091	1	0.087	-0.27	0.077	1.00
BC	-1.19	1	0.087	-1.37	-0.02	1.00
A^2	-0.45	1	0.12	-0.70	-0.20	1.00
B^2	-0.68	1	0.12	-0.93	-0.44	1.00
C^2	-0.66	1	0.12	-0.91	-0.42	1.00

Table 4.15: Analysis of Variance (ANOVA) for Response Surface Quadratic Modelfor Cu^{2+} Sorption onto CFK Composite

Source	Sum of Squares	Degree of Freedom(df)	Mean Square	F- Value	P- Value Prob > **F**	Inference
Model	9701.41	9	1077	360.95	<0.0001	Significant
A-Concentration	7788.24	1	7788.24	2607.91	<0.0001	
B-temperature	85.88	1	85.88	28.76	<0.0001	
C-time	2.60	1	2.60	0.87	<0.3535	Not Significant
AB	22.72	1	22.72	7.61	<0.0074	
AC	0.98	1	0.98	0.33	0.5692	Not Significant
BC	17.77	1	17.77	5.95	<0.0172	
A^2	1776.81	1	1776.81	594.97	0.0001	
B^2	1.44	1	1.44	0.48	<0.4895	Not Significant
C^2	4.96	1	4.96	1.66	<0.2015	Not Significant

Table 4.16: Quadratic Model Statistical Values for Cu^{2+} Sorption onto CFK Composite

Std. Dev	1.73
Mean	67.20
R-Square	0.9786
Adj. R-Square	0.9759
Pred. R-Square	0.9730
C. V %	2.57
Press	25.17
Adeq Precision	37.760

Table 4.17:Coefficient Estimates and Parameter Interactions of the EmpiricalModelsfor Cu^{2+} Sorptiononto CFK Composite

Factor	Coefficient Estimate	Degree of Freedom(df)	Standard Error	95%Cl Low	95% Cl High	VIF
Model	73.28	1	0.51	72.27	74.30	
A-Concentration	-12.01	1	0.24	-12.48	-11.54	1.00
B-temperature	1.26	1	0.24	0.79	1.73	1.00
C-time	-0.22	1	0.24	-0.69	0.25	1.00
AB	0.79	1	0.29	0.22	1.37	1.00
AC	0.16	1	0.29	-0.41	0.74	1.00
BC	0.70	1	0.29	0.13	1.28	1.00
A^2	-9.94	1	0.41	-10.75	-9.12	1.00
B^2	0.28	1	0.41	-0.53	1.10	1.00
C^2	0.53	1	0.41	-0.29	1.34	1.00

Moreso, Table 4.18 shows the result of the analysis of variance (ANOVA) for response surface quadratic model for Ni^{2+} sorption with F-value of 234.23 implying a good model fit.

The quadratic model statistical values for Ni^{2+} sorption is shown in Table 4.19. The table shows an R^2 value of 0.96 indicating a good model fit.

Also, Table 4.20 depicts the result of the coefficient estimates and parameter interactions of the empirical models for Ni^{2+} sorption. Again, the concentration term of -9.70 has the highest negative effect on Ni^{2+} sorption.

Table 4.21 shows the result of the predicted and actual values for Pb^{2+}, Cu^{2+} and Ni^{2+} sorption and reflects a good agreement between the two as their values are close to each other.

Table 4.18: Analysis of Variance (ANOVA) for Response Surface Quadratic Model for Ni^{2+} Sorption onto CFK Composite

Source	Sum of Squares	Degree of Freedom(df)	Mean Square	F- Value	P- Value Prob > **F**	Inference
Model	6300.23	9	700.03	234.23	<0.0001	Significant
A-Concentration	5083.19	1	5083.19	1700	<0.0001	
B-temperature	206.31	1	206.31	69.03	<0.0001	
C-time	6.98	1	6.98	2.33	<0.1310	Not Significant
AB	15.85	1	15.85	5.30	<0.0242	
AC	0.092	1	0.092	0.031	0.8612	Not Significant
BC	174.11	1	174.11	58.26	<0.0001	
A^2	793.97	1	793.97	265.66	0.0001	
B^2	4.69	1	4.69	1.57	<0.2147	Not Significant
C^2	15.05	1	15.05	5.03	<0.0280	

Table 4.19: Quadratic Model Statistical Values for Ni^{2+} Sorption onto CFK Composite

Std. Dev	01.73
Mean	57.61
R-Square	0.96
Adj. R-Square	0.9633
Pred. R-Square	0.9576
C. V %	3.00
Press	275.91
Adeq Precision	45.788

Table 4.20: Coefficient Estimates and Parameter Interactions of the Empirical Models for Ni^{2+} Sorption onto CFK Composite

Factor	Coefficient Estimate	Degree of Freedom(df)	Standard Error	95%Cl Low	95% Cl High	VIF
Model	62.31	1	0.51	61.30	63.32	
A-Concentration	-9.70	1	0.24	-10.17	-9.23	1.00
B-temperature	1.95	1	0.24	1.49	2.42	1.00
C-time	0.36	1	0.24	-0.11	0.83	1.00
AB	-0.66	1	0.29	-1.24	-0.089	1.00
AC	0.051	1	0.29	-0.52	0.63	1.00
BC	-2.20	1	0.29	-2.77	-1.62	1.00
A^2	-6.64	1	0.41	-7.45	-5.83	1.00
B^2	0.51	1	0.41	-0.30	1.32	1.00
C^2	-0.91	1	0.41	-1.73	-0.10	1.00

Table 4.21: Predicted and Actual Values for Pb^{2+}, Cu^{2+} and Ni^{2+} Sorption onto CFK Composite

S/N	Concentration (ppm)	Temperature (^oC)	Time (mins)	Pb Actual (%)	Pb Pred. (%)	Cu Actual (%)	Cu Pred. (%)	Ni Actual (%)	Ni Pred. (%)
1	200.00	75.00	60.00	90.70	91.23	56.73	54.85	45.58	45.06
2	100.00	50.00	60.00	97.39	96.72	76.58	75.50	67.13	64.76
3	100.00	25.00	60.00	96.11	96.99	75.35	74.62	65.67	64.86
4	200.00	25.00	60.00	95.73	95.59	49.26	49.33	46.69	46.88
5	150.00	25.00	60.00	97.11	96.74	72.29	71.91	61.66	62.51
6	150.00	50.00	10.00	95.49	96.78	76.57	75.81	60.46	61.04
7	100.00	50.00	35.00	97.70	97.75	76.64	75.36	63.02	65.37
8	200.00	25.00	35.00	95.8	93.62	50.56	49.44	44.37	45.18
9	200.00	75.00	10.00	94.77	94.75	52.18	53.56	46.85	48.64
10	100.00	75.00	35.00	97.33	97.32	74.51	76.12	67.87	68.50
11	100.00	75.00	10.00	97.86	98.20	75.21	76.31	67.86	69.47
12	100.00	50.00	10.00	97.26	97.45	76.61	76.27	67.66	64.15
13	100.00	75.00	60.00	95.06	95.12	76.65	76.95	64.98	65.69

14	200.00	75.00	35.00	93.92	97.32	52.28	53.55	48.16	47.77
15	200.00	25.00	10.00	93.99	94.32	52.11	50.85	44.16	41.66
16	150.00	50.00	60.00	96.33	95.87	68.66	68.82	60.29	61.75
17	150.00	25.00	35.00	95.88	96.67	70.45	72.31	60.98	60.86
18	100.00	25.00	10.00	95.92	95.33	75.05	76.79	57.62	59.84
19	150.00	75.00	10.00	97.88	96.93	76.99	75.65	67.95	65.70
20	150.00	50.00	35.00	97.14	96.98	74.08	73.28	61.43	62.31
21	100.00	25.00	35.00	97.09	96.82	76.45	75.17	64.10	63.26
22	150.00	25.00	10.00	95.77	95.27	72.76	74.53	57.46	57.39
23	150.00	75.00	60.00	93.60	93.62	75.57	75.84	60.51	62.02
24	150.00	75.00	35.00	95.66	95.93	76.68	74.83	67.88	64.77
25	200.00	50.00	60.00	93.99	94.10	52.84	51.81	46.07	45.46
26	200.00	50.00	35.00	95.54	95.32	49.98	51.21	46.44	45.97
27	200.00	50.00	10.00	95.38	95.22	50.72	51.92	42.67	44.64

CHAPTER FIVE

5.0 DISCUSSIONS

5.1 Characterization of the Adsorbents Using Fourier Transform Infra-Red (FTIR) Analysis.

5.1.1 FTIR analysis of kaolin (K)

Figure 4.1 shows the FTIR spectra of kaolin. The spectraindicate a number of absorption peaks showing the nature of Kaolin. The spectra analysis was run in between650-4000 cm^{-1} region. In the 3,500-4000 cm^{-1} frequency range, kaolin shows bands at 3,690.1 cm^{-1} and 3,623.0 cm^{-1} due to stretching vibrations of hydroxyl groups. This is similar to the bands at 3,690.1 and 3,623.0 cm^{-1} obtained by Salwa *et al*.(2015) for kaolin. The band at 3690 cm^{-1} is attributed to the hydroxyl group sitting at the edges of the kaolin platelets and corresponds to the hydroxyl group at the surface of the alumina octahedral layers that interact with the oxygen or nitrogen atoms of other incoming species.

The band at 3623 cm^{-1} is connected with the internal hydroxyl groups. Asymmetric Si-O-Si stretching vibration isresponsible for the band at 1114 cm^{-1}, the band at 998 cm^{-1} is attributed to the bending Al-OH vibration (hydroxyl groups sitting on the alumina faces), whereas the Al–OH bond vibrations is visibly characterized by the band appearing at the wave number 909 cm^{-1}. This is similar to the reports of FTIR for kaolin by Melia *et al.*(2012). Similarly, Wu and Ullah.(2013) indicated that the band at 749 cm^{-1} corresponds to Si-O-Al vibrations for kaolin.

5.1.2 FTIR analysis of chicken feather (CF)

FTIR analysis of the spectra of chicken feather (CF) is as shown in Figure 4.2. The spectra show a number of distinguishable peaks indicating the complex nature of chicken feather. The spectrum at 3690.10cm^{-1} indicates O-H group from water of the feather fibre. The peak at 3265.10 cm^{-1} was due to N–H (amine) group from an amino acid from chicken feather(CF). The peak at 2922.20 cm^{-1} shows the C–H stretch. The band due to the C-C of the alkyl group of the amino acid of the CF fibre is indicated by the peak at 1923.30 cm^{-1}. The bands obtained in this work for CF is similar to those obtained in the work by Egwuatu *et al*. (2014).

The characteristic peak at 2087.30 cm^{-1} corresponds to nitrile C–N stretch and the peak that appears at 1632.60 cm^{-1} is assigned to C=O group of amino acid and the ones at 1520.80 cm^{-1}and 1446.20 cm^{-1}show the N-H bending vibration and C=C stretch. The peaks which appeared around 1388.60 cm^{-1} region in the spectra shows C–H bending formation. Also, the peak at 1233.70 cm^{-1}is related to C-O (carboxylic acid) originating mainly from amino acid of the feather fibre. The peak at 1155.50 cm^{-1} indicated the nitrile C–N stretch. The band at 1032.50cm^{-1} is assigned to PO_4^{3-} band. The information from FTIR of CF in this study conforms well to those obtained for CF by Egwuatu *et al*.(2014).

5.1.3 FTIR analysis of chicken feather-kaolin composite (CFK)

Fourier transform infra-red spectroscopy (FTIR) analysis of the spectra of CFK composite is as shown in Figure 4.3. After the formation of the composite, sharp band at 3690.1 cm^{-1} in the chicken feather spectra has shifted to 3734.8 cm^{-1} indicating an interaction between CF and the K. The band at 3,690.1cm^{-1} due to stretching vibrations of hydroxyl groups of the K is still

present in the FTIR spectrum of CFK but with reduced intensityindicating Kinteracted with CF in CFK.

Therefore, the result indicated that in the CFK composite, the CF provided an efficient and strong support for the kaolin in forming the composite via the interaction between the nitrogen atom of the amino group of the protein keratin in CF, and the oxygen atom of the hydroxyl group on the kaolinite surface in the kaolin with more number of hydroxyl, carboxyl, amino and alcohol groups available for adsorption of metal ions.This result proof the second theoretical believe that despite intercalation, the interaction between CF and K could occur at the surface rather than by insertion of CF into the lamella spacing in K.

There was clear evidence of interaction in the appearance of new adsorption bands at wavenumbers 3649.1cm^{-1}, 3619.2 cm^{-1} and 3425.4 cm^{-1} whichwere assigned to O-H and N-H; inter hydrogen bond's vibration between the kaolin and the chicken feather. The band at 3265.1 cm^{-1} in the CF spectra which shifted to 3291.2 cm^{-1} in the CFK also suggested interaction between CF and K. This observation of interaction was supported by the appearance of several C-H stretch and alkyl group bands due to the CF contribution to the composite at the region around 1950 cm^{-1} to 2950cm^{-1} which were not originally present in the spectra of kaolin alone. Though, the C=O stretching in carboxyl or amide group at 1632.6cm^{-1} in the spectra of CF remained unchanged in the composite,the adsorption bandsat 1520.8 cm^{-1} and 1446.2cm^{-1}showing the N-H bending vibrationand C=C stretch in CF have now shifted to 1554 cm^{-1} and 1408.9 cm^{-1} respectively in CFK, whichfurther indicates that interaction has taken place between CF and K. This assertion conforms to the findings put forward byRatna and Sobha. (2015).

Further, the band at 1032.50cm^{-1} assigned to PO_4^{3-} groupin CF spectra has shifted to 1092.10cm^{-1} in CFK (Figure 4.3). This also indicated that there was an interaction between CF and K in the

CFK composite.This is also in conformity to the work of Egwuatu *et al*. (2014). Therefore, the FTIR analysis suggeststhe interaction between CF and K in CFK leading to the creation of more active bondingsites in CFK due to the presence of new O-H and N-H groups at the region between 3000 cm^{-1} to 4000cm^{-1} in CFK.

5.2 Scanning Electron Microscope (SEM) Analysis of the Adsorbents

5.2.1 SEM analysis of kaolin

The scanning electron micrograph of kaolin (K) is presented in Figure 4.4 and shows its morphological features. The SEM micrograph reveals the presence of large particles that appeared to have been formed by loose masses of particles stacked together in form of agglomerates or each on top of the last, showing hexagonal platelets of kaolinite mineral.

5.2.2 SEM analysis of chicken feather (CF)

Figure 4.5 shows the SEM micrograph of CF revealing its surface morphology as a function of its shape and size which in turn leaves an impact on CF adsorption capacity. The feathers have long shafts with barbs and barbules attached to it. It can be deduced that the chicken feather has a fibrous structure in which a crystalline microfibrils are embedded. The morphological characteristics of the sample as shown in the SEM micrograph also reveals a structure with knots and hooks. The micrograph also reveals a hollow structure and the presence of void on the surface. This is similar to the result of Débora *et al*. (2012) for CF.

5.2.3 SEM analysis of chicken feather-kaolin composite (CFK)

The SEM micrograph of the CFK in Figure 4.6 reveals that the K particles were found attached to the surface of the CF fibre along the barbs and the barbules in the matrix possibly through a certain degree ofhydrogen bonding between the two phases leading to the formation of more active sorption sites on the surface of CFK. This feature is also envisaged to enhanceadsorption capacity of CFK.

The surface morphology of the particles of the sample at the surface reveals the surface of the CF fibres rougher, having a brittle structure with fragments of kaolin adhering to its surface in the CFK, with protein degradation, which is due to the formation of overlapping layers and implies that the kaolinite particles grow at the surface of the CF fibres. This is also speculated to enhance heavy metal sorption to the surface. The presence of K particles on the surface of CF is expected to reduce the voids in CF and as such, the hollow structure of CF was not preserved in CFK.

Since, adsorption capacity depends upon the porosity or surface morphology as well as functional groups present on the adsorbent surface, supported by the appearance of more hydroxyl bands at the 3000 cm^{-1}- 4000cm^{-1} region of the FTIR spectrum of CFK, adsorption capacity of CFH was enhanced.

This result also shows that, the intercalation, even after passing through an additional guest displacement reaction step to expand the spacing between K layers and enhance the insertion of CF fibres between them, failed to have CF fibres inserted, instead, the CF fibres, by virtue of its size and hollow nature trapped the K particles on its surface via hydrogen bonding and as such, the second theoretical assumption of surface attachment after intercalation remained valid.

5.3X-ray Diffraction (XRD) Analysis of the Adsorbents

5.3.1 Analysis of the X-ray diffractogram of kaolin (K)

The X-ray diffractogram of K as shown in Figure 4.7 shows well defined reflections at 2θ value of 12.41◦ corresponding to the d values of 7.13 Å. These peaks correspond to the reflections from [001], which are typical characteristic peaks of kaolinite. This is similar to the work of Sachin *et al*.(2013). The present of kaolinite mineral (K) in the diffractogram was also indicated by peaks existing at 2θ values 25, 38.56, 45.94, 51.28, and 55.42^{o} respectively (Figure 4.7).

5.3.2 XRD analysis of chicken feather (CF)

The X-ray diffractogram of CF sample(Figure 4.8) indicated thatCF barbs contains mainly beta-keratins, fibrous proteins. This assertion conforms to the work of Kirschner*et al*, (1987). According to Meyers*et al.* (2008) and also corroborated by Greenwold and Sawyer. (2011).

The CF barb fibre shows a very broad peak at 8.49^{o} and 19.28^{o} and 20.59^{0} which specifically corresponds to the b-sheet structure. The peaks scattering at interplanar distance 10.5A^{0} and 9.2A˚ corresponding to 2θ values of 8.49^{0} and 9.61^{0} demonstrates all of the characteristics of a b-keratin diffraction pattern.

The X-ray diffractogram analysis also showed amorphous nature of the CF, with peaks at 2θ positions of 17.78^{0}, 21.14^{0}, 23.90^{0}, 28.68^{0}, 35.31^{0}, 41.19^{0} and 43.69^{0} and the corresponding d-spacing of 4.93A^{0}, 4.20A^{0}, 3.72A^{0}, 3.11A^{0}, 2.54A^{0}, 2.19A^{0} and 2.07A^{0}. This result is similar to that by Ratna *et al*.(2015). The diffraction pattern showed sharp crystallinity peak at 24.54^{0}, 26.09^{0}, 34.92^{0}, 38.39^{o}, 44.59^{o}, 56.22^{o} and 67.94^{o} correspond to the d spacing of 3.63A^{0}, 3.41A^{0}, 2.57A^{0}, 2.34A^{0}, 2.03A^{0}, 1.63A^{0}, 1.38A^{0} and (021), (210), (012), (022), (-132), (251)and (-521) plans reflection. This is similar to the work of Rizzo *et al*.(2006). Therefore, CF beta keratin fiber is semi-crystalline fibrous material.

5.3.3XRD analysis of chicken feather-kaolin composite (CFK)

Figure 4.9 shows the X-ray diffractogram of CFK. There was no observable change in the intensity and the interplanar spacing of the kaolinite peak at 12.41◦ corresponding to the d values of 7.13 Å, indicating that the CF particles did not pack between the lamella spacing of K,rather, particles of K are attached to the surface of CF particles in CFK. The CFK SEM result also corroborates this.

The new peaks that appear at 11.63^0 d-spacing of $7.6A^0$ with 003 reflections and 13.74^0, d-spacing of $6.44A^0$ with 110 reflections goes to show that an interaction has occurred in between the CF and K. This interaction has also been confirmed by the results from SEM and FTIR analysis of the composite. The peaks scattering at interplanar distance $10.5A^0$ and 9.2 A˚ corresponding to 2θ values of 8.49^0 and 9.61^0 which demonstrateall of the characteristics of a b-keratin diffraction pattern in CF no longer appear in CFK, which implies the degradation of the protein keratin structure of CF due to the presence of K on its surface. Also, the amorphous nature of the CF appeared to have been lost.

5.4Bruneur-Emmette-Teller (BET) Analysis of the Adsorbents

5.4.1Analysis of BET results for kaolin, chicken feather and chicken feather-kaolin composite

From Table 4.1, the BET results for CF, K and CFK indicated that there was an increase in the surface area 352.5m^2/g in Kto 424.8m^2/g in CFK and a pore volume increase from 21.66cc/g

in K to 24.27cc/gin CFK, but CF has the highest surface area of 711.9m^2/g and pore volume of 36.29cc/g. However, CFK has the highest pore size of 2.132nm followed by K (2.131nm) and then CF (2.105nm). The presence of CF which served as a base upon which K particles were attached in the composite CFK makes ithave higher surface area and pore volume than K.

Also, the presence of CF in the composite CFK contributes more actively adsorbing groups(as already established by the results from FTIR, SEM and XRD) and this is believed to be responsible for the increase in the pore size of CFK than K and CF which in turn enhances its adsorption more.

5.5Kinetics Study of the Adsorption

The Kinetic studies for the adsorption of Pb^{2+}, $Cu^{2+}$and Ni^{2+} on CFK were investigated using pseudo-first order kinetic, pseudo-second order kinetic and intra-particle diffusion models. The Figures 4.10a-4.10c arefor pseudo-first order model and theFigures 4.11a-4.11c are for pseudo-second order modelrespectively. The Table 4.2a shows the pseudo-first order parameters while the pseudo-second order parameters are shown in Table 4.2b. The intra-particle diffusion model plots are shown in Figures 4.12a–4.12c and their parameters are recorded in Table 4.3.

5.5.1 Analysis of pseudo-first order kinetic

The pseudo-first order plots in Figures 4.10a-4.10c did not give a perfect straight line for any of the three metals, and their R^2values in Table 4.2a are very poor and far from unity for all three metals and the difference between the Q_{exp} and Q_{cal} is very large. These findings indicate that the kinetic data of Pb^{2+}, Cu^{2+} and Ni^{2+} cannot be well predicted by pseudo-first order model. This is similar to the report of Adeyinka *et al*. (2017) in his work on adsorption of heavy metals onto thermally treated egg quail shell.

5.5.2 Analysis of pseudo-second order kinetic

The kinetic data of the metal ions were further investigated using pseudo-second order kinetic model. As shown in Figures 4.11a-4.11c, pseudo-second order kinetic plot of (t/qt) versus (t)

gave a perfect straight line for the adsorption of Pb^{2+}, Cu^{2+} and Ni^{2+} onto CFK composite implying that, the adsorption process fitted well into the pseudo-second order kinetic model.

The values of model parameters k_1, k_2, h, Q_{cal} and correlation coefficients (R^2) are gotten from the plots and presented in Table 4.2b. As shown in the result, the R^2 values of 0.999 for Pb^{2+}, 1 for $Cu^{2+}$and 0.9999 for $Ni^{2+}$for the pseudo-second order rate mechanismare greater than 0.99. They are not only reasonable but are also substantially higher than those obtained for the first order mechanism. Furthermore, the Q_{cal} values calculated from the second order kinetic model agreed reasonably well with the values obtained experimentally (Q_{exp}). Again, this further indicates that the adsorption of Pb^{2+}, Cu^{2+} and Ni^{2+}onto CFK composite follow the pseudo second-order model.

The rate constant of the pseudo-second order adsorption (k_2) obtained for Pb^{2+} was found to be higher than that calculated for Cu^{2+} and Ni^{2+} (Table 4.2b). This indicates that the uptake of Pb^{2+} onto CFK from the aqueous solution was more rapid and favorable.

The initial adsorption rate, h (mg/g.min) at $t \rightarrow 0$ is defined as: $h = K_2 q_e^2$ (17)

Where k_2 is the pseudo-second order rate constant (g/mg.min) and qe is the amount of adsorbate adsorbed by adsorbent at equilibrium. According to the values obtained for the initial adsorption rate (h) as shown in Table 4.2b, Pb^{2+}has higher value than Cu^{2+} and Ni^{2+}. This shows that initial adsorption of Pb^{2+} by CFK is the fastest and in a mixture of metals of this group, Pb^{2+} may be quantitatively removed before others. This interpretation is similar to the report of Adeyinka *et al*. (2017) in his work on adsorption of heavy metals onto thermally treated egg quail shell.

5.5.3 Analysis of intra-particle diffusion rate equation

It is possible to have outer surface diffusion as well as intra-particle diffusion from outer surface of the adsorbent into the pores (Pandey *et al*, 2009). The adsorption of a sorbate into the sorbent occurs in three steps which are: Film diffusion, pore diffusion and intra-particle transport (Pant *et al*, 2004). However, there is the possibility of pore diffusion being the rate determining step in the batch process, but the sorption parameter which in most cases controls the batch process for most of the contact time is the intra-particle diffusion.The intra-particle diffusion model was applied to further investigate the kinetic process in order to explain the mechanism of diffusion.

Using equation (6), q_t was plotted against $t^{1/2}$ in order to determine K_d and l. The plots for Pb^{2+}, Cu^{2+} and Ni^{2+} are shown in Figures 4.12a–4.12c and their parameters are recorded in Table 4.3.

From Figures 4.12a-4.12c, the linear plots for all three metals did not pass through the origin. This means that there were differences in the rate of mass transfer in the initial and final stages (rapid initial stage and slow second stage) of the sorption. This also implies that intra-particle diffusion was not the only rate controlling step but other surface phenomena were actively involved in the sorption process. This conforms to the report by Das and Mondal. (2011) on theirequilibrium, kinetic and thermodynamic studies on the use of calcerous clay soil for the removal of lead from aqueous solution.

Also, from Table 4.3, the l value for Pb^{2+} is higher than that of Ni^{2+} and Cu^{2+} denoting a greater contribution of the surface sorption for Pb^{2+} than the other two metals at the rate determining step, it was followed by Ni^{2+} and then Cu^{2+} .

5.6 Adsorption Isotherms

Adsorption isotherms are mathematical models that explain the distribution of the adsorbate species in liquid and solid phases, depending on whether the solid surface is heterogeneous,

homogeneous, the coverage type and the likely hood of interaction between the adsorbate species. In this work, equilibrium data were analyzed using the Freundlich isotherm, Langmuir isotherm and Dubinin-Radushkevich isotherm expressions.

5.6.1 Analysis of Langmuir model

The Langmuir. (1916) model assumes that uptake of metal ions occurs on a homogenous surface by monolayer adsorption without any interaction between adsorbed ions. The Langmuir isotherm model was chosen for the estimation of maximum adsorption capacity corresponding to complete monolayer coverage on the CFK surface. The plots of (1/qe) against (1/Ce) for Pb^{2+}, $Cu^{2+}$and $Ni^{2+}$are shown in Figures 4.13a- 4.13c and the linear isotherm parameters, q_m, K_L and the R^2 values are presented in Table 4.4.

Figures 4.13b and 4.13c indicate better fit to Langmuir model than Figure 4.13a because they give better straight lines and have higher R^2 values. Table 4.4 shows the Langmuir isotherm parameters for all the three metals. The higher the K_L value, the more favourable is the monolayer adsorption. The adsorption coefficient, K_L that is related to the apparent energy of sorption according to Table 4.4 for Ni^{2+}(2.54 l/g) was greater than that of Cu^{2+}(0.56 l/g) and Pb^{2+}(-1.14 l/g). The data therefore indicated that, the effectiveness of CFK in the monolayer adsorption of the three metals from an aqueous system was Ni^{2+}> Cu^{2+}> Pb^{2+}. This interpretation is similar to the report of Adeyinka *et al*. (2017) in his work on adsorption of heavy metals onto thermally treated egg quail shell.

This preferential sorption behaviour could be explained in terms of ionic radii of the metal ions (Pb^{2+} = 1.19A°, Cu^{2+} = 0.73A°; Ni^{2+} = 0.69A°). The element with smaller ionic radius will compete faster for exchange sites during physical adsorption than those of larger ionic radius.

The sorption capacity, q_{max} measures the maximum sorption capacity corresponding to complete monolayer coverage. Table 4.4 also shows that the q_{max} for $Cu^{2+}$is (78.13 mg/g) which is greater than Ni^{2+}(44.25 mg/g) and Pb^{2+}(-9.35mg/g). This implies that, in this multi component system comprising Pb^{2+}, $Cu^{2+}$and Ni^{2+}; Pb^{2+}does not fit well into the Langmuir model, its q_{max} value of -9.35 is not just the smallest compared to 78.13 for Cu^{2+} and 44.25 for Ni^{2+} but it is also negative, with R^2 value of 0.6544 as against 0.9205 for Cu^{2+} and 0.9089 for Ni^{2+} indicating that Pb^{2+}did not follow the Langmuir model and monolayer adsorption by CFK composite; but this is possible with respect to $Cu^{2+}$and Ni^{2+} adsorption onto CFK composite.

The highest q_{max} and R^2 values was for Cu^{2+}followed by that of Ni^{2+}as presented in Table 4.4. This implies that Langmuir isotherm is best fitted for Cu^{2+}adsorption in this work followed by $Ni^{2+}$with just a very slight difference. So, the ideal order for fitness to Langmuir isotherm is Cu^{2+}> Ni^{2+}> Pb^{2+}. This explanation is similar to the report of Adeyinka *et al*. (2017) in his work on adsorption of heavy metals onto thermally treated egg quail shell.

5.6.2 Analysis of Langmuir isotherm separation factor (SF) for adsorption of Pb^{2+}, Cu^{2+} and Ni^{2+} on CFK

Furthermore, favourability of adsorption of the three metal ions onto the CFK composite was tested using the essential features of the Langmuir isotherm model, expressed in terms of a dimensionless constant called separation factor (SF). The SF value for the adsorption of Pb^{2+}, $Cu^{2+}$and Ni^{2+}onto CFK composite at initial concentration of 50 ppm (lowest concentration studied) and 250 ppm (highest concentration studied) are listed in Table 4.5.

The smaller the SF value, the more favourable the relationship between the adsorbent and the adsrobate and the higher the adsorption. As indicated in Table 4.5, the SF parameters for the

three metals are less than unity signifying that CFK is an ideal adsorbent capable of adsorbing all the three metal ions selected in this study from aqueous medium. However, the SF value of Cu^{2+}> Ni^{2+}> Pb^{2+}, obtained in study shows that in a mixed metal ion system or multi component system of this metals, Pb^{2+}will compete for the binding sites better and faster than Ni^{2+} and Cu^{2+}, this is why percentage adsorption of $Pb^{2+}$is higher than that of $Cu^{2+}$and Ni^{2+}.

5.6.3 Analysis of Freundlich isotherm

The Freundlich. (1906) equation is an empirical equation based on adsorption on a heterogeneous surface.

The Freundlich model was chosen to estimate the adsorption intensity of the adsorbate on the adsorbent surface. The experimental data from the batch sorption study of the three metal ions on CFK composite were plotted using the linear Freundlich isotherm equation, the graphs for the three metal ions were as shown in Figures 4.14a-4.14c and the linear Freundlich isotherm constants for Pb^{2+}, $Ni^{2+}$and Cu^{2+}on CFK are presented in Table 4.6.

The Freundlich isotherm parameter 1/n is a measure of the intensity of adsorption of metal ions onto the CFK surface.It takes values from 0.1- 0.5 while the Freundlich exponent, n, should have values ranging from 1 to 10 to be classified as favorable adsorption (Chantawong *et al*., 2001). The higher the 1/n value, the more favourable the adsorption. The high 1/n value of Pb^{2+}(0.47) in Table 4.6 in comparison to Cu^{2+}(0.1) and Ni^{2+}(0.04), indicates the preferential sorption of Pb^{2+}than $Cu^{2+}$and Ni^{2+} onto CFK composite.

The Freundlich isotherm is also used to indicate the ability of the CFK composite to remove these three metal ions from aqueous medium even at high concentrations. The K_F which is an indicator of the ultimate adsorption capacity was obtained from the intercept on the graph. The

higher the K_f value, the higher the maximum adsorption capacity. So, the K_f value of Pb^{2+}(115.58 l/g) obtained is greater than that of Cu^{2+}(42.52 l/g) and Ni^{2+}(32.79 l/g) suggesting and confirming that Pb^{2+} has greater tendency and ease of adsorption by CFK than the other two metals.

This remarkable difference is due to the considerable difference in their hydration radii and hydration enthalpies. The hydration radii of the metal ions are 4.01A^o for Pb^{2+}, 4.19A^o for $Cu^{2+}$and 4.50A^o for Ni^{2+} (Afrodita and Mirjana. 2014). Ideally, the smallest cation will be adsorbed faster and in larger quantities than the larger cations because the smaller the cations, the easier it is for it to pass through the pores and channels of the adsorbent (CFK). Therefore, the smaller the hydrated radius, the higher the affinity for adsorption onto the CFK surface. This explanation conforms to the report of Afrodita and Mirjana.(2014) in his work on adsorption on the effect of competing cations (Cu, Zn, Mn, Pb) absorbed by natural zeolite.

Similarly, adsorption is also related to hydration enthalpy, which is the energy that permits the detachment of water molecules from cations. Hence, it determines the ease of interaction between the cations and the adsorbent. Cations with low hydration energies are preferably sorbed than the ones with high hydration energies. This implies that the more a cation is hydrated, the stronger is its hydration enthalpy and the less it can interact with the adsorbent. Consequently, $Pb^{2+}$with hydration energy of 1481 kJ/mol will be sorbed preferably compare to $Cu^{2+}$and $Ni^{2+}$with 2010 kJ/mol and 2105 kJ/mol hydration energies respectively. This is in good conformity to the report of Afrodita and Mirjana. (2014) in his work on adsorption. Therefore, the order of sorption for the metals is $Pb^{2+} > Cu^{2+} > Ni^{2+}$.

Although, both the Langmuir and Freundlich isotherms provide good fit for Cu^{2+} with respect to the R^2 values, its R^2 value of 0.9212 in Freundlich which is slightly higher than 0.9205 in Langmuir shows that the the Freundlich model provides better fit for Cu^{2+} adsorption in this study. Also, Pb^{2+} R^2 value of 0.8002 in Freundlich isotherm which is higher than 0.6544 in Langmuir model signifies that Pb^{2+} adsorption follows the Freundlich model. On the other hand, the 0.9089 R^2 value for Ni^{2+} in Langmuir model as against 0.8779 in Freundlich isotherm indicates that the Langmuir model is better fitted for Ni^{2+} adsorption than the Freundlich model. The R^2 values also imply that, overall, whereas the Langmuir model describes well the adsorption of Ni^{2+}, the Freundlich model on the other hand, was better able to describe the adsorption of Cu^{2+} and Pb^{2+}, so there is a mix model fit. Therefore, the adsorption of Pb^{2+} and Cu^{2+} followed the heterogenous route while the adsorption of Ni^{2+} is more of a monolayer process.

5.6.4 Dubinin–Radushkevich isotherm (D-R) model

This isotherm assumes that the characteristics of the sorption curve are related to the porosity of the biosorbents (Abdelwahab, 2007). This model was also used to evaluate the mean energy of sorption. The plots and parameters of the Dubinin-Radushkevich isotherm for Pb^{2+}, $Cu^{2+}$and Ni^{2+} sorption are shown in Figures 4.15a- 4.15c and Table 4.7.

As indicated in the R^2 values of the metals in Table 4.7 and Figures 4.15a–4.15c, the Dubinin-Radushkevich model also provides a good fit for the adsorption of the metals. The D-R isotherm constant Q_{DR} represents the sorption capacity and the higher its value, the higher the adsorption. Pb^{2+} has a greater value of 351.08 mmol/g as against 41.84 mmol/g for $Cu^{2+}$and 38.00 mmol/g for Ni^{2+}. Therefore, in a multi-component system such as this, Pb^{2+} will be preferentially

adsorbed, followed by Cu^{2+} and then Ni^{2+}. The value of the mean energy of sorption (E) is used to determine whether the adsorption process is through chemisorption or physisorption. Its value in the range of 1-8 kJ/mol for the transfer of one mole of an ion is indicative of physisorption whereas its value in the range of 20-40 kJ/mol implies a chemical adsorption process. From Table 4.7, the values for all the three metals studied are less than 8 kJ/mol and this further confirms physisorption as the dominant mechanism through which the adsorption of these metals occurred onto CFK composite. Similar interpretation was given by Jusheng and Xin. (2013) in their isotherm study on lead adsorption onto novel silica-based hybrid adsorbent.

5.7 Thermodynamic Studies

This study was done so as to investigate the spontaneity of the adsorption process, be it endothermic or exothermic and whether the process is accompanied by increase or decrease in entropy on the surface of the adsorbent during adsorption. The plot of ΔG versus temperature were shown in Figures 4.16a-4.16c and the values for all the parameters involved were determined and presented in Tables 4.8 and 4.9.

The plot of ΔG versus temperature (Figures 4.16a-4.16c) were found to be linear signifying good fit. The ΔG values for all three metals at the different temperatures investigated (Table 8) were all negative signifying that the adsorption process is feasible and spontaneous. The positive ΔH values shows that the adsorption process is endothermic. The value of heat of adsorption (ΔH) which were less than 20 kJ/mol (Table 9) for all the three metals studied depicts physisorption. The positive value of ΔS signifies increased degree of disorderliness (entropy) at the interface of solid-liquid system during the adsorption of the metals. This is similar to the report by Adeyinka *et al.* (2017)on the adsorption of heavy metals onto thermally treated egg quail shell.

5.8 Analysis of the Comparison of the Adsorption of Pb^{2+}, Cu^{2+} and Ni^{2+} onto CFK at an Initial Concentration of 100 ppm, Temperature of 75^{o}C and Time of 10 min for Single and Multi-Component System

This comparison was necessary in order to understand the effect the presence of each metal has over the adsorption of the others by CFK composite if they are all present in a given wastewater. As can be observed from Table 4.10, the adsorption of Pb^{2+} was not significantly affected by the presence of the other two metals as the difference between its adsorption for single and multi-component systems is very insignificant. However, there was a slight increase in adsorption of Pb^{2+} for the single component system with 99.88% adsorption against the multi-component system with 98.86% adsorption.

On the other hand, the presence of the other metals affected significantly the adsorption of both Cu^{2+} and Ni^{2+}. There was a reduction in adsorption from 99.78 to 83.61 for Cu^{2+} and a decrease from 86.43 to 68.49 for Ni^{2+} which represents a significant decrease in their adsorption due to competition with other metal species. This can be attributed to the remarkable differences in their hydration radii and hydration enthalpies which had already been discussed under the Freundlich isotherm.

5.9 Analysis of the Comparison of the Adsorption of Pb^{2+}, Cu^{2+} and Ni^{2+} onto Chicken Feather-Kaolin Composite (CFK), Kaolin (K) and Chicken Feather (CF) at an Initial Concentration of 100 ppm, Temperature of 75^{o}C and Time of 10 min for Multi-Component System

Although, based on the results obtained from BET analysis (Table 4.1) for the three adsorbents, chicken feather (CF) has a higher surface area than the kaolin (K) and the chicken feather-kaolin composite (CFK). It was however observed from the results in Table 4.11 that CFK has the

highest sorption capacity followed by CF for Pb^{2+}, Cu^{2+} and Ni^{2+} respectively and shows that the CFK composite performs better in adsorbing the metals studied than the individual starting materials of K and CF proving the goal of the research successful. This means that the surface area is not the only factor responsible for the sorption capacity of an adsorbent.

According to Ping *et al*. (2009), "the sorption capacity of materials is mainly controlled by two factors, the specific surface area and the character of the surface. The factor having the dominant effect will control the adsorption process of a given adsorbent more". In this study, BET was used to investigate the possible reason for the adsorption capacity of K, CF and CFK. It was found out that, despite the fact that the surface area of CF (711.9 m^2/g) is larger than that of CFK (424.8 m^2/g), CFK performs better in adsorbing the heavy metals from a multi- component solution than CF. Therefore, the dominant factor that affects the sorption capacity of CFK, K and CF is not the surface area but the character or property of the surface. It has already been established in this work based on the FTIR results of K, CF and CFK that CFK has more groups on its surface which enhances its sorption capacity than individual K and CF and this is believed to be responsible for the higher sorption capacity of CFK compared to individual K and CF though CF has a higher surface area than CFK. Their adsorption capacities were studied and the results presented in Table 4.11. It shows from Table 4.11 that CFK with 98.86% Pb^{2+} removal, 83.61% Cu^{2+} removal and 68.49% Ni^{2+} removal capacity from the multi-element system has higher sorption capacity than both CF with 80.35% Pb^{2+} removal, 75.00% Cu^{2+} removal, 67.39% Ni^{2+} removal and K with 69.90% Pb^{2+} removal, 73.48% Cu^{2+} removal and 65.46% Ni^{2+} removal respectively.

5.10 Statistical Analysis of the Adsorption Model for Pb^{2+}

5.10.1 Analysis of variance (ANOVA) for response surface quadratic model for Pb^{2+}sorption onto CFK composite

The use of Design Expert software version 7.0.0 to analyse the fitness of the model based on analysis of variance (ANOVA), gave the results of the regression model as presented in Table 4.12. Statistical testing of the model by the Fischer's statistical test for analysis of variance (ANOVA) yields an F-value of 74.05 with a low p-value ($P<0.0001$) which implies that the model is significant. Similar explanation was given by Gul. (2016) in his work on the application of full factorial experimental design and response surface methodology for chromite beneficiation by knelson concentrator.

There is only a 0.01% chance that a model with F-value as large as this could occur due to noise. Values of Prob > F less than 0.0500 as shown in Table 4.12indicates thatmodel terms are significant. In this case A, B, C, AB, BC, A^2, B^2, $C^2$are significant model terms. Values greater than 0.1000 indicate the model terms are not significant, in this case, the interaction term due to AC is not significant.

5.10.2 Analysis of the quadratic model statistical values for Pb^{2+} sorption onto CFK composite

Table 4.13 shows the model R-square value is nearer to unity($R^2 = 0.9037$) and implies that the quadratic model is the best fit for the observed adsorption of lead metal onto the composite CFK.The predicted R-squared value of 0.8758 is in reasonable agreement with the adjusted R-squared value of 0.8915 (difference is less than 0.2). The standard deviations of the predicted model was 0.52.

Gul. (2016) gave similar interpretation in his work on full factorial design. Adequate precision measures the signal to noise ratio of an experiment and a ratio greater than 4 is desirable. Therefore, theratio of 37.760 for lead metal in this work indicates an adequate signal, thusthe model can be used to navigate the design space for the metal being considered.

5.10.3 Coefficient estimates and parameter interactions of the empirical models for Pb^{2+} sorption onto CFK composite

The coefficient estimates and parameter interactions of the empirical models are tabulated in Table 4.14.Final equation in terms of coded factors for Pb^{2+}:

$$Pb = +96.98 -1.21* A -0.37* B -0.46* C -0.61* A * B -0.097* A * C -1.19* B * C -0.45* A^2 - 0.68*B^2-0.66*C^2 \quad (13)$$

The estimated coefficient values calculated for main effects of the process variables as shown in Table 4.14 and equation 13 reveals that, B and C have significant negative effect and concentration has the highest negative effect (-1.21) on the removal efficiency. This implies that the higher the concentration, the lower the removal efficiency.All the interaction terms (AB and BC) have negative effects except for the interaction between A and C which effect is insignificant, similar to the report by Gul.(2016) in his work on full factorial design.The quadratic effects A^2, B^2 and C^2 all have negative effects on Pb^{2+} adsorption from the solution.

5.10.4Analysis of the normal probability plot for Pb^{2+}sorption onto CFK composite

The normal probability plot is used to check for normality of residuals for Pb^{2+}. As depicted from the normal probability plot of internally studentized residuals in Appendix IV, it shows that it is normal with a good shape as most points were on the straight line. This is also supported by the work of Gul.(2016).

5.10.5 Analysis of predicted versus actual values for Pb^{2+}sorption onto CFK composite

The plot of the predicted versus actual values also known as the studentized residuals versus predicted values plot is used to check for constant error. The plot shown in Appendix V indicates that all the points are concentrated or randomly scattered around the straight line and this is a very good pointer to the effectiveness of the model.

5.10.6Externally studentized residuals analysis for Pb^{2+}sorption onto CFK composite

The externally studentized residual plot shown in Appendix VI is used to discover or check for outliers. Any point that is located beyond the plus or minus 3.5 region is an outlier and as can be seen from the figure, all the points fell ramdomly within the allowed range and as such, there were no outliers with respect to the experimental results gotten for Pb^{2+} sorption.

5.11Analysis of the Predicted Response (Pb^{2+}) of the Process to the Independent Variables

This was done using graphs in the form of contours and in three dimensional (3D) space to help to visualize the shape of the response surface in respect to the operating experimental parameters.

5.11.1 Effect of concentration and temperature on the adsorption of Pb^{2+} from the solution

Appendices VIIa and VIIb represent the contour and 3D plots which show the effect of concentration and temperature on the percentage removal efficiency of Pb^{2+} from the multi-elemental wastewater using CFK composite at the centre level of time (35 min). From the Appendices, a higher percentage removal of Pb^{2+} from the system was obtained at higher temperature and at lower concentration.

Within the limits of the tested parameters in this work, the percentage removal was found to increase at the beginning as the temperature is being increased and the concentration is being increased, but further increase in concentration leads to a significant decrease in Pb^{2+} adsorption. This can be attributed to the increase in the concentration of the adsorbate as against a fixed number of available active sites on the adsorbent.And the increase in percentage removal of Pb^{2+} by an increase in temperature can be explained by the fact that increase in temperature leads to increase in the rate of diffusion of the adsorbate molecules from bulk to the external boundary layer and into the internal pores of the adsorbent material. This result is consistent with that of Mekonnen *et al.* (2015).

5.11.2 Effect of concentration and time on the adsorption of Pb^{2+} from the solution

Appendices VIIIa and VIIIb represent the contour and 3D plots which indicate the effect of concentration and time on the percentage removal efficiency of Pb^{2+} from the multi- elemental wastewater using CFK composite at the centre level of temperature($50^{o}C$) . From the Appendices, a higher percentage removal of Pb^{2+} from the system was obtained at lower time and at lower concentration as well, while decrease in adsorption was observed at higher concentration and time.

The decrease in adsorption capacity with increase in time and concentration could be attributed to desorption resulting from weakening and breaking of bond between adsorbate and adsorbent occasioned by electrostatic repulsion between already adsorbed adsorbate on the adsorbent and

the ones in the bulk solution. This result conforms to that of Karthikeyan *et al*.(2005) andMekonnen *et al*.(2015).

5.11.3 Effect of time and temperature on the sorption of Pb^{2+} from the solution

Appendices IXa and IXb represent the contour and 3D plots and show the effect of temperature and time on the percentage removal efficiency of Pb^{2+} from the multi- elemental wastewater using CFK composite at the centre level of concentration (150ppm). From the results, it can be deduced that increasing the time and decreasing the temperature tends to favour higher adsorption of Pb^{2+}. Also, decreasing the time while increasing the temperature leads to increase in the percentage removal of the metal from the solution. This is due to the fact that increase in temperature increases the rate of adsorption as a result of increase in the rate of difusion of adsorbate onto the adsorbent surface and inside of its pores.

However, decreasing both time and temperature decreases the percentage adsorption capcity of the adsorbent for Pb^{2+}. This is so because at low temperature, mobility of the metal ion is low and this results to a low rate of difusion of adsorbate onto the external and internal surface of the adsorbent, hence low percentage removal capacity.

Also, increasing both time and temperature decreases the percentage amount of Pb^{2+} that can be removed from the multi- elemental solution.This is because, it has already been established in this study that increase in temperature favours Pb^{2+} adsorption leading to the occupation of the adsorbent's active sites and establishment ofequilibrium within a short time.

It therefore follows that maintaining such high temperature for longer time decreases the percentage adsorption due to desorption occasioned by non-availability of more active sites and increase in the thermal energy that may induce higher agitation or vibration of the adsorbed metals onto the surface of the adsorbent, leading to weakening of the adsorbent-to-adsorbate

surface bond, so the bond eventually cleaves causing desorption.This result is in good agreement with the report by Hamadi *et al*. (2001) and Mekonnen *et al*. (2015).

5.11.4Study of the interactionplots between the parameters for Pb^{2+} removal from the solution

The interaction effects plots are used to indicate the mean response of two factors at all feasible combinations of their settings.

5.11.4.1 Interation between concentration and temperature during Pb^{2+}sorption

In Appendix X, the lines are not parallel but rather they are crossing over each other which signifies an interaction between the temperature and concentration. At high tempearture and low concentration, percentage metal adsorption capacity is high.

On the other hand, increasing the concentration at high temperature decreases the percentage removal of the metal from the solution.Decreasing both concentration and temperature decreases percentage adsorption capcity of the adsorbent for Pb^{2+} than when the concentration is low and the temprature is high within the parameters analyzed and is in good conformity to the report of Mtaallah*et al*.(2017).

5.11.4.2 Interation between time and concentration for Pb^{2+} sorption onto CFK composite

Appendix XI shows a plot of the interation between time and concentration. The result shows clearly that the two lines are parallel indicating no interaction between the two independent variables within the range of parameters chosen in the course of this research. This further confirm the result of analysis of variance (ANOVA) in Table 4.12which gave "Prob > F" value of 0.2695 for the AC, indicating that the interaction term AC (concentration and time) is not significant as also reported by Gul.(2016).

5.11.4.3 Interaction between temperature and time for Pb^{2+} sorption onto CFK composite

The lines in Appendix XIIare not parallel but rather are crossing over each other which signifies an interaction between temperature and time. Increasing the time and decreasing temperaure simultaneously favours higher adsorption capacity. Also, decreasing the time while increasing the temperature leads to increase in the percentage removal of the metal from the solution. On the other hand, decreasing both time and temperature decreases the percentage adsorption capcity of the adsorbent for Pb^{2+}due to low rate of diffusion and short time of contact. This is similar to the report byMtaallah *et al*.(2017).

5.11.4.4 Analysis of the cube plot for Pb^{2+}sorption onto CFK composite

Appendix XIII shows the cube plot for Pb^{2+}adsorption from the solution. It can be inferred from the result that, at 25^{o}C, 10min and 100ppm, 95.33% of Pb^{2+} was predicted to be removed from the multi- component system but when the temperature wasincreased to 75^{o}C, percentage adsorption was predicted to rise to 98.20% signifying a 2.87% increase in adsorption.

However, when the concentration was increased to 200ppm at 10 min, there was no significant effect of changing the temperature from 25^{o}C with 94.32% adsorption to 75^{o}C with 94.75% adsorption, indicating that, at high concentration, temperature increase has no significant effect on the percentage adsorption of Pb^{2+} from the solution. The 98.20% removal of Pb^{2+} at 100ppm as against 94.75% at 200ppm both at 75^{o}C (3.45 difference) shows a decrease in adsorption due to increase in concentration of the adsorbate.

On the other hand, when the time was increased to 60min, at concentration of 200ppm, predicted percentage adsorption was observed to be higher at lower temperature (25^{o}C gave 95.59% adsorption) than at higher temperature (75^{o}C gave 91.25%).This is because longer time and high

temperature weakens the force holding the adsorbate and adsorbent together and hence desorption sets in. Similar report was put forward by Mtaallah *et al*.(2017).

5.12 Statistical Analysis of the Adsorption Model for Cu^{2+} Sorption onto CFK Composite

5.12.1 Analysis of variance (ANOVA) for response surface quadratic model for Cu^{2+}sorption

The use of Design Expert software version 7.0.0 to analyse the fitness of the model based on analysis of variance (ANOVA), gave the results of the model for as presented in Table 4.15. Statistical testing of the model by the Fischer's statistical test for analysis of variance (ANOVA) produced an F-value of 360.95 with a low p- value ($P<0.0001$) for Cu^{2+}sorption which implies the model is significant and this is similar to the report by Gul.(2016).

There is only a 0.01% chance that a model with F-value this high could occur due tonoise. Values of Prob > F less than 0.0500 as shown in the table indicates that certain model terms are significant while others are not. In this case A, B, AB, BC, A^2 are significant model terms. Values greater than 0.1000 indicate the model terms are not significant, in this case, the term C, the interaction term due to AC and the quadratic terms B^2 and C^2 are not significant.

5.12.2 Quadratic model statistical values for Cu^{2+}sorption onto CFK composite

Table 4.16 shows the model R-square value of 0.9786 is nearer to unity and implies that the quadratic model is the best fit for the observed adsorption of copper metal onto the composite CFK. The Predicted R-squared value of 0.9730 is in reasonable consistency with the adjusted R-squared value of 0.9759 (difference is less than 0.2). This deduction is similar to the one given by Gul. (2016) in his work on full factorial design.

Adequate precision measures the signal to noise ratio of an experiment and a ratio greater than 4 is desirable. The ratio of 45.482 for copper metal in this work is well above 4 and thus shows that the signal is adequate, hence the model can be used to navigate the design space for the metal being adsorbed. The standard deviations of the predicted model was found to be 1.73.

5.12.3 Coefficient estimates and parameter interactions of the empirical models for Cu^{2+} sorption onto CFK composite

The coefficient estimates and parameter interactions of the empirical models are shown in Table 4.17. Final equation in terms of coded factors for Cu^{2+}:

$$Cu = +73.28 - 12.01 * A + 1.26 * B - 0.22 * C + 0.79 * A * B + 0.16 * A * C + 0.70 * B * C - 9.94 * A^2 + 0.28 * B^2 + 0.53 * C^2 \quad (14)$$

The estimated coefficient values calculated for main effects of the process variables as shown in Table 4.17 and equation 14, reveals that concentration has the highest negative effect (-12.01) on the removal efficiency. This implies that the higher the concentration, the lower the removal efficiency, time has a negative effect too. This also agrees with the report put forward by Gul.(2016).

On the other hand, the temperature has a positive effect (1.26). This means that the higher the temperature, the higher the efficiency of adsorption for copper.The interaction terms (AB and BC) have positive effects and AC has the least positive effect. The quadratic effect A^2has a negative effect while both B^2 and C^2have positive effects on Cu^{2+} adsorption in this work.

5.12.4Analysis of the normal probability plot for Cu^{2+}sorption onto CFK composite

The normal probability plots as shown in Appendix XIV is used to check for normality of residuals for Cu^{2+}. From the normal probability plot, it indicates a normal plot with a good shape

as most points were on the straight line. This deduction is in line with the one given by Gul. (2016) in his work on full factorial design.

5.12.5Analysis of predicted versus actual values for Cu^{2+}sorption onto CFK composite

The plot of the predicted versus actualvalues is as seen in Appendix XV, this studentized residuals versus predicted values plot is used to check for constant error. The result reveals that all the points are concentrated or randomly scattered around the straight line and this is a very good pointer to the effectiveness of the model for Cu^{2+} sorption from the solution.

5.12.6Externally studentized residuals analysis for Cu^{2+}sorption onto CFK composite

The externally studentized residual plot shown in Appendix XVI is used to check for outliers. Any point that is located beyond the plus or minus 3.5 region is an outlier. The result indicated that, all the points are ramdomly sacattered within the permissible range and therefore, there is no outlier with respect to the experimental results obtained for Cu^{2+}.

5.13 Analysis of the Predicted Response (Cu2+) of the Process to the Independent Variables

This was carried out using graphs in the form of contours and in three dimensional (3D) space to help to visualize the shape of the response surface in respect to the operating experimental parameters.

5.13.1 Effect of concentration and temperature on the adsorption of Cu^{2+} from the solution

Appendices XVIIa and XVIIbillustrate the effect of temperature and concentration on the percentage adsorption of Cu^{2+} from the multi-elemental wastewater using CFK composite at the

centre level of time (35min). It can be seen from the results that there is no significant effect of temperature on the percentage adsorption of Cu^{2+} at low concentration,this indicates that, at low concentration,irrespective of the temperature, percentage adsorption of Cu^{2+} is always high in the range of the parameter levels studied.

However, increasing the concentration generally leads to a significant decrease in the percentage adsorption of Cu^{2+} at low temperatures but a slight increase in adsorption was observed when the temperature was increasedboth at high and low concentrations. The phenomenon of low adsorption at high concentration was duetotheincreasein the numberof metal particles as against a fixed active sites on the adsorbent. This result is consistent with that of Mekonnen *et al.* (2015).

5.13.2 Effect of concentration and time on the adsorption of Cu^{2+} from the solution

Appendices XVIIIa and XVIIIb illustrate the effect of time and concentration on the percentage adsorption of $Cu^{2+}$from the multi- elemental wastewater using CFK composite at the centre level of temperature ($50^{o}C$). From the results, it can be stated that, there is no significant effect of changing thetime on the percentage adsorption of Cu^{2+} at a constant concentration in the range of the parameter levels analyzed.

However, increasing the concentration leads to a significant lowering of the percentage adsorption of Cu^{2+} due to the increase in the number of metal particles beyond the capacity of the active sites on the adsorbent as stated by Karthikeyan *et al*.(2005) and Mekonnen *et al*.(2015).

5.13.3 Effect of time and temperature on the adsorption of Cu^{2+} from the solution

Appendices XIXa and XIXb illustrate the effect of time and temperature on the percentage adsorption of $Cu^{2+}$from the multi-elemental wastewater using CFK composite at the centre level of concentration (150ppm). From the results, variation of time and temperature has no

significant effect on percentage adsorption of Cu^{2+} from the solution. However, decreasing the temperature and increasing time leads to a slight decrease in percentage adsorption of Cu^{2+}as a result of decrease in the rate of diffusion caused by low mobility of the metal ion. On the other hand, a slight increase in perentage adsorption of $Cu^{2+}$was obtained by increasing both the temperature and time. These result agrees well with the result obtained by Hamadi *et al*. (2001) and Mekonnen *et al*. (2015).

5.13.4Study of the interactions between the parameters for Cu^{2+} removal from the multi elemental system

5.13.4.1 Interaction between concentration and temperature for Cu^{2+} sorption onto CFK composite

In Appendix XX, the lines converge at one end which implies they will eventually cross over each other and thus signifies an interaction between the temperature and concentration. At high temperature,whether the concentration is high or low, percentage adsorption of Cu^{2+} was higher than at low temperatures in the range of the parameter levels studied. However, increasing the concentration leads to a significant decrease in the percentage adsorption of Cu^{2+} and conforms to the findings by Mtaallah *et al*.(2017).

5.13.4.2 Interaction between time and concentration for Cu^{2+} sorption onto CFK composite

Appendix XXI shows a plot of the interation between time and concentration.

The result indicated that the two lines are not only parallel but are also far apart, indicating no interaction between the two independent variables within the range of the parameters chosen and

tetsed in this study. This further confirm the result of analysis of variance (ANOVA) in Table 4.15with Prob > F value of 0.5692 for the AC, implying that the interaction term AC (concentration and time) is not significant. It has also been observed that at low concentration,whether the time is short or long, the percentage adsorption of Cu^{2+} is always significantly higher thanwhen the concentration is high. The result is also similar to the report by Gul.(2016).

5.13.4.3 Interaction between time and temperature for Cu^{2+} sorption onto CFK composite

The lines in Appendix XXI are not parallel but rather are crossing over each other which signifies an interaction between the temperature and time. There was no significant change in percentage adsorption of Cu^{2+} due to either change of time or temperature at the center level of concentration. However, a slight increase in perentage adsorption of Cu^{2+} was obtained at both high temperature and time than at higher temperature and lower time. This conforms to the report put forward by Mtaallah *et al*.(2017).

5.13.4.4 Analysis of cube plot for Cu^{2+} sorption onto CFK composite

Appendix XXIII shows the cube plot for Cu^{2+} from the solution. It can be inferred from this result that, at 25^{o}C, 10 min and 100ppm, 76.79% of Cu^{2+} was predicted to be removed from the multi- component system but when the temperature was increased to 75^{o}C, percentage adsorption was predicted to be 76.31% reflecting insignificant temperature effect on adsorption of Cu^{2+} at low concentration. However, when the concentration was increased to 200ppm at 10 min, it was 50.85% removal of Cu^{2+} at 25^{o}C and 53.55% removal at 75^{o}C representing a 2.7% rise in adsorption.

There was a significant reduction in adsorption from 76.79% at 100ppm, 25^{o}C and 10min to 50.85% at 200ppm under the same condition of temperature and time.The 76.31% removal of

Cu^{2+} at 100ppm as against 53.55% at 200ppm both at 75^{o}C (22.76% difference) shows a decrease in adsorption due to increase in concentration of the adsorbate. On the other hand, when the time was increased to 60min, predicted percentage adsorption was observed to be lower at lower temperature (25^{o}C) and increases slightly at higher temperature (75^{o}C) for all concentrations studied. This interpretation is consistent with that of Mtaallah *et al*. (2017) in his work on full factorial design applied to cadmium adsorption onto activated alumina.

5.14 Statistical Analysis of the Model for Ni^{2+} Sorption onto CFK Composite

5.14.1 Analysis of variance (ANOVA) for response surface quadratic model for Ni^{2+}sorption onto CFK composite

The Design Expert software version 7.0.0 was used to analyse the fitness of the model base on analysis of variance (ANOVA), and the results of the model is as presented in Table 4.18. The model produced an F-value of 234.23 with a low p-value ($P<0.0001$) which denotes that the model is significant similar to the work ofGul.(2016).

There is only a 0.01% chance that a model with such a high F- value could be due to noise. Values of Prob > F less than 0.0500 as shown in the Table 4.18 indicates that certain model terms are significant while others are not. In this case A, B, AB, BC, A^2, C^2 are significant model terms.

Values greater than 0.1000 indicate that the model terms are not significant, in this case, the model terms C, $B^2$and the interaction term due to AC are not significant.

5.14.2 Analysis of the quadratic model statistical values for Ni^{2+}sorption onto CFK composite

Table 4.19 shows the model R-square value of 0.9674 is nearer to unity and implies that the quadratic model fits best for the observed adsorption of Ni^{2+} onto the composite CFK. The Predicted R-squared value of 0.9576 is in reasonable agreement with the adjusted R-squared value of 0.9633 (difference is less than 0.2). This is consistent with the interpretation given by Gul. (2016).

Adequate precision measures the signal to noise ratio of an experiment and a ratio greater than 4 is desirable. The ratio of 45.788 for adsorption of Ni^{2+} in this work is well above 4 and thus implies that the signal is adequate, the model can therefore be used to navigate the design space for Nickel metal. The standard deviations of the predicted model was found to be 1.73.

5.14.3 Analysis of the coefficient estimates and parameter interactions of the empirical models for Ni^{2+} sorption onto CFK composite

The coefficient estimates and parameter interactions of the empirical models are tabulated in Table 4.20 and further affirmed in the model equation in terms of coded factors below (equation 15).

Final equation in terms of coded factors for Ni^{2+}:

$$Ni = +62.31 - 9.70 * A + 1.95 * B + 0.36 * C - 0.66 * A * B + 0.051 * A * C - 2.20 * B * C$$

$$-6.64 * A^2 + 0.51 * B^2 - 0.91 * C^2 \quad (15)$$

The estimated coefficient values calculated for main effects of the process variables as shown in Table 4.20 and equation 15, reveals that concentration has the highest negative effect (-9.70) on the Ni^{2+} removal efficiency of the adsorbent CFK. This implies that the higher the concentration, the lower the adsorption of Ni^{2+}. On the other hand, temperature has positive

effects (1.95). This means that the higher the temperature, the higher the efficiency of adsorption for Ni^{2+} from the solution while time has an insignificant effect on the percentage removal of Ni^{2+}. The interaction terms AB and BC have negative effects and AC has no significant effect. The quadratic terms A^2 and C^2 have negative effects while B^2 has positive effect on the percentage sorption of $Ni^{2+}$and this is similar to the report by Gul.(2016).

5.14.4Analysis of the normal probability plot for Ni^{2+}sorptiononto CFK composite

The normal probability plot is used to check for normality of residuals for Ni^{2+}. As can be seen from the normal probability plot of internally studentized residuals in Appendix XXIV, it indicates a good normality with a good shape as most points lied on the straight line for Ni^{2+} adsorption from the solution. This deduction conforms with the report by Gul. (2016) in his work on full factorial design.

5.14.5Analysis of predicted versus actual values for Ni^{2+} sorption onto CFK composite

The plot of the predicted versus actual values is as shown in Appendix XXV, the studentized residuals versus predicted values plot is used to check for constant error. The result showed that all the points are concentrated or randomly scattered around the straight line. This is a very good indication that the experimental values obtained had good relationship and closeness to the predicted values.

5.14.6Externally studentized residuals analysis for Ni^{2+} sorptiononto CFK composite

The externally studentized residual plot shown in Appendix XXVI is used to check for outliers. Any point that is located beyond the plus or minus 3.5 region is an outlier. It can be observed

from the result that, all the points are ramdomly sacattered within the permissible limit which implies that there are no outliers with respect to the experimental data reported for Ni^{2+} adsorption in this work.

5.15 Analysis of the Predicted Response (Ni^{2+}) of the Process to the Independent Variables

This was carried out using graphs in the form of contours and in three dimensional (3D) space to help to visualize the shape of the response surface in respect to the operating experimental data.

5.15.1 Effect of concentration and temperature on the adsorption of Ni^{2+} from the solution

Appendices XXVIIa and XXVIIb show the effect of concentration and temperature on the percentage adsorption of Ni^{2+} from the multi- elemental solution using CFK composite at the centre level of time (35 min) . It can be observed from the resultsthat, at a higher temperature and at lower concentration, a higher percentage removal of Ni^{2+} from the solution was obtained when the time was fixed at 35 minute. This implies that, increase in temperature favours increase in Ni^{2+} adsorption from the bulk solution due to increase in the rate of difusion of the adsorbate molecules onto the boundary layer and into the internal pores of the adsorbent ocasioned by increase in the mobility of metal ion.The sorption process is therefore endothermic.

Within the limits of the tested parameters in this work, adsorption decreases significantly as the concentration of the metal is being increased. This can be attributed to the increase in the concentration of the adsorbate as against a fixed number of available active sites on the adsorbent which soon become occupied and reaches equilibrium. This explanation is consistent with that of Mekonnen *et al.* (2015).

5.15.2 Effect of concentration and time on the adsorption of $Ni^{2+}$from the solution

AppendicesXXVIIIa and XXVIIIb illustrate the effect of time and concentration on the percentage adsorption of $Ni^{2+}$from the multi-elemental wastewater using CFK composite at the centre level of temperature ($50^{o}C$). It can be inferred from the results that, there is no significant change in percentage adsorption when the time is varied at low concentration in the range of the parameter levels analyzed and this also complements the result presented in Table 4.18 (ANOVA). However, percentage adsorption increases significantly as the concentration decreases at a constant time. On the other hand, increasing the concentration leads to a significant reduction in percentage adsorption of $Ni^{2+}$from the solution due to increase in the number of metal particles as against fixed number of active sites. The adsorbent active sites have now been fully occupied. This is similar to the deduction made by Mekonna *et al*. (2015).

5.15.3 Effect of time and temperature on the adsorption of $Ni^{2+}$from the solution.

Appendices XXIXa and XXIXb illustrate the effect of time and temperature on the percentage adsorption of $Ni^{2+}$from the multi- elemental wastewater using CFK composite at the centre level of concentration (150ppm). As can be seen from the results, there is no sinificant change in percentage adsorption of Ni^{2+}due to varation of time and temperature at the center level of concentration and adsorption is generally low at all conditions verified. However, decreasing the temperature and increasing the time leads to a slight decrease in percentage adsorption of Ni^{2+}. This is because, at low temperature, adsorbate molecules move slowly and as such, rate of difusion is low. Also, at longer time, desorption sets in, though a slight increase in perentage adsorption of Ni^{2+} was obtained by increasing the temperature and decreasing the time, similar to the work of Hamadi *et al*. (2001) and Mekonnen *et al*.(2015).

5.15.4Study of the interactions between the parameters for Ni^{2+} removal

5.15.4.1 Interaction between concentration and temperature for Ni^{2+} sorption onto CFK composite

Appendix XXX shows that, at high tempearture, be it at a low or high concentration, percentage adsorption of Ni^{2+} was always higher than when the temperature was low in the range of the parameter levels studied. However, increasing the concentration leads to a significant decrease in

the percentage adsorption of Ni^{2+} both at low and high temperatures, similar to the report by Mtaallah *et al*. (2017) in his work.

5.15.4.2 Interaction between concentration and time for Ni^{2+} sorption onto CFK composite

Appendix XXXI shows a plot of the interation between time and concentration. The result shows clearly that the two lines are parallel but are very close and appeared to converge at higher concentration. This implies that, within the range of parameters chosen in the course of this research and considering the relationship between time and concentration, there is no significant difference in percentage adsorption of Ni^{2+} when time is changed at a given concentration.

However, percentage adsorption continues to decrease at higher concentrations.This is a further confirmation of the result of analysis of variance (ANOVA) in Table 4.18 which gave Prob > F value of 0.8612 for the AC, indicating that the interaction term AC (concentration and time) is not significant. Gul. (2016) gave similar interpretation to this effect in his work.

5.15.4.3 Interaction between time and temperature for Ni^{2+} sorption onto CFK composite

The lines in Appendix XXXII are crossing over each other which indicates an interaction between the two variables(temperature and time). At lower temperature and longer time, percentage adsorption of $Ni^{2+}$is higher than at lower temperature and shorter time.

On the other hand, increasing the temperature and reducing the time leads to a signficant increase in percentage adsorption of Ni^{2+}. Therefore, time and temperature antagonistically affect adsorption of Ni^{2+} from the bulk solution. This is in agreement with the interpretation of Mtaallah *et al*. (2017) in his work.

5.15.4.4 Analysis of the cube plot for Ni^{2+}sorption onto CFK composite

Appendix XXXIII shows the cube plot for $Ni^{2+}$from the solution. It can be inferred from the result that, at 25^{o}C, 10 min and 100ppm, 59.84% of $Ni^{2+}$was predicted to be removed from the multi- component system but when the temperature was increased to 75^{o}C, percentage adsorption was predicted to rise to 69.47% signifying a 9.63% increase in adsorption, but when the concentration was increased to 200 ppm at 10 min, still at 25^{o}C, Ni^{2+} adsorption decreases to 41.66% representing a significant drop in adsorption at high concentration.

Furthermore, at 200ppm, when temperature was increased to 75^{o}C maintaining time at 10 min, percentage adsorption rose again to 48.64% but not as high as 69.47% at low concentration (100ppm) under this same condition of temperature and time implying that at high concentration, the favourability of increase in adsorption was not as strong as when the concentration is low.The 69.47% removal of Ni^{2+}at 100ppm as against 48.64% at 200ppm both at 75^{o}C (20.83% difference) shows a substantial decrease in adsorption due to increase in concentration of the adsorbate.

On the other hand, when the time was increased to 60 min, there was no substantial difference in adsorption with regard to temperature change but concentration still has prominent effect. At 100ppm, 64.88% was removed and at 200ppm, it dropped to 46.88% at the 25^{o}C consideration, and 65.69% at 100ppm for 75^{o}C consideration also dropped to 45.06% at 200ppm indicating that

adsorbate concentration has the most significant effect on Ni^{2+} adsorption. Similar explanation was given by Mtaallah *et al*. (2017) in his work.

5.16Analysis of the Predicted and Actual Values for Pb^{2+}, Cu^{2+} and Ni^{2+} Sorption onto CFK Composite

The predicted and experimental values are presented in Table 4.21. A total of 27 tests were conducted for the three-factor-three level full factorial design with three replication during this experimental study giving rise to a total of 81 runs but the average results of each triplicate are presented.

The actual data collected from the tests were used to construct the empirical models representing the heavy metal removal efficiency as process response to the independent variables considered. Table 4.21 also shows the predicted responses of the process variables. Based on this, model equations for the three responses of Pb^{2+}, Cu^{2+} and Ni^{2+} ions removal from wastewater were generatedand they are as presented in equations 16, 17 and 18 below repectively:

Final equation in terms of actual factors for Pb^{2+}:

Pb =+86.51691+0.056781*Concentration+0.23451*Temperature+0.16301*Time-4.88000E-004*Concentration*Temperature7.77778E-005*Concentration*Time-1.90978E003

*Temperature*Time-1.79704E-004*Concentration^2-1.09126E-003*Temperature^2-1.06104E-003*Time^2(16)

Final equation in terms of actual factors for Cu^{2+}:

Cu = +27.26543 +0.91567*Concentration-0.12950*Temperature-0.14357*Time+6.35556E-004*Concentration*Temperature+1.31778E-004*Concentration*Time+1.12400E-

003*Temperature*Time-3.97415E-003*Concentration^2+4.52741E-004*Temperature^2+8.40296E-004*Time^2 (17)

Final equation in terms of actual factors for Ni^{2+}:

Ni = +17.55203+0.62806*Concentration+0.19934*Temperature+0.28664*Time-5.30889E-004 * Concentration*Temperature+4.04444E-005*Concentration*Time-3.51867E-003 * Temperature *Time-2.65659E-003*Concentration^2+8.16296E-004*Temperature^2-1.46281E-003*Time^2 (18)

As can be seen from Table 4.21, the differences between the actual or experimental values and the model's predicted values are relatively small and unbiased. This implies that the predicted values are in consistent with the observed experimental results, therefore,the models fit the data well.

5.17Process Optimization

The optimized independent variable levels for making the percentage adsorption maximum for the three responses (Pb^{2+}, Cu^{2+} and Ni^{2+}) were also determined using the numerical optimizationoptionof the optimization module of the Design Expert version 7.0.0 by utilizing thedevelopedmodels for each response tosearchthefactor space for the best combinations and conditions to obtaining the highest percentage adsorption in the range of the experimental parameters studied. The results show that a percentage adsorption of 97.03% for Pb^{2+}, 75.50% for $Cu^{2+}$and 66.26% for $Ni^{2+}$from the multi-elemental solution of Pb^{2+}, $Cu^{2+}$and Ni^{2+}can be achieved by adjusting the variables to the following levels: Concentration of 147.19ppm, temperature of 75^{o}C and time of 10 minute. This is in close agreement with the maximum adsorption data of 97.88% for Pb^{2+}, 76.99% for $Cu^{2+}$and 67.95% for Ni^{2+}obtained experimentally under the following conditions of concentration of 150ppm, temperature of 75^{o}C and time of 10 minute.

CHAPTER SIX

6.0 SUMMARY/CONCLUSION/RECOMMENDATION

6.1 Summary

The FTIR result showed the appearance of more bands in chicken feather-kaolin composite(CFK) which indicates the presence of more adsorbing groups on the surface of CFK than in kaolin (K) and chicken feather (CF) alone and that is why CFK was a better adsorbent for the metals (Pb^{2+}, Cu^{2+} and Ni^{2+}) adsorbedfrom the solution than individual K and CF.

The SEM micrograph revealed the kaolin(K) particles adhere to the surface of the chicken feather(CF). Therefore, the CF served as a base providing an efficient and strong support for K in forming the composite via hydrogen bonding,thus increasing the adsorption capacity of CFK with the presence of more number of hydroxyl, carboxyl, amino and alcohol groups and shows that the second theoretical assumption that CF could have K particles trapped in its entanglement through hydrogen bonding held sway and that inserting CF into the interplanar spacing of K did not work due to the fibrous nature of CF and its larger size.

XRD difractogram showed well defined peaks due to Kaolin in K, semi-crystalline nature of CF and an increased crystallinity in CFK which was indicated by the appearance of more peaks in CFK composite.

BET results corroborated the SEM and FTIR results by revealing an increase in the surface area of 352.5m^2/g in K to 424.8m^2/g in CFK and a pore volume increase from 21.66cc/g in K to 24.27cc/g in CFK, a characteristic that plausibly favours better ability to adsorb metals onto CFK. Though CF (711.9m^2/g) has a larger surface area than CFK (424.8 m^2/g), CFK has more groups on its surface which influences its sorption capacity positively upwards than individual K and CF.

Batch adsorption studies was carried out so as to understand the mechanism of adsorption through isotherm, thermodynamics, equilibrium and kinetic studies. The kinetic study was done using the pseudo-first order, pseudo-second order and intra-particle diffusion models respectively.

The equilibrium study was performed using the Langmuir isothermand the result shows that Ni^{2+} follows the monolayer route while Pb^{2+} and Cu^{2+} obey the Freundlich isotherm and Dubinin-Radushkevich isotherm result reveals that the adsorption process was by physisoption.Thermodynamic study was also performed and its result shows that the sorption process onto CFK composite was spontaneous and endothermic.

A three level full factorial design and Response Surface Methodology (RSM) was employed in order to optimize the process and understand the interactive effects of operating parameters. From this, the optimum conditions for the adsorption study was obtained and gave a percentage adsorption of 97.03% for Pb^{2+}, 75.50% for $Cu^{2+}$and 66.26% for $Ni^{2+}$from the multi-elemental

solution containing Pb^{2+}, $Cu^{2+}$and Ni^{2+}, achieved at concentration 147.19 ppm, temperature of 75^{o}C and time of 10 minute.

6.2 Conclusion

TheCFK composite was used to sorb Pb^{2+}, Cu^{2+} and Ni^{2+} from a multi-elemental system. The order of preference for the sorption was Pb^{2+}> Cu^{2+}> Ni^{2+}.

The study of the pseudo-first order and pseudo-second order models revealed that the adsorption process follows the pseudo-second order model.

The intra-particle diffusion model revealed a two stage adsorption process, a rapid initial stage and slow second stage which was followed by equilibrium stage.

The equilibrium studies revealed that, while both Langmuir and Freundlich isotherms were possible mechanism routes for Cu^{2+} and Ni^{2+}, though Cu^{2+} fits better than Ni^{2+}; Pb^{2+}on the other hand, fits into Freundlich isotherm only. Ni^{2+} followed a monolayer adsorption process while Pb^{2+} and Cu^{2+} followed the heterogeneous route.

The Dubinin-Radushkevich isotherm study showed that the adsorption mechanism was through physisorption. This was also corroborated by the result of the thermodynamic studies which showed low heat of adsorption that corresponds to the physisorption process.

The thermodynamic studies revealed that the adsorption process is spontaneous, endothermic and accompanied by an entropy increase.

The full factorial design and response surface methodology for the optimization indicated that the percentage adsorbed was 97.03% for Pb^{2+}, 75.50% for Cu^{2+} and 66.26% for Ni^{2+} from the multi-elemental solution, achieved by adjusting the variables to the following levels: Concentration of 147.19 ppm, temperature of 75^{o}C and time of 10 minute.

6.3 Recommendation

1. In this study, simulated wastewater was used. It is therefore recommended that further studies using industrial effluents be done.

2. Sodium acetate was used as the intercalating agent due to its affordability, but other intercalating agents should be employed for further studies.

6.4 Contribution to Knowledge

The result of this study creates a base for the use of CF, K and CFK for large-scale production of non-conventional adsorbents, thereby offering a lot of promising benefits for commercial purposes in the future.

The result further projects that this low-cost adsorbent will perform well in removing heavy metals at low cost and can be adopted and extensively used in the industries not only to minimize cost, but also to increase profitability.

The study also reveals a classic case of having the bye-product of an industry (chicken feather, a hitherto waste product of the poultry industry) becoming as important as the product itself.

Part of its contribution to knowledge was that, the living organisms and the surrounding environment will also benefit as a result of the decrease or elimination of potential toxicity which may be caused either by the presence of solid wastes generated by chicken feathers in the environment or heavy metals in water thus contributing to the maintenance and sustenance of the surrounding environment by significantly reducing the overall percentage of heavy metals in wastewater, thus having a significant impact on public health.

Furthermore, the optimization study revealed that, within the parameter limits used in this research, the factor combination for optimum adsorption is: Concentration of 147.19 ppm, temperature of 75^{o}C and time of 10 minute.

REFERENCES

Abdelwahab, O. (2007). Kinetics and isotherm studies of copper (II) removal from wastewater using various adsorbents.*Egyptian Journal of Aquatic Research*, 33(1),125-143.

Adebowale, K.O., Unuabonah, I.E. and Olu-Owolabi, B.I. (2005).Adsorption of some heavy metal ions on sulfate and phosphate-modified kaolin.*Applied Clay Science*.29, 145–148.

Adeyemo, A. A., Adeoye I.O. and Bello, O.S. (2015). Adsorption of dyes using different types of clays: A review.*Applied Water Science,*5(4), 407-423.

Adeyinka, S.Y., Idowu, I.O. and Sorphia, E.E. (2017).Thermodynamic studies of the adsorption of heavy metals from aqueous solution by thermally treated quail egg shell. *Journal of Environmental Science and Technology*, 10, 245-257.

Ada, K., Ergene, A., Tan, S. and Yalcin, E. (2009). Adsorption of remazol brilliant blue-R using ZnO fine powder: equilibrium, kinetic and thermodynamic modeling studies. *Journal of Hazard Materials*. 165, 637–644.

Afrodita, Z. and Mirjana, G. (2014).Effect of competing cations (Cu, Zn, Mn, Pb) adsorbed by natural zeolite.*International Journal of Science, Engineering and Technology*. 02(5), 483-492.

Al-Asheh, S.,Fawzi, B. and Dheaya, A.(2002).Adsorption of copper, zinc and nickel ions from single and binary metal ion mixtures on to chicken feathers. *Adsorption Science and Technology*, 20(9), 407-423.

Al-Asheh, S., Banat, F.and Al-Rousan, D. (2003).Beneficial reuse of chicken feathers in removal of heavy metals from wastewater.*Journal of Cleaner Prod*uction,11, 321–326.

Aluigi, A., Vineis, C., Varesano, A., Mazzuchetti, G., Ferrero F. and Tonin, C. (2008). Structure and properties of keratin/poly ethylene oxide (PEO) blend nanofibres. *European Polymer Journal*, 44(8), 2465-2475.

Ara´ujo, E. M., M´elo, T. J. A., Santana, L. N. L., Neves,G.A., Ferreira, H.C.,Lira, H.L., …. Araújo, I.S. (2004).The influence of organo-bentonite clay on the processing and mechanical properties of nylon 6 and polystyrene composites.*Materials Science and Engineering B*, 112(2-3),175–178.

Arias, M., Barral, M.T. and Mejuto, J.C. (2002).Enhancement of copper and cadmium adsorption on kaolin by the presence of humic acids.*Chemosphere*, 48, 1081–1088.

Ashori, A. (2008). Wood-plastic composites as promising green-composites for automotive industries.*Bioresource Technology*, 99, 4661-4667.

Asmatulu, R. (2002).Removal of discolouring contaminants of an east Geogia kaolin clay and its dewatering.*Turkish Journal of Engineering and Environmental Sciences*, 26(5), 447-453.

Auta, M. and Hameed, B.H. (2012).Modified mesoporous clay adsorbent for adsorption isotherm and kinetics of methylene blue.*Chemical Engineering Journal*, 198**–**199, 219–227.

Barone, J. R. and Schmidt, W. F. (2005). Polyethylene reinforced with keratin fibers obtained from chicken feather. *Composites Science and Technology*, 65, 173-181.

Bergeson, L. L. (2008). The proposed lead NAAQS: Is consideration of cost in the clean air act's future?.*Environmental Quality Management*, 18(1), 79-84.

Bhattacharyya, K.G. and Gupta, S.S. (2011). Removal of Cu(II) by natural and acid-activated clays: An insight of adsorption isotherm, kinetic and thermodynamics. *Desalination*, 272, 66–75.

Bhattacharyya, K. G. (2008). Adsorption of a few heavy metals on natural and modified kaolinite and montmorillonite: a review, *Advances in Colloid and Interface Science*,140(2), 114–131.

Bi, C., Long, Y., Xia, L.and Jessica. L.W. (2016). Poultry keratin based decolorants for dyeing wastewater treatment.*Journal of Bioresources and Bioproducts*, 1(1), 30-35.

Carrillo, F.J., Macanás, X., Colom, J., Cañavate, G., Molins, M.D. and Álvarez, N.G. (2012). Use of chicken feathers waste for the fabrication of composite materials. *15th European Conference on Composite Materials*, Venice, Italy, 1-8.

Chantawong, V., Harvey, N.W. and Bashkin, V.N. (2001).Comparison of heavy metal adsorptions by thai kaolin and ballclay.*Asian Journal of Engineering and Environmental science.* 1, 33–48.

Cheung, H.Y., Ho, M.P., Lau, K.T.and Cardona, F.H.D.(2009).Natural fibre-reinforced composites for bioengineering and environmental engineering applications. *Composites, Part B*, 40,655-663.

Churchman, G.J. (2002).Formation of complexes between bentonite and different cationic polyelectrolytes and their use as sorbents for non-ionic and anionic pollutants.*Applied Clay Science*, 21(3-4),177–189.

Dąbrowski, D. (2001).Adsorption— from theory to practice, *Advances in Colloid and Interface Science*, 93(1-3),135-224.

Dalida, M.L.P., Mariano, A.F.V., Futalan, C.M., Kan, C.C., Tsai, W.C. and Wan, M.W. (2011).Adsorptive removal of Cu(II) from aqueous solutions using non-crosslinked and crosslinked chitosan-coated bentonite beads. *Desalination*, 275, 154–159.

Das, B. and Modal, N.K. (2011). Calcerous Soils a New Adsorbent to Remove Lead from Aqueous Solution: Equilibrium, Kinetics and Thermodynamic Studies. *UniversalJournal Environmental Resource and Technology*, 1(4), 515-530.

Davydova, S.(2005).Heavy metals as toxicants in big cities.*Microchemical Journal*,79, 133–136.

Débora D. B., Rasiah L., Loilde, D. B., Juliana, R., de, M.P., Brismark, G., da Rocha, A.O.G. andSania, M.B.D. (2012).Physical and morphological structure of chicken feathers (keratin biofibre) in natural, chemically and thermally modified forms. *Materials Sciences and Applications*,3, 887-893.

De la Rosa, G., Reynel-Avila, H. E., Bonilla-Petriciolet, A., Cano-Rodriguez, I., VelascoSantos, C. and Martinez-Hernandez, A. L. (2008). Recycling poultry feathers for Pb^{2+} removal from wastewater: kinetic and equilibrium studies. *International Journal of Chemical and Biomolecular Engineering,* 1, 185-193.

Demirbas, E. (2003). Adsorption of cobalt (II) from aqueous solution onto activated carbon prepared from hazelnut Shells. *Adsorption Science and Technology*, 21, 951- 963.

Deng, Y., White, G. N.and Dixon, J. B. (2002).Intercalation and surface modification of smectiteby two Non- anionic Sulfactant.*Journal of Colloid and Interface Science*,250, 379.

Dos-Santos, V.C.G., Grassi, M.T. and Abate, G. (2015). Sorption of Hg(II) by modified K10 montmorillonite: influence of pH, ionic strength and the treatment with different cations. *Geoderma*, 237–238, 129–136.

Dubinin, M.M. (1960). The Potential Theory of Adsorption of Gases and Vapors for Adsorbents with Energetically Non- uniform Surface. *Chemical Review*, 60, 235-266.

Egwuatu, C.I., Umedum, N.L., Anarado, C.J.O. and Eboatu, A.N. (2014).Chicken feather as sequestrant for lead ions in aqueous solution.*International Journal of Modern Analyticaland Separation Sciences,* 3(1), 51-66.

Ekici, S., Is,ıkver, Y. and Saraydın, D. (2006). Poly (acrylamide-sepiolite) composite hydrogels: preparation, swelling and dye adsorption properties. *PolymerBulletin*,57(2),231– 241.

Elbokl, T.A. and Detellier, C. (2006). Aluminosilicate nanohybrid materials: Intercalation of polystyrene in kaolinite. *Journal of Physical and Chemistry of Solids*, 67, 950 – 955.

Food and Agriculture Organization of the United Nations.(2010). Agribusiness Handbook: Poultry meat and Eggs. *Investment Centre Division.FAO*. *Rome, Italy*, 1-77.

Freundlich, H.M.F. (1906). Uber die adsorption in Losungen. Z. *Physical Chemistry*-Leipzig, 57A, 385-470.

Frost, R.L., Kristof, J., Schmidt, J.M. and Kloprogge, J.T. (2001).Raman spectroscopy of potassium acetate-intercalated kaolinites at liquid nitrogen temperature.*Spectrochim Acta A Molecular and Bimolecular Spectroscopy*, 57, 603-609.

Gao, X.J., Riabinina, O., Li, J., Potter, C.J., Clandinin, T.R. and Luo, L. (2015). A transcriptional reporter of intracellular Ca^{2+} in *Drosophila*. *Nature Neuroscience*, 18(6), 917-925.

Greenwold, M.J. and Sawyer, R.H. (2011).Linking the molecular evolution of avian beta (β) keratins to the evolution of feathers.*Journal of Experimental Zoology Part B: Molecular and Developmental Evolution*,316B, 609–616.

Golub, M.S.(2005).Metals, fertility and reproductive toxicity.*CRC Press, Boca Raton Florida, USA*, p. 153.

Guhados, G., Wan, W. and Hutter J.L. (2005).Measurement of the elastic modulus of single bacterial cellulose fibres using atomic force microscopy. *News Releases*, 21, 6642-6646.

Gul, A.S. (2016).Application of full factorial experimental design and response surface methodology for chromite beneficiation by knelson concentrator.*Minerals,* 6(5), 10.

Gupta, S. S.andBhattacharyya, K. G. (2006). Removal of Cd(II) from aqueous solution by kaolinite, montmorillonite and their poly(oxo zirconium) and tetrabutylammonium derivatives. *Journal of Hardardous Materials*, 128(2-3), 247-57.

Gupta, V. K., Mittal, A., Kurup, L. and Mittal, J. (2006).Adsorption of a hazardous dye, erythrosine, over hen feathers.*Journal of Colloid and Interface Sciences,*304, 52-57.

Gupta, V.K. and Suhas, L. (2009).Application of low-cost adsorbents for dye removal – A review.*Journal of Environmental Management,* 90, 2313–2342.

Hamadi, N.K., Chen, X.D., Farid, M.M. and Lu, M.G.Q. (2001). Adsorption kinetics for the removal of chromium(VI) from aqueous solution by adsorbents derived from used tyres and sawdust, *Chemical Engineering Journal*, 84, 95–101.

Hazrat, A., Khan, E. and Saja, M.A. (2013).Phytoremediation of heavy metals—Concepts and applications.*Chemosphere*, 91, 869–881.

Ho, Y.S.and McKay, G. (1999). Pseudo-second order model for sorption processes. *Process Biochemistry,* 34, 451–465.

Hughes, M.F. (2002). Arsenic toxicity and potential mechanisms of action. *Toxicology Letters*, 133, 1– 16.

Hui, K. S., Chao, C. Y. H. and Kot, S. C. (2005).Removal of mixed heavy metal ions in wastewater by zeolite 4A and residual products from recycled coal fly ash.*Journal of Hazardous Materials*, 127(1-3), 89-101.

Hussein, S.M., Shihab, O.H., Ibrahim, S.S. and Ahmed, N.M. (2015).Interaction between kaolin and urea in organoclay and its impact on removing methylene blue from aqueous solution.*World Journal of Nano Science and Engineering*, 5, 1-9.

Ijagbemi, C.O., Baek, M.H. and Kim, D.S. (2009).Montmorillonite surface properties and sorption characteristics for heavy metal removal from aqueous solutions.*Journal of Hazardous Materials*, 166, 538–546.

Ijagbemi, C.O., Baek, M.H. and Kim, D.S. (2010).Adsorptive performance of un-calcined sodium exchanged and acid modified montmorillonite for Ni^{2+} removal: Equilibrium, kinetics, thermodynamics and regeneration studies. *Journal of Hazardous Materials*, 174**,** 746–755.

Isabel, M.L., Kyung, S., Ro, G. B., Reddy, D. L. B. and Klasson, K. T. (2015).Efficacy of chicken litter and wood biochars and their activated counterparts in heavy metal clean up from wastewater. *Agriculture*,5(3), 806-825.

Isah, A.L. (2010 June, 6). Death toll in Zamfara lead poisoning hits 300*, The Guardian*, pp. 1-2.

Ismadji, S., Soetaredjo, F.E. and Ayucitra, A.(2015).Clay materials for environmental remediation.*Springer Briefs in Green Chemistry for Sustainability*, 25, 1-124.

Itagaki, T., Komori, Y., Sugahara.and Kuroda, K. (2001). Synthesis of a kaolinite–poly(β-alanine) intercalation compound.*Royal Society of Chemistry,* 11, 3291-3295.

Jia, X., Li, Y., Zhang, B., Cheng, Q.and Zhang, S. (2008).Groundwater arsenic contamination in Bangladesh and West Bengal, India.*Material Resources Bulletin,* 43, 611.

Jiang, M., Jin, X., Lu, X. and Chen, Z. (2011). Adsorption of Pb(II), Cd(II), Ni(II) and Cu(II) onto natural kaolinite clay. *Desalination,*252, 33–39.

Jusheng, L. and Xin W. (2013). Novel Silica-Based Hybrid Adsorbents: Lead(II) Adsorption Isotherms, *The Scientific World Journal*.2013, 577-584.

Kadirvelu, K. and Namasivayam, C. (2000). Agricultural by-products as metal adsorbents: sorption of lead (II) from aqueous solutions onto coir-pith carbon. *Environmental Technology,* 21(10),1091-1097.

Kar, P. and Misra M. (2004).Use of keratin fibre for separation of heavy metals from water. *Journal of Chemical Technology and Biotechnology,* 79,1313-1319.

Karthikeyan, T., Rajgopal, S. and Miranda, L.R. (2005). Chromium (VI) adsorption from aqueous solution by Hevea brasilinesis sawdust activated carbon. *Journal of Hazardous Materials*, 124, 192–199.

Kelle, H.I. and Udeozo, I.P. (2015). Assessment of crude oil mopping efficiency of ground chicken feathers: Kinetic and adsorption isotherm studies. *American Chemical Science Journal,* 9(4), 1-19.

Kelleher, B.P., Sutton, D.and Odwyer, T.F. (2002).*The effect of kaolinite intercalation on the structural arrangements of* N-*methylformamide and 1-methyl-2-pyrrolidone*.*Journal of Colloid and Interface Science,* 255, 219.

Keskinkan, O., Göksu, M.Z.L., Başıbüyük, M. and Forster, C.F. (2004). Heavy metal adsorption properties of a submerged aquatic plant (Ceratophyllumdemersum). *BioresourceTechnology,* 9, 197–200.

Khan, S.A., Riaz-ur-Rehman, A. and Khan, M.A. (1995). Adsorption of Cr(III), Cr(VI) and silver (I) on Bentonite.*Waste Management,* 155(4), 271–282.

Khosa, M.A. and Ullah A.A. (2013). Sustainable Role of Keratin Biopolymer in Green Chemistry: A Review. *Journal of Food Processing & Beverages,* 1(1), 8.

Khosa, M.A., Wu, J. and Ullah, A. (2013).Chemical modification, characterization, and application of chicken feathers as novel biosorbents.*Royal Society of Chemistry Advances*, 10, 1038.

Kirschner, D.A., Inouye, H., Duffy, L.K., Sinclair, A., Lind, M. and Selkoe, D.J. (1987). Synthetic peptide homologous to beta protein from Alzheimer disease forms amyloid-like fibrils in vitro. *Proceedings of the National Academy of Sciences*, 84, 6953–6957.

Komori, Y.and Koroda, K. (2000).Polymer clay nano composites, John Wiley and Sons, England, p. 3-16.

Kowshik, C.S.S., Hiremath, P., Shettar, M. and Naik, N. (2017). A study on chicken feather filled hybrid glass fibre-polymer composite. *Materials Science Forum*, 904, 151–154.

Králik, M. (2014).Adsorption, chemisorption, and catalysis.*Chemical Papers*, 68, 10.

Lagergren, S. (1898).About the theory of so-called adsorption of soluble substances.*Kungliga Svenska Vetenskapsakademiens Handlingar*, 24, 1-39.

Langmuir, I. (1916). The Constitution and Fundamental Properties of Solids and Liquids.*Journal of American Chemical Society*, 38, 2221-2295.

Lawrence, C.E., Simon, O.G., Oyewemi, A.I. and Solomon, G.B.(2013).Kinetics of adsorption of nickel ion on kankara kaolinite.*Journal of Practices and Technologies*,22,83-92.

Leeson, S. and Walsh, T. (2004). Feathering in commercial poultry—II. Factors influencing feathergrowth and feather loss.*World's Poultry Science Journal*,60,52–63.

Li, A., Zhang, J. and Wang, A. (2007).Preparation and slow-release property of a poly (acrylic acid)/attapulgite/sodium humate superabsorbent composite.*Journal of Applied Polymer Science*,103.

Li, Q., Wu, S., Liu, G., Liao, X., Deng, X., Sun, D., Hu, Y. and Huang, Y. (2004).Simultaneous biosorption of cadmium (II) and lead (II) ions by pretreated biomass of Phanerochaetechrysosporium.*Separation, Purification and Technology*,34, 135–142.

Ma'rquez, G.E., Ribeiro, M.J.P. and Ventura, L.J.M.J.A. (2004). Removal of nickel from aqueous solutions by claybased beds. *Ceramics International*, 30, 111–119.

Martínez, H. A.L., Velasco-Santos, C., de-Icaza M. and Castaño, V.M. (2007). Dynamical, mechanical and thermal analysis of polymeric composites reinforced with keratin biofibres from chicken feathers. *Composites: Part B*, 38,405-410.

McGaghie, W.C., Bordage, G.and Shea J.A. (2001). Problem statement, conceptual framework and research question. *Academic Medicine*, 76(9), 923-924.

McGovern, V. (2000).Recycling poultry feathers: more bang for the cluck.*Environmental Health Perspect*, 108(8), 366-369.

Mekonnen, E., Yitbarek, M. and Soreta, T.R. (2015). Kinetic and thermodynamic studies of the adsorption of Cr(VI) onto some selected local adsorbents. *South African Journal of Chemistry*, 68**,** 45–52.

Melia.G., Sorya, N.F., Fenouillot, R. and Nacerddine, H. (2012). Effects of kaolin surface treatments on the thermomechanical properties and onthe degradationof Polypropylene. *International Journal of Polymer Science*,2012,1-9.

Meyers, M.A., Chen, P.Y., Lin, A. Y.M. and Seki, Y. (2008). Biological materials: Structure and mechanical properties. *Progress in Material Science*, 53, 1–206.

Meziane, O., Bensedira A., Guessoum M. and Haddaoui, N. (2017). Preparation and characterization of intercalated kaolinite with urea, dimethyl formamide and an alkylammonium salt using guest displacement reaction. *Journal of Material and Environmental Sciences*, 8(10),3625-3635.

Mittal, A. (2006a).Use of hen feathers as potential adsorbent for the removal of a hazardous dye, brilliant blue FCF, from wastewater.*Journal of Hazardous Materials*, B128, 233-239.

Mittal A. (2006b).Adsorption kinetics of removal of a toxic dye, malachite green from waste water by using hen feathers.*Journal of Hazardous Materials*, 133, 196-202.

Molins, G., Álvarez, M.D., Garrido, N., Macanás, J. and Carrillo, F. (2012). Chicken feathers based composites: A life cycle assessment: 15th *European Conference on composite materials, Venice, Italy*, 276, 1-18.

Mtaallah, S., Marzouk, I. and Hamrouni, B. (2017). Factorial experimental design applied to adsorption of cadmium on activated alumina. *Journal of water reuse and desalination*, 8(1), 76-85.

Muhammad, A.K., Jianping, W.and Aman, U.(2013).Chemical modification, characterization, and application of chicken feathers as novel biosorbents.*Royal Society of Chemistry Advances*, 3(43), 20800-20810.

Murray, H.H.(2007).Applied clay mineralogy: Occurrences, processing and application of kaolins, bentonites, palygorskite-sepiolite, and common clays.*Clays and Clay Minerals*, 55(6), 644-645.

Nilsson, R. (1971). Removal of metals by chemical treatment of municipal wastewater.*Journal of Water Resources*,5, 51-60.

Ojo, M. (2016 May 1). Nigeria among 10 Countries without access to water.*The Nation*, pp. 54.

Olejnik, S., Posner, A.M. and Quirk, J.P. (1970).Kaolinite-pyridine intercalation compound derived from hydrated kaolinite. *Clays and Clay Minerals*, 8, 421-434.

Oliveira, L. C. A., Rios, R.V.R.A., Fabris, J.D, Sapag, K., Garg, V.K. and Lago R. M. (2003). Clay-iron oxide magnetic composites for the adsorption of contaminants in water. *Applied Clay Science*,22(4),169–177.

Onifade, A.A, Al-Sane, N.A., Al-Musallam, A.A. and Al-Zarban, S. (1998). A review: Potentialsfor biotechnological applications of keratin-degrading microorganisms and their enzymes for nutritional improvement of feathers and other keratins as livestock feed resources. *Bioresource Technology*, 66, 1-11.

Orhan, Y. and Buyukgungor, H. (1993).The removal of heavy metals by using agricultural wastes.*Water Scienceand Technology*, 28(2), 247-255.

Orumwense, F. (1996). Removal of lead from water by adsorption on a koalinitic clay. Journal of Chemical Technology & Biotechnology**,** 65, 363-369.

Pandey, S. and Mishra, S. B. (2011).Organic-inorganic hybrid of chitosan/organoclay bio nanocomposites for hexavalent chromium uptake.*Journal of Colloid and Interface Science*, 361(2),509–520.

Pandey, S. S. P., Sabi, S. K. and Sharma, S. S. (2009). Batch adsorption studies for the removal of Cu(II) ions by zeolite NaX from aqueous steam. *Proceedings of the World Congress on Engineering and Computer Science*, *San Francisco, U.S.A*, 1, 122-127.

Pandima, D.M. and Muthukumaran, C. (2013).Adsorption kinetics of acid brown dye from aqueous solution using biowaste,*Asian Journal of Science and Technology*, 4(08),001-005.

Pant, K.K.and Sing, T.S. (2004). Equilibrium, kinetics and thermodynamics study for adsorption of As(II) ions on activated alumina. *Separation and Purification Technology*, 3, 139-147.

Ping, S., Zhao-Tie, L. and Zhong-Wen, L. (2009). Particles from bird feather: A novel application of an ionic liquid and waste resource. *Journal of Hazardous Materials*, 170(2-3), 511-1282.

Poole, A.J., Church J.S. and Huson, M.G. (2009). Keratin as a protein biopolymer: Extraction from waste biomass and applications.*Biomacromolecules*, 10, 1–8.

Prum, R. O. and Brush, A.H.(2002).The evolutionary origin and diversification of feathers. *TheQuarterly Review of Biology*,77(3), 261-295.

Rai, A.K., Upadhyay, S.N., Kumar, S. and Upadhyay, Y.D. (1998). Heavy metal pollution and its control through a cheaper method: A review. *Journalof Indian Association for Environmental Management*, 25, 22-51.

Rajani, S. (2011).Advances in application of natural clay and its composites in removal of biological, organic and inorganic contaminants from drinking water.*Advances in Materials Science and Engineering*, 2011, 1-17.

Rajesh, K.K. and Kanjan U. (2014).Treatability study of low cost adsorbentsfor heavy metal removal from electroplating industrial effluent: A review.*International Journal of Chemical Technology Research*, 6(2),1446-1452.

Randall, J. M., Hautala, E. and McDonald, G. (1978). Binding of heavy metal ions by formaldehyde polymerized peanut skins. *Journal of Applied Polymer Science*, 22(2), 379-387.

Ratna, K. A. and Sobha, K. (2015).Cost effective and eco-friendly method for copper removal by adsorption with Emu feather (*Dromaius novaehollandiae*) and chitosan (*Agaricus bisporus*) composite.*International Journal of ChemTech Research*, 8(4),1769-1782.

Rintoul, L., Frost, R. L., Kristof, J. and Kloprogge, J. T. (2000).Raman spectroscopy of urea and urea-intercalated kaolinites at 77K.Spectrochim Acta A Molecular andBiomolecular Spectroscopy,56(9), 1681-1691.

Rizzo, N.W., Gardner, K.H., Walls, D.J., Keiper-Hrynko, N.M., Ganzke, T.S. and Hallahan, D.L. (2006). Characterization of the structure and composition of gecko adhesive setae. *Journal of the Royal Society Interface*, 3, 441–451.

Sachin, K., Achyut, K.P. and Singh R. K. (2013). Preparation and characterization of acids and alkali treated kaolin clay.*Bulletin of Chemical Reaction Engineering and Catalysis*,8(1), 61 – 69.

Sadeeq, A.G. (2010 June, 7). Zamfara releases 240 million naira over mining death, *Daily Trust*, pp. 2.

Salwa, A.A., Mohamed, A.T., Elham, M.A. and Mostafa, I.Q.(2015).Characterization and application of kaolinite clay as solid phase extractor for removal of copper ions from environmental water samples.*International Journal of Advanced Research,* 3(3), 1-21.

San, C. A.G., Castello, R., Luengo, M. and Vizcayno, C. (2009).Acid activation of mechanically and thermally modified kaolins.*Materials Research Bulletin*,44, 2103–2111.

Schmidt, W.F., Codling, E.E., Thomas, C.G. and Line, M. J. (1997).Binding of heavy metals ions to fibers and filters from poultry feathers. In *Proceedings of Nonwovens Conference* (pp. 105-107),Memphis, TN, TAPPI Press, Atalanta, GA.

Šćiban, M., Klašnja, M. and Škrbić, B. (2008). Adsorption of copper ions from water by modified agricultural byproducts. *Desalination*, 229, 170–180.

Sen, S.G. and Bhattacharyya, K.G. (2006). Removal of Cd(II) from aqueous solution by kaolinite, montmorillonite and their poly(oxo zirconium) and tetrabutylammonium derivatives: *Journal of Hazardous Materials*, 128(2-3),247–257.

Sharma, D.C.and Foster, C.F. (1994).A preliminary examination into the adsorption of hexavalent chromium using low-cost adsorbents.*Bioresource Technology*, 47, 257–264.

Singh, A.K. Singh, D.P. and Singh, V.N. (1988).Removal of Zn(II) from water by adsorption on Chinaclay.*Environment Technological Letter,* 9(10), 1153 -1162.

Suyam, K., Fukazawa, Y.and Sukumura, H. (1996).Biosorption of precious metal ions by chicken feather.*Applied Biochemistry and Biotechnology*, 57/58,67-74.

Tesfaye, T., Sithole, B., Ramjugernath, D. and Chunilall, V. (2017). Valorisation of chicken feathers: Characterisation of physical properties and morphological structure. *Journal of Cleaner Production,*149, 349–365.

Thyagarajan, D., Barathi, M. and Sakthivadivu, R. (2013).Scope of poultry waste utilization. *Journal of Agriculture and Veterinary Science*, 6(5), 29-35.

Trevino, C. H., Jua´ rez-Aguilara, L.G., Mendoza-Castilloa, D.I., Hernández-Montoya, V., Bonilla-Petriciolet, A. and Montes-Morán, M.A. (2013) Synthesis andadsorption properties of activated carbons from biomass of *Prunus domestica and Jacaranda mimosifolia*for the removal of heavy metals and dyes from water. *Industrial Crops and Products*, 42, 315– 323.

Ullah, A., Vasanthan, T., Bressler, D., Elias, A.L. and Wu, J. (2011). Bioplastics from feather quill. *Biomacromolecules*, 12, 3826-3832.

United States Department of Agriculture (USDA).(2014). Poultry—Production and Value. *National Agricultural Statistics Service,*Washington, DC, USA.

Van-Dam., J.E.G., and Bos, H.L. (2004).The environmental impact of fibre crops in industrial applications. *Food and Agriculture Organization of the United Nations*(*FAO), Rome,* pp. 33.

Van, O. H. (1977).An Introduction to Clay Colloid Chemistry,(2nd edition).*Wiley Interscience, NewYork, USA*,pp. 236-237.

Waid,O. and Hossam, A. (2007).Removal of Pb^{2+} ions from aqueous solutions by adsorption on kaolinite clay.*American Journal of Applied Sciences*,4(7), 502-507.

Wang, W., Li, A., Zhang, J. and Wang, A. (2008). Study on superabsorbent composite: Effect of thermal treatment and acid activation of attapulgite on water absorbency of poly(acrylicacid)/attapulgite superabsorbent composite.*Polymer Composites*,28(3),397–404.

Wang, Y. and Björn, L.O. (2014).Heavy metal pollution in Guangdong province, China, and the strategies to manage the situation.*Frontiers in Environmental Science,* 2, 1–12.

Weber, W. J. and Morris, J. C. (1963).Kinetics of adsorption on carbon from solution.*Journal* of*Sanitory Engineering Division. American Society of Civil Engineering*,89(SA2), 31-40.

Wu, J. and Ullah, A. (2013). Feather- based thermoplastics: Effects of different plasticizers on material properties.*Macromolar Materials and Engineering*, 298, 153–162.

Yan, G. Y. and Viraraghavan, T. (2001).Heavy metal removal in a biosorption column by immobilized *M. rouxii* biomass.*Bioresources Technology*, 78, 243-249.

Yavuz, O. and Saka, C. (2013).Surface modification with cold plasma application on kaolin and its effects on the adsorption of methylene blue.*Applied Clay Science*, 85, 96-102.

Yu, Y., Zhuang, Y.Y. and Wang, Z.H. (2001).Adsorption of watersoluble dye onto functionalized resin.*Journal of Colloid Interface Science*,242, 288–293.

Zaini, M.A.A., Amano, Y. and Machida, M. (2010). Adsorption of heavy metals onto activated carbons derived from polyacrylonitrile fibre. *Journal of Hazardous Materials*,180, 552–560.

Zarraa, M. A. (1995). A study on the removal of chromium (VI) from waste solutions by adsorption on to sawdust in stirred vessels.*Adsorption Science Technology*,12(2), 129-138.

Zhang, B., Li, Y., Pan, X., Jia, X. andWang B.(2007). Tailored organic-inorganic materials. *Journal of Physics and Chemistry of Solids*, 68, 135-142.

Zhang, X. R.and Xu, Z. (2007).Microwave-assisted intercalation of 1-alkanols and 1,ω-alkanediols into α-zirconium phosphate. Evidence of conformational phase transitions in the bimolecular film of alkyl chains.*Materials Letters*, 58(1-2), 95-101.

Zouboulis, A. I. and Kydros, K. A. (1993).Use of red mud for toxic metals removal: the case of nickel. *Journal of Chemical Technology and Biotechnology*, 58, 95-101.

APPENDICES

Appendix I: List of Chemicals

The chemicals used for this experiment are:

I. $Pb(NO_3)_2$ (purity: 99%).

II. $Cu(NO_3)_2.3H_2O$ (purity: 99%).

III. $NiCl_2.6H_2O$. (purity: 99%)

IV. Sodium acetate (purity: 99%).

V. Dilute hydrochloric acid (10%), 98% purity.

VI. Dilute sodium hydroxide (10%), 98 purity.

VII. Distilled water was used to prepare sample solutions and with detergents to wash the chicken feathers, Kaolin and other apparatuses.

Appendix II: List of Apparatuses Equipment

The following apparatuses and equipment are used in this study:

I. Glassware of various sizes: Measuring Cylinder, Conical flask, Crucible, water bath shaker, Whatman filter paper (size 42), Reagent bottles, Modern analytical balance (for weighing samples).

II. Thermometer for temperature determination.

III. pH meter (was used to measure the pH at every point in the process to ensure that it was kept constant).

IV. Fourier transform infrared spectrophotometer (FTIR).

V. Atomic adsorption spectrophotometer (AAS).

VI. Scanning electron Microscope (SEM).

VII. X-ray Diffraction Spectrophotometer (XRD).

VIII. Brunauer-Emmette-Teller (BET).

Appendix III: Calculations

Workings on the mass of the different metal salts used for the preparation of 1000 ppm multi-component stock solution of Pb^{2+}, Cu^{2+} and Ni^{2+}.

The formula mass of $Pb(NO_3)_2$ is 331 g and it is of 99% purity

The molar mass of Pb is 207 g, therefore the mass of $Pb(NO_3)_2$ needed to prepare 1000 ppm Pb is:

207 g Pb is contained in 331 g $Pb(NO_3)_2$, but 1 g of Pb is required to prepare 1000 ppm stock solution, therefore, 1 g Pb will be contained in 331/207 = 1.599 g $Pb(NO_3)_2$.

99% purity is: 100 * 1.599/99 = 1.615 g $Pb(NO_3)_2$.

The formula mass of $Cu(NO_3)_2.3H_2O$ is 242 g and it is of 99% purity.

The molar mass of Cu is 64 g, therefore the mass of $Cu(NO_3)_2.3H_2O$ needed to prepare 1000 ppm Cu is:

64 g Cu is contained in 242 g $Cu(NO_3)_2.3H_2O$, but 1 g of Cu is required to prepare 1000 ppm stock solution, therefore, 1 g Cu will be contained in 242/64 = 3.781 g $Cu(NO_3)_2.3H_2O$.

99% purity is: 100 * 3.781/99 = 3.819 g $Cu(NO_3)_2.3H_2O$.

The formula mass of $NiCl_2.6H_2O$ is 129.6 g and it is of 99% purity.

The molar mass of Ni is 58.7 g, therefore the mass of $NiCl_2.6H_2O$ needed to prepare 1000 ppm Ni is:

58.7 g Ni is contained in 129.6 g $NiCl_2.6H_2O$, but 1 g of Ni is required to prepare 1000 ppm stock solution, therefore, 1 g Ni will be contained in 129.6/58.7 = 2.208 g $NiCl_2.6H_2O$.

99% purity is: 100 * 2.208/99 = 2.23o g $NiCl_2.6H_2O$.

To get the volume of the stock solution required for the preparation of the 100 cm^3 of the different concentrations (50 ppm, 100 ppm, 150 ppm, 200 ppm and 250 ppm) used in this work, the serial dilution method (equation 1) was used:$C_1V_1 = C_2V_2$ or $V1 = C_2V_2/C_1$

For 50 ppm: C_1 = 1000 ppm, V_1= ?, C_2 = 50 ppm, V_2 = 100 cm^3

V_1 = 50 * 100/1000 = 5 cm^3

For 100 ppm: C_1 = 1000 ppm, V_1= ?, C_2 = 100 ppm, V_2 = 100 cm^3

V_1 = 100 * 100/1000 = 10 cm^3

For 150 ppm: C_1 = 1000 ppm, V_1= ?, C_2 = 150 ppm, V_2 = 100 cm^3

V_1 = 150 * 100/1000 = 15 cm^3

For 200 ppm: C_1 = 1000 ppm, V_1= ?, C_2 = 200 ppm, V_2 = 100 cm^3

V_1 = 200 * 100/1000 = 20 cm

For 250 ppm: C_1 = 1000 ppm, V_1= ?, C_2 = 250 ppm, V_2 = 100 cm^3

V_1 = 250 * 100/1000 = 25 cm^3

Appendix IV: Normal Plot for Pb^{2+} Sorption onto CFK Composite

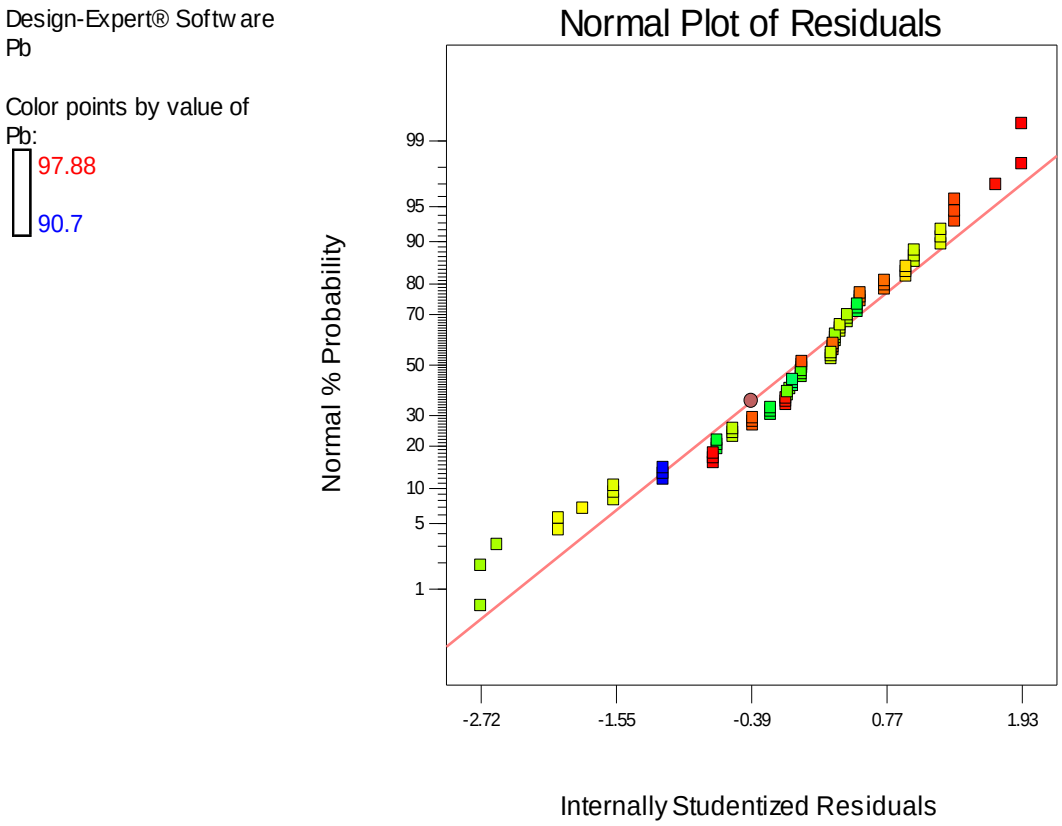

Appendix V: Predicted Versus Actual Plot for Pb^{2+} Sorption onto CFK Composite

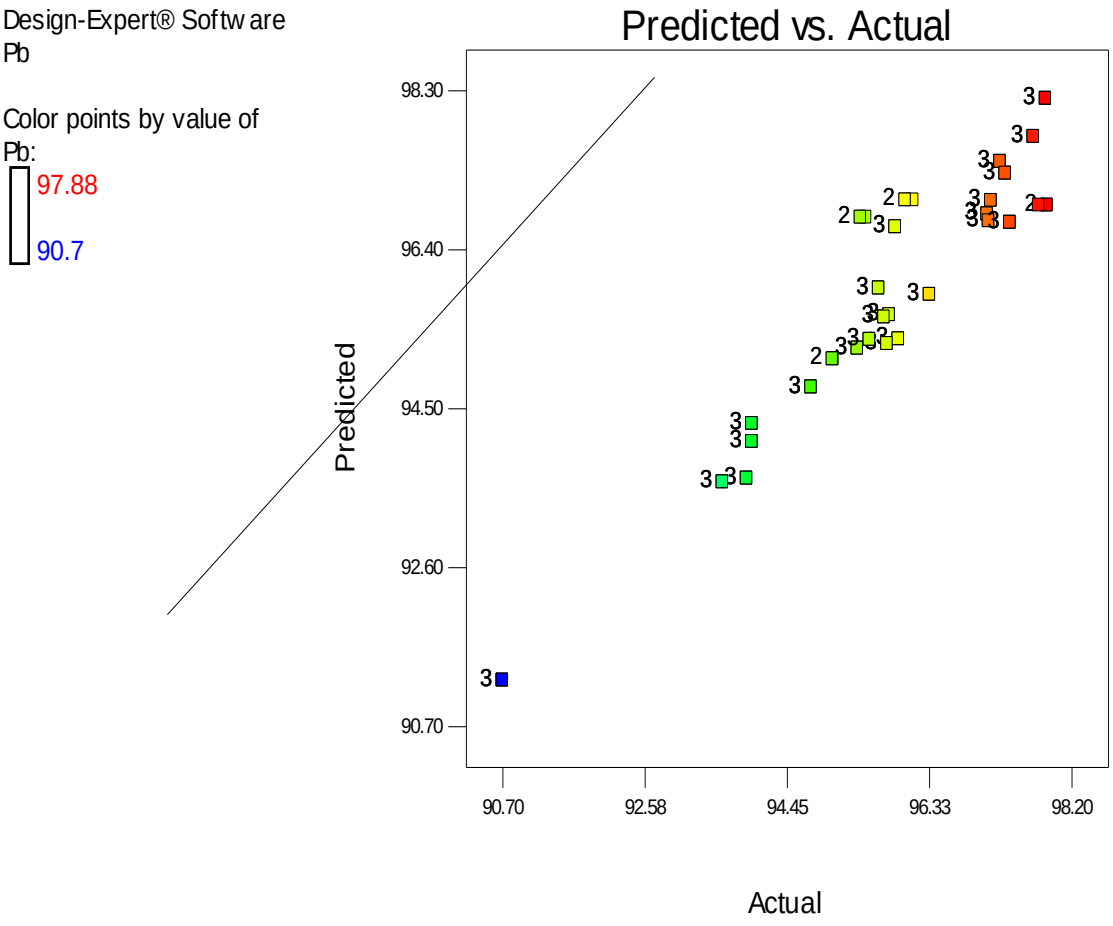

Appendix VI: Externally Studentized Plot for Pb^{2+} Sorption onto CFK Composite

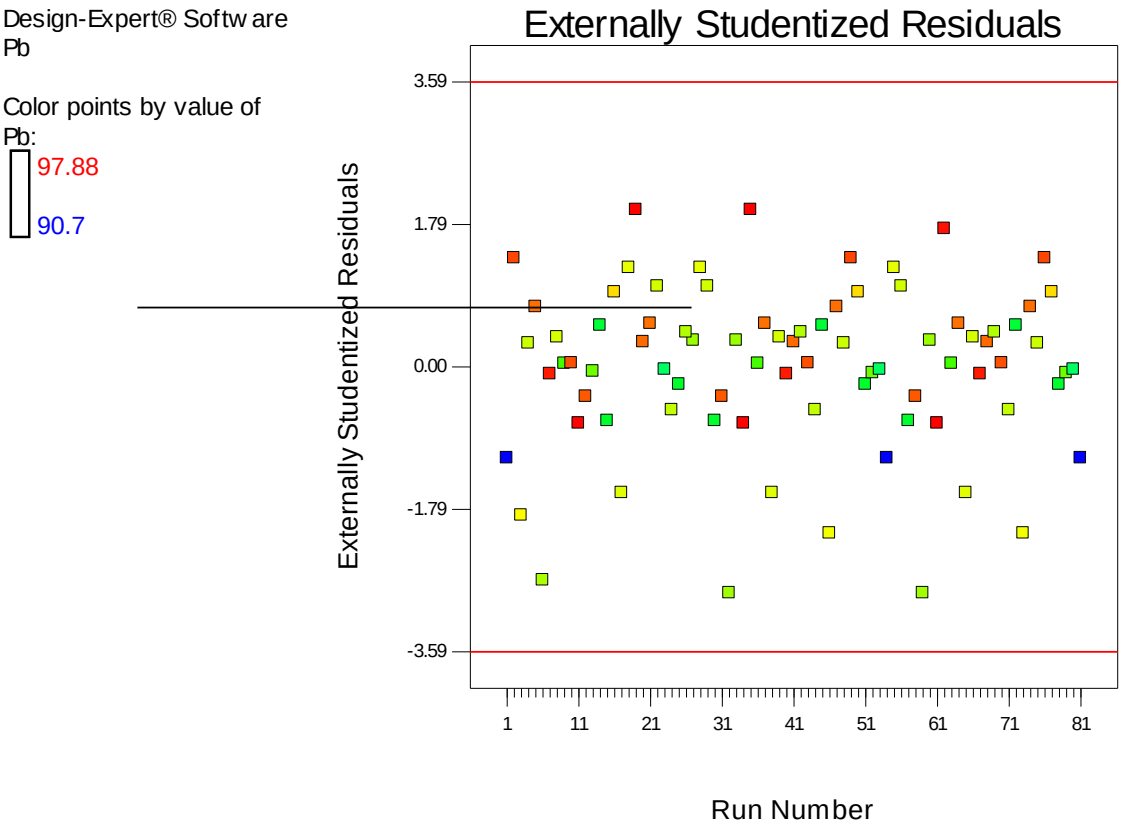

Appendix VIIa: Contour Response Surface Plot Representing the Effect of Concentration and Temperature on the Sorption of Pb^{2+} from the Aqueous Medium

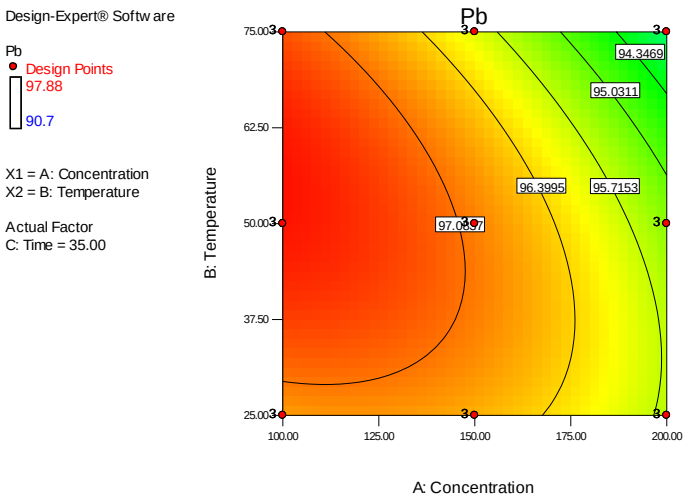

Appendix VIIb: 3D Response Surface Plot Representing the Effect of Concentration and Temperature on the Sorption of Pb^{2+} from the Aqueous Medium

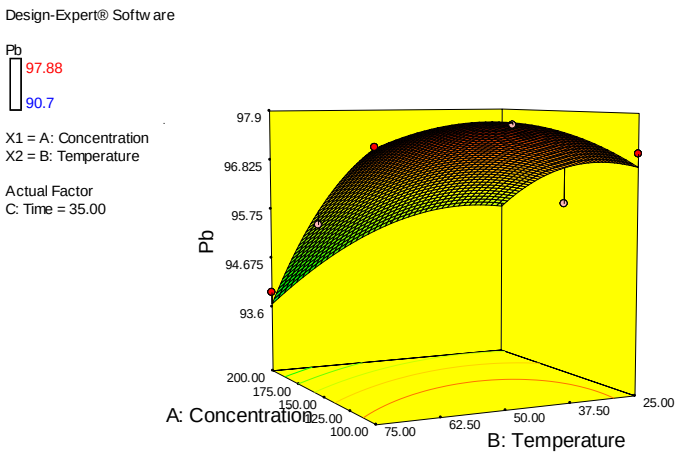

Appendix VIIIa: Contour Response Surface Plot Representing the Effect of Concentration and Time on the Sorption of Pb^{2+} from the Aqueous Medium

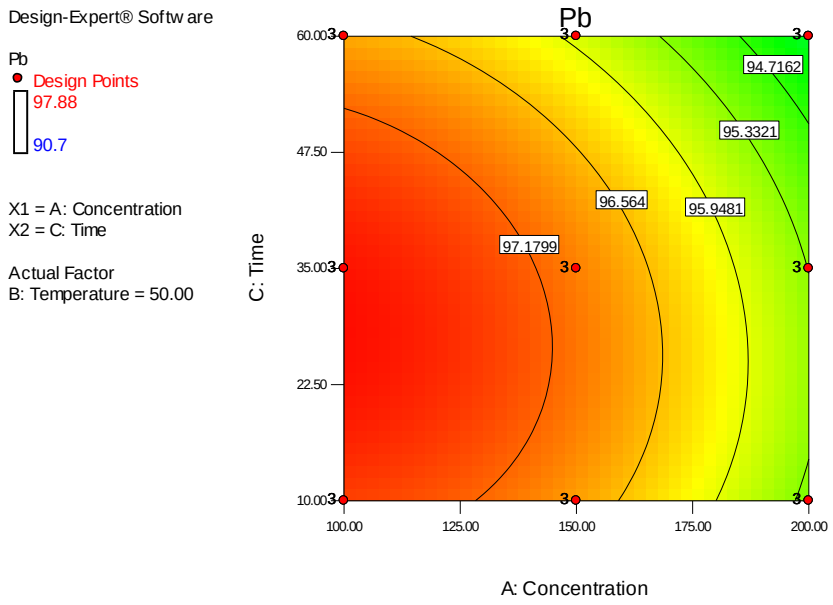

Appendix VIIIb: 3D Response Surface Plot Representing the Effect of Concentration and Time on the Sorption of Pb^{2+} from the Aqueous Medium

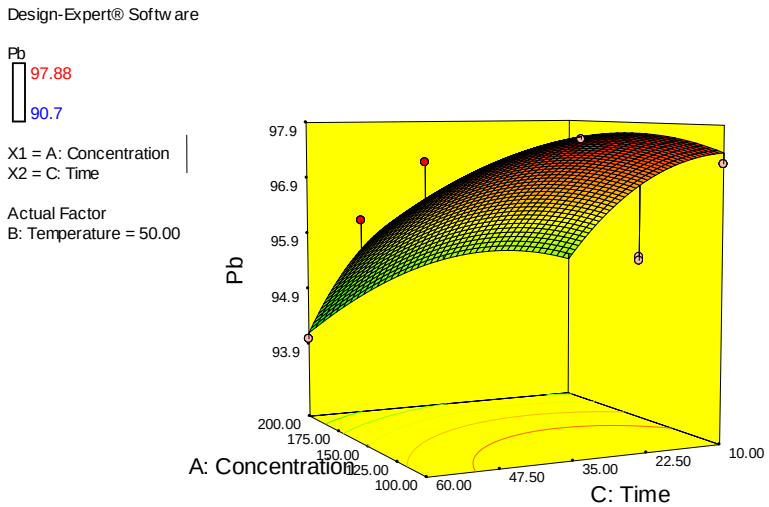

Appendix IXa: Contour Response Surface Plot Representing the Effect of Time and Temperature on the Sorption of Pb^{2+} from the Aqueous Medium

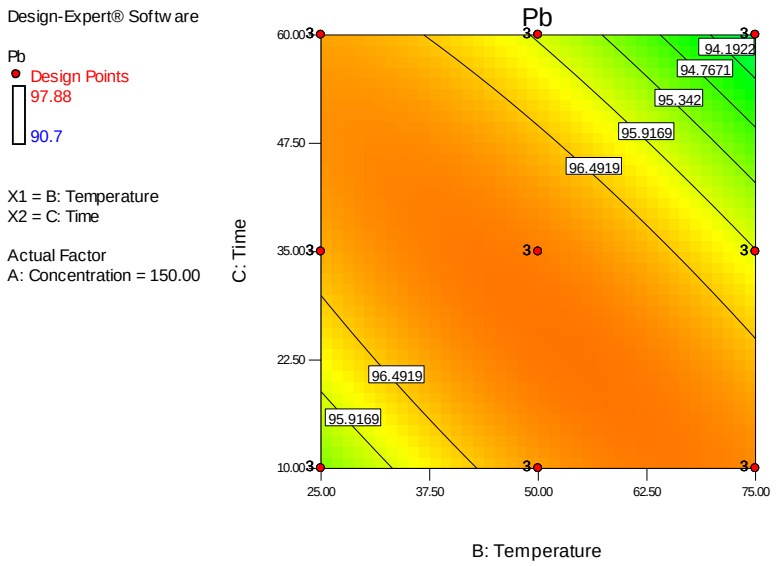

Appendix IXb: 3D Response Surface Plot Representing the Effect of Time and Temperature on the Sorption of Pb^{2+} from the Aqueous Medium

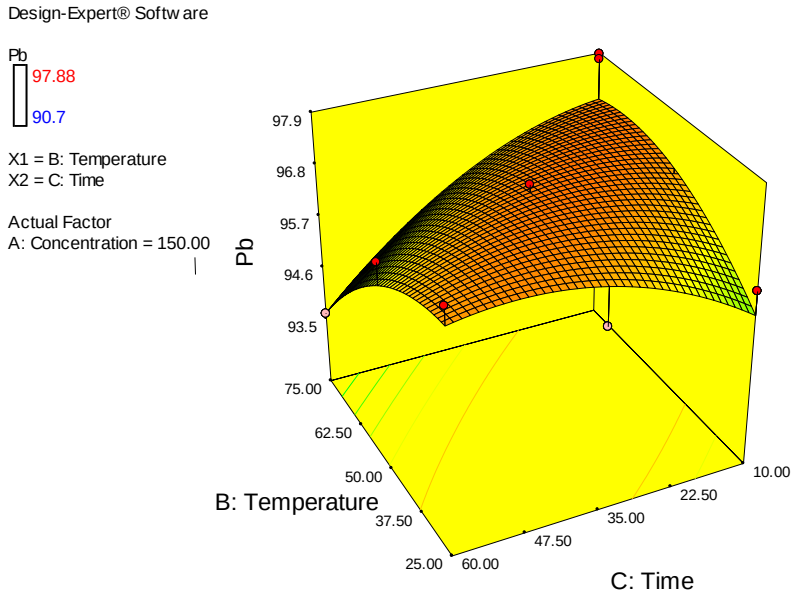

Appendix X: Plot of the Interaction between Concentration and Temperature for Pb^{2+} Sorption onto CFK Composite

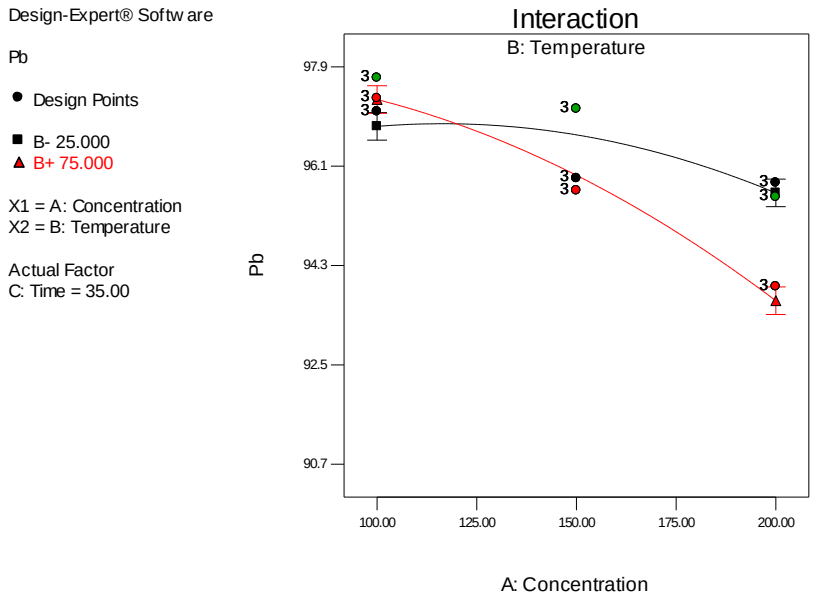

Appendix XI: Plot of the Interaction between Time and Concentration for Pb^{2+} Sorption onto CFK Composite

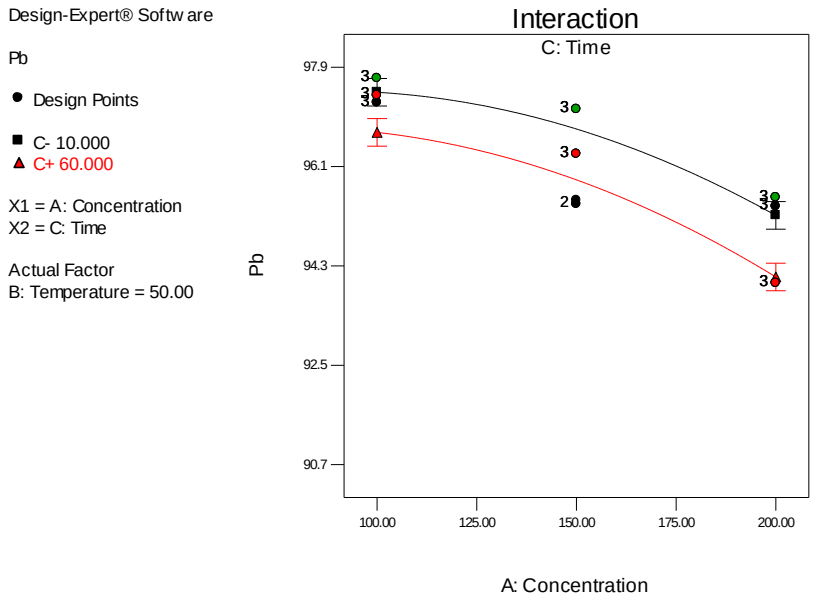

Appendix XII: Plot of the Interaction between Temperature and Time for Pb^{2+} Sorption onto CFK Composite

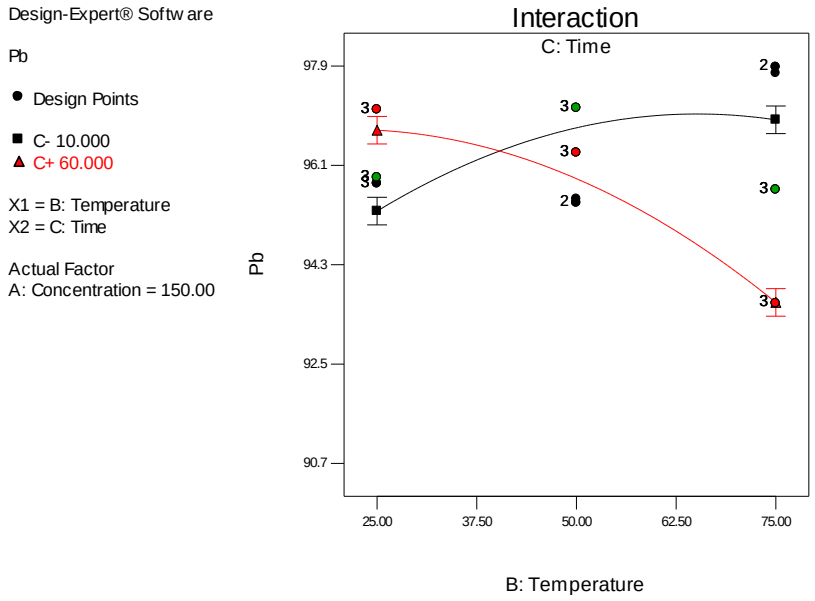

Appendix XIII: Cube Plot for Pb^{2+} Sorption onto CFK Composite

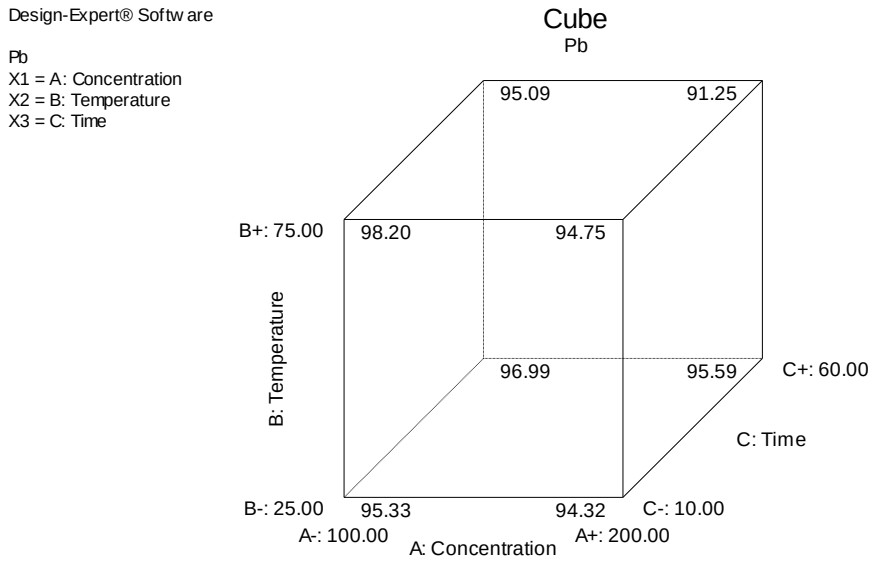

Appendix XIV: Normal Plot for Cu^{2+} Sorption onto CFK Composite

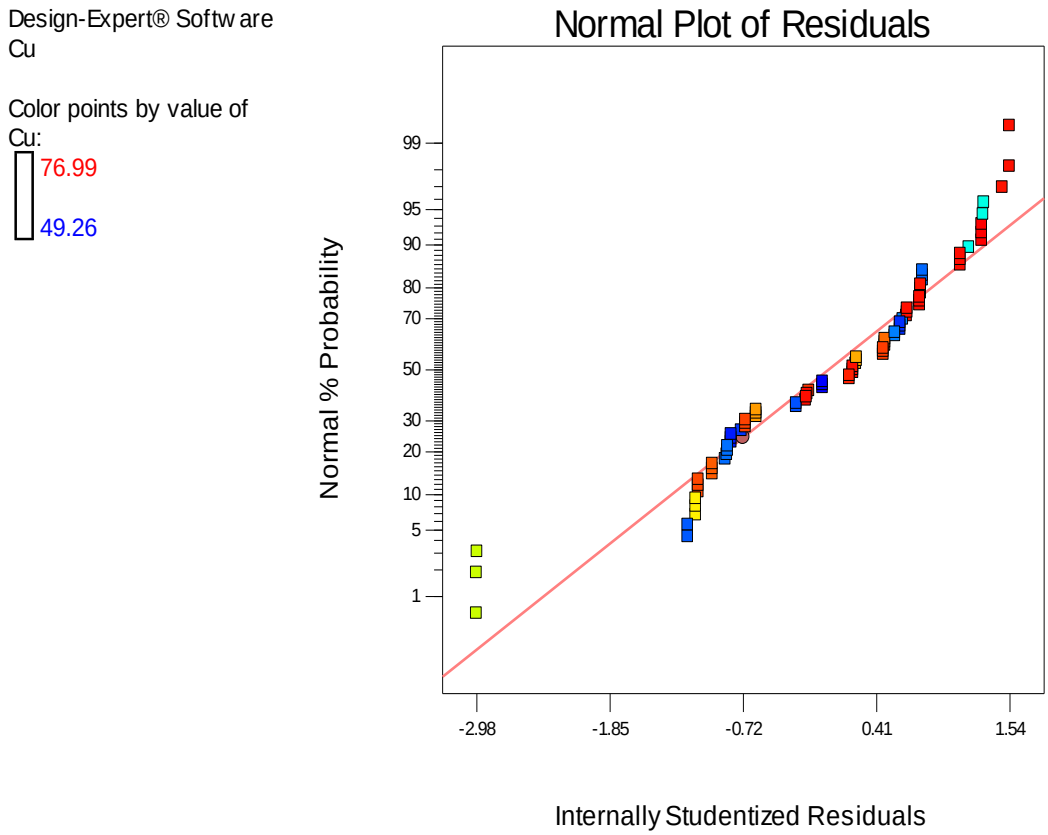

Appendix XV: Predicted Versus Actual Values Plot for Cu^{2+} Sorption onto CFK Composite

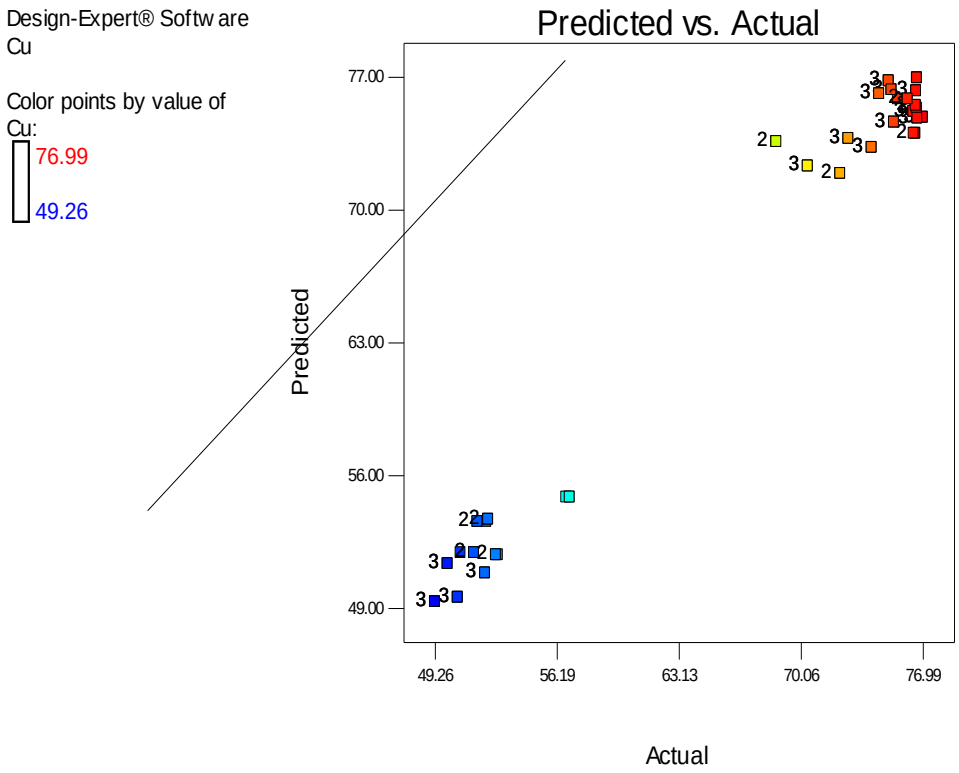

Appendix XVI: Externally Studentized Residual Plot for Cu^{2+} Sorption onto CFK Composite

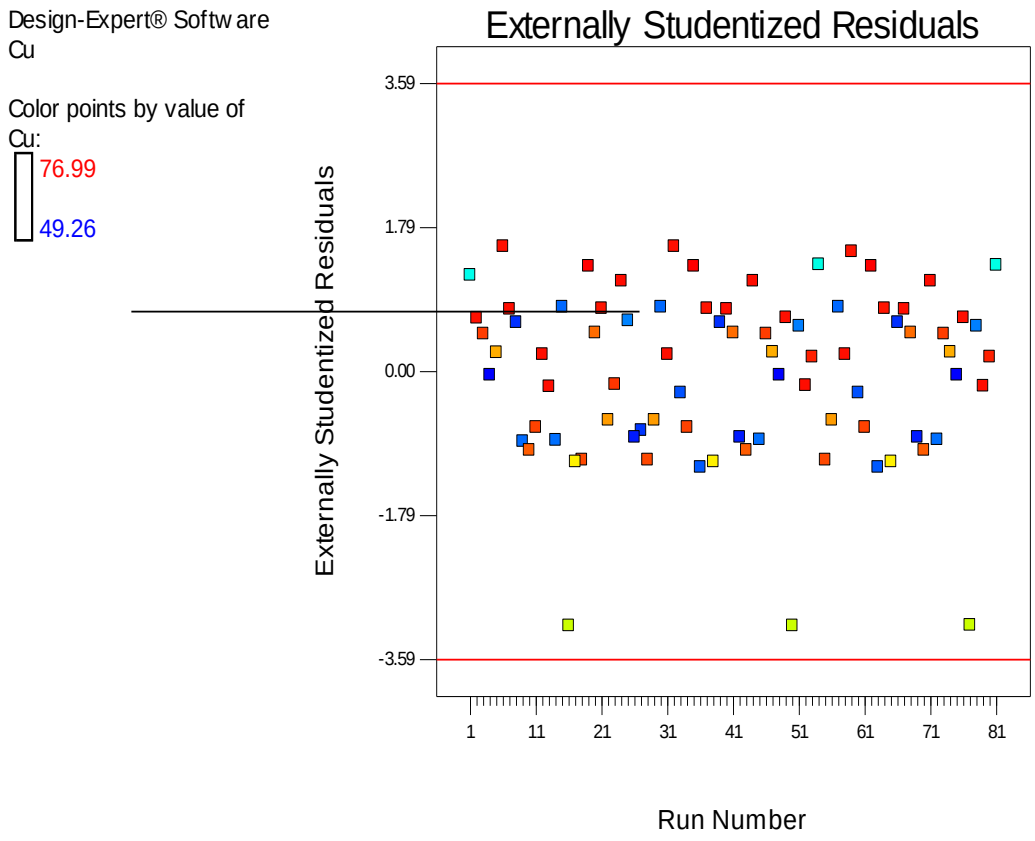

Appendix XVIIa: Contour Response Surface Plot Representing the Effect of Concentration and Temperature on the Sorption of Cu^{2+} from the Aqueous Medium

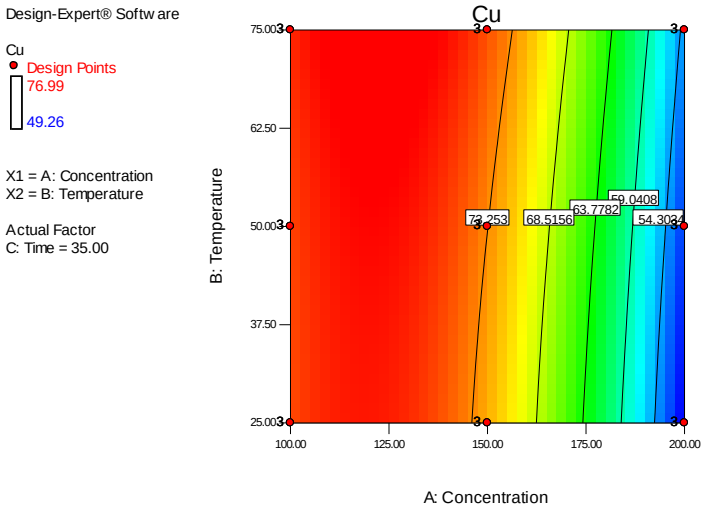

Appendix XVIIb: 3D Response Surface Plot Representing the Effect of Concentration and Temperature on the Sorption of Cu^{2+} from the Aqueous Medium

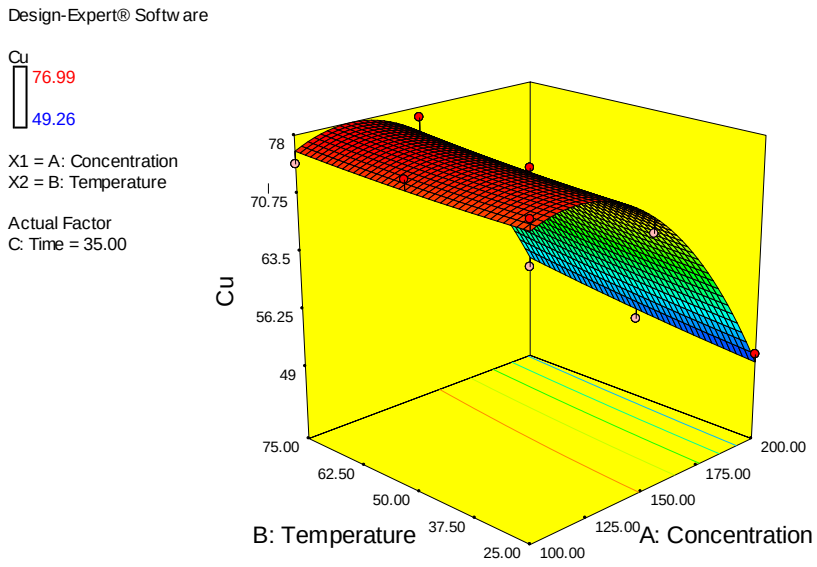

Appendix XVIIIa: Contour Response Surface Plot Representing the Effect of Concentration and Time on the Sorption of Cu^{2+} from the Aqueous Medium

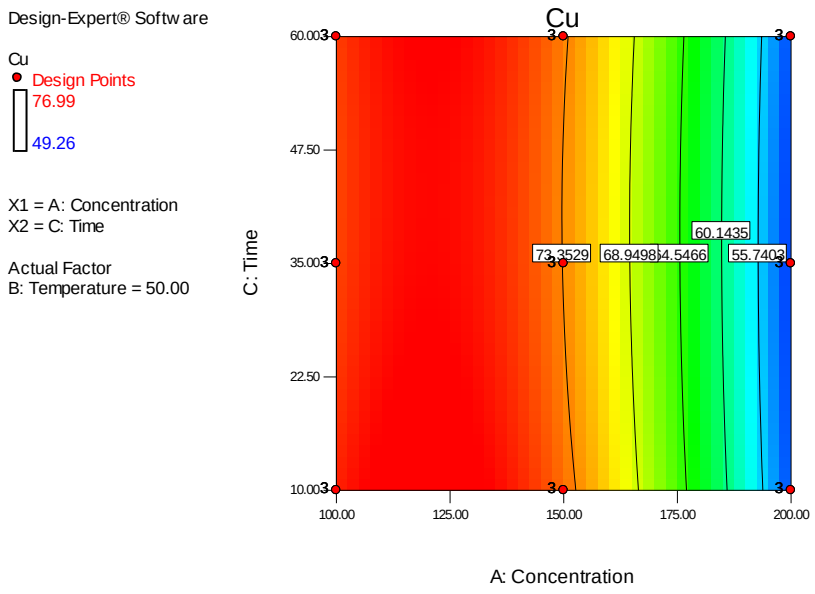

Appendix XVIIIb: 3D Response Surface Plot Representing the Effect of Concentration Time on the Sorption of Cu2+ from the Aqueous Medium

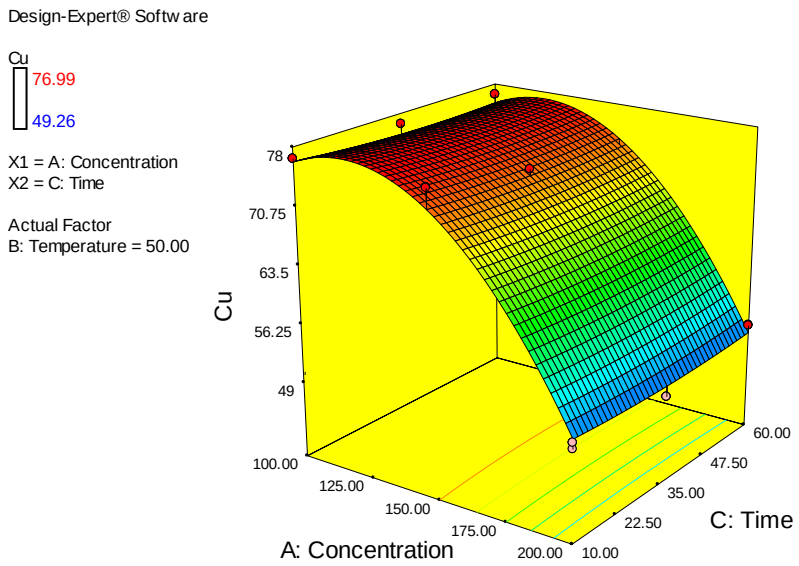

Appendix XIXa: Contour Response Surface Plot Representing the Effect of Time and Temperature on the Sorption of Cu^{2+} from the Aqueous Medium

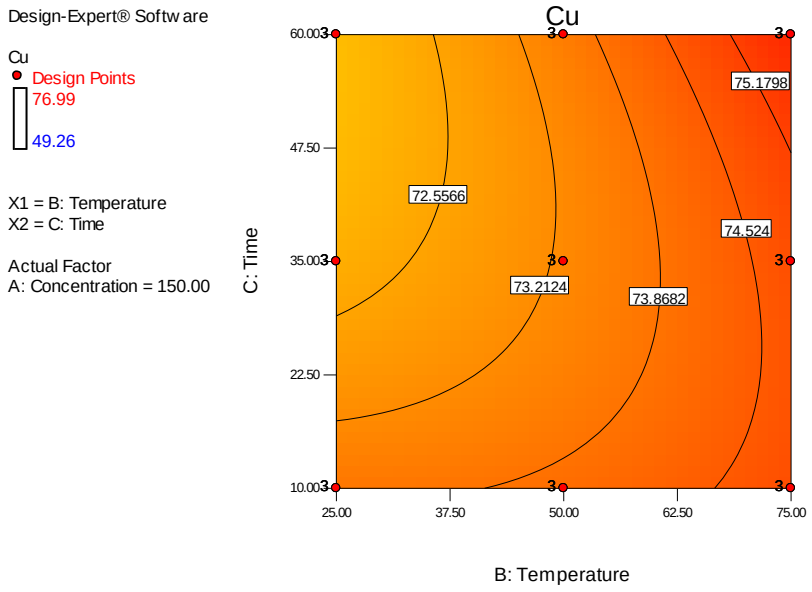

Appendix XIXb: 3D Response Surface Plot Representing the Effect of Time and Temperature on the Sorption of Cu^{2+} from the Aqueous Medium

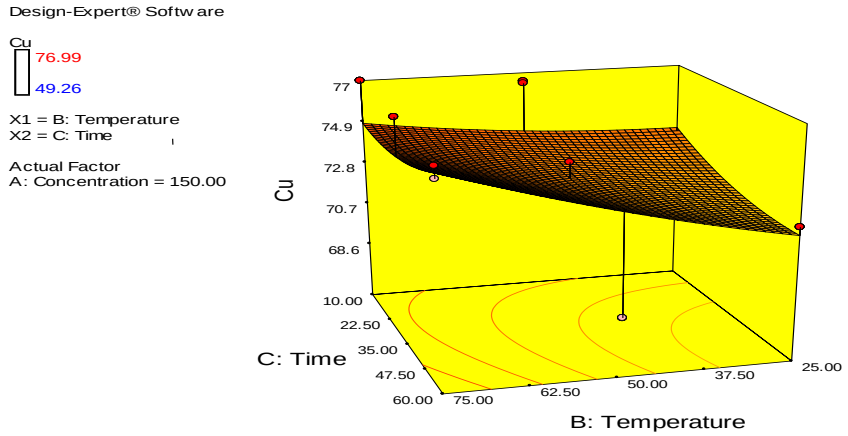

Appendix XX: Plot of the Interaction between Concentration and Temperature for Cu^{2+} Sorption onto CFK Composite

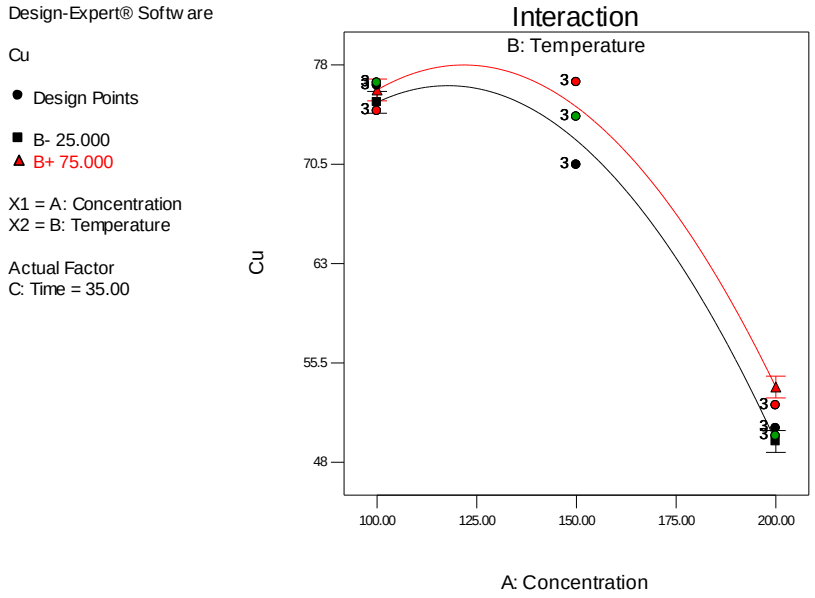

Appendix XXI: Plot of the Interaction between Time and Concentration for Cu^{2+} Sorption onto CFK Composite

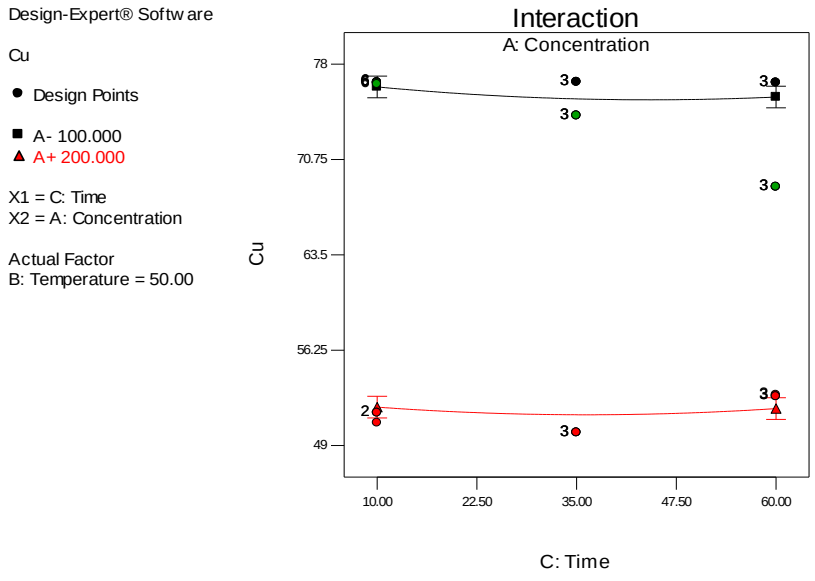

Appendix XXII: Plot of the Interaction between Time and Temperature for Cu^{2+} Sorption onto CFK Composite

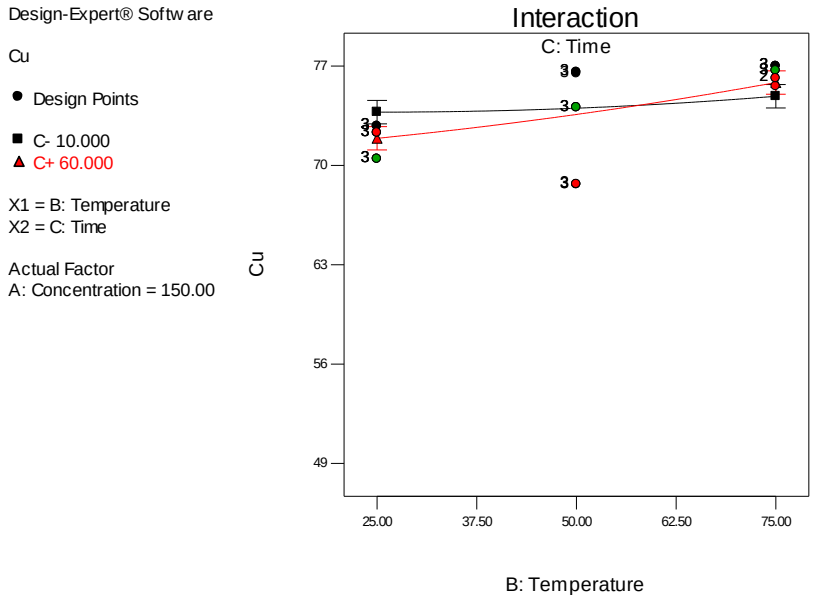

Appendix XXIII: Cube Plot for Cu^{2+} Sorption onto CFK Composite

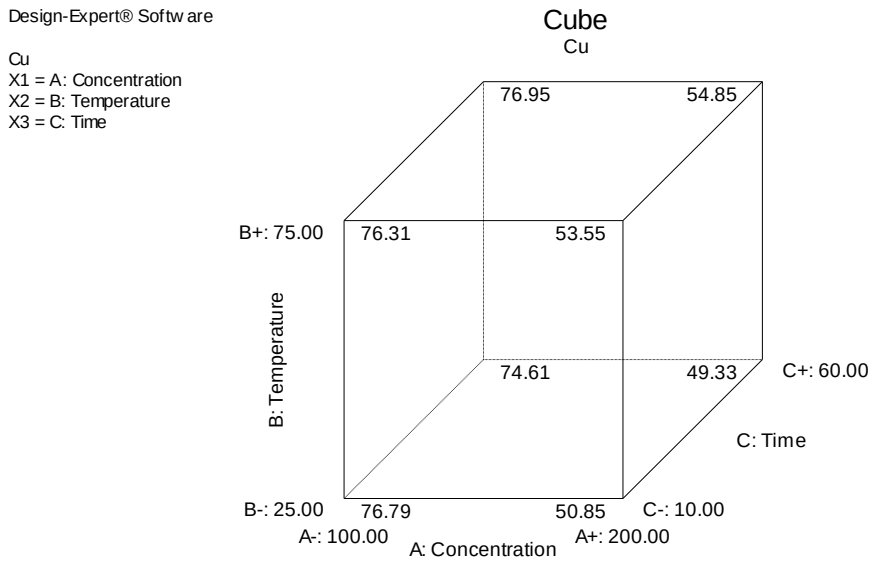

Appendix XXIV: Normal Probability Plot for Ni^{2+} Sorption onto CFK Composite

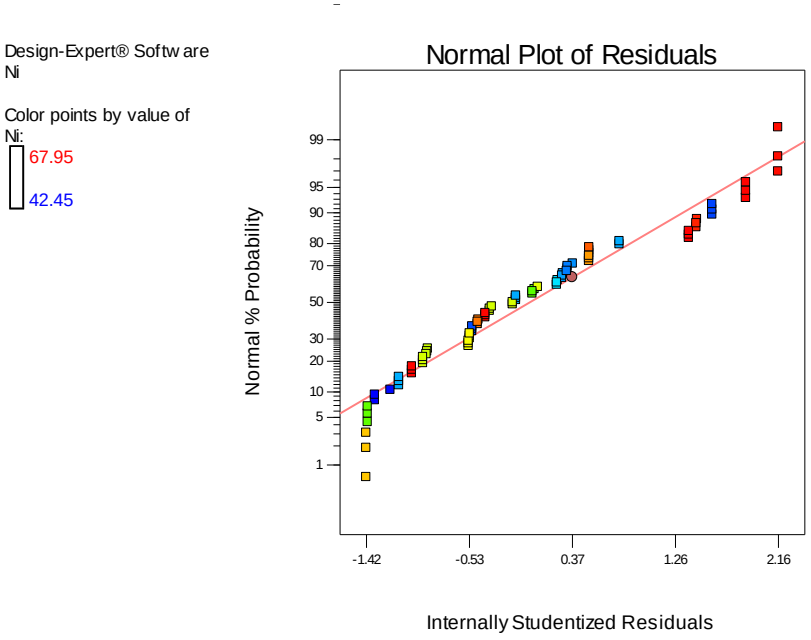

Appendix XXV: Plot of Predicted Versus Actual Values for Sorption onto CFK Composite

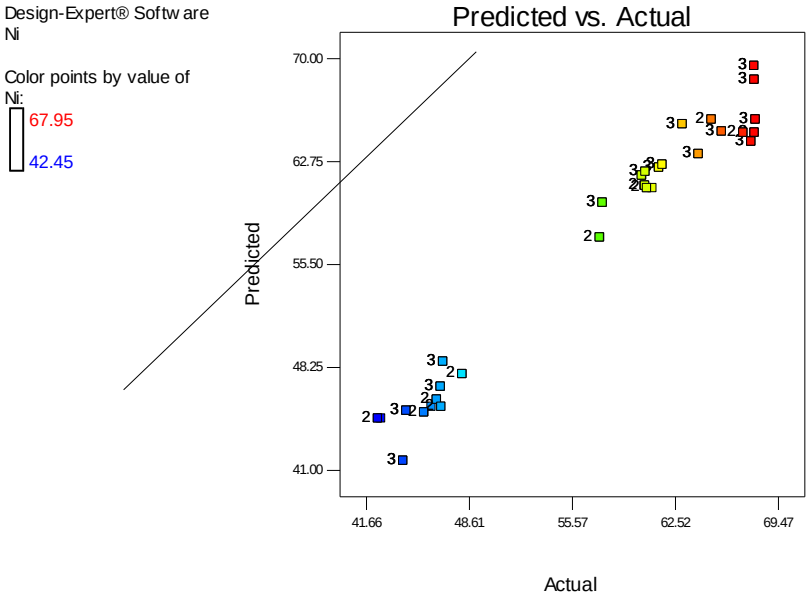

Appendix XXVI: Externally Studentized Residual Plot for Ni^{2+} Sorption onto CFK Composite

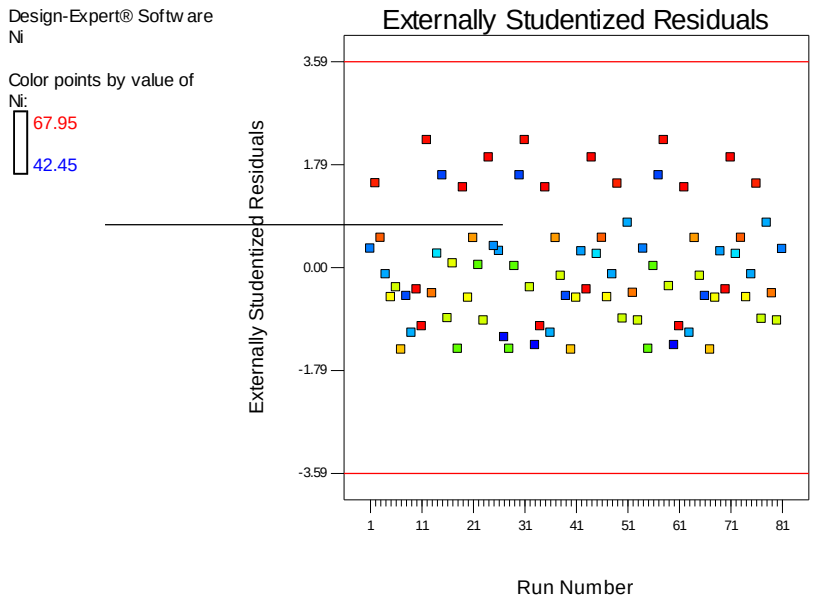

Appendix XXVIIa: Contour Response Surface Plot Representing the Effect of Concentration and Temperature on the Sorption of Ni^{2+} from the Aqueous Medium

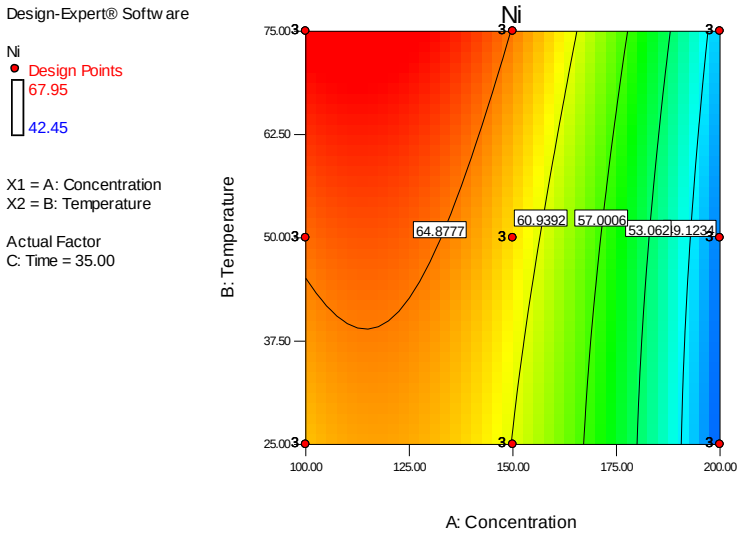

Appendix XXVIIb: 3D Response Surface Plot Representing the Effect of Concentration and Temperature on the Sorption of Ni^{2+} from the Aqueous Medium

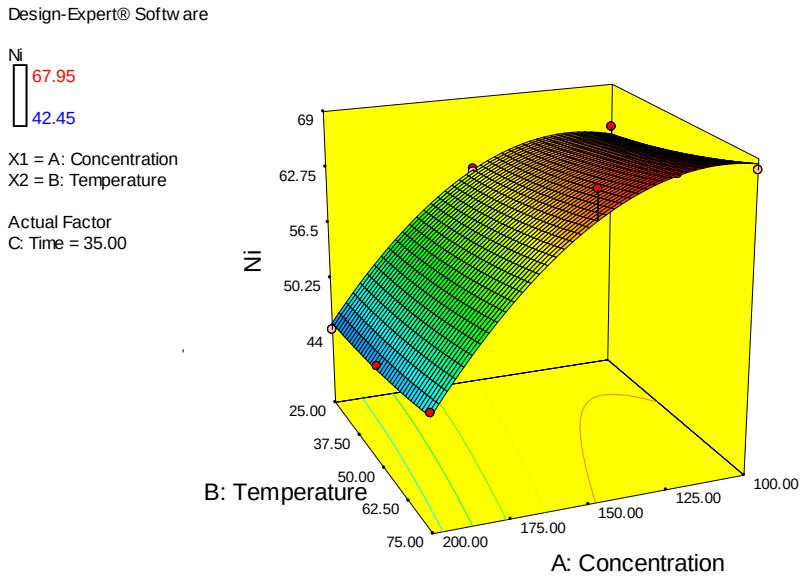

Appendix XXVIIIa:Contour Response Surface Plot Representing the Effect of Concentration and Time on the Sorption of Ni^{2+} from the Aqueous Medium

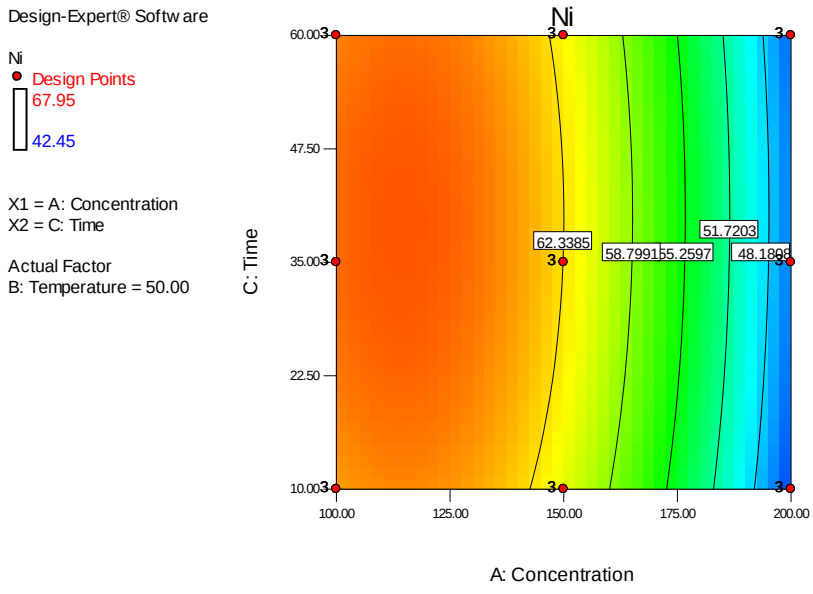

Appendix XXVIIIb: 3D Response Surface Plot Representing the Effect of Concentration and Time on the Sorption of Ni^{2+} from the Aqueous Medium

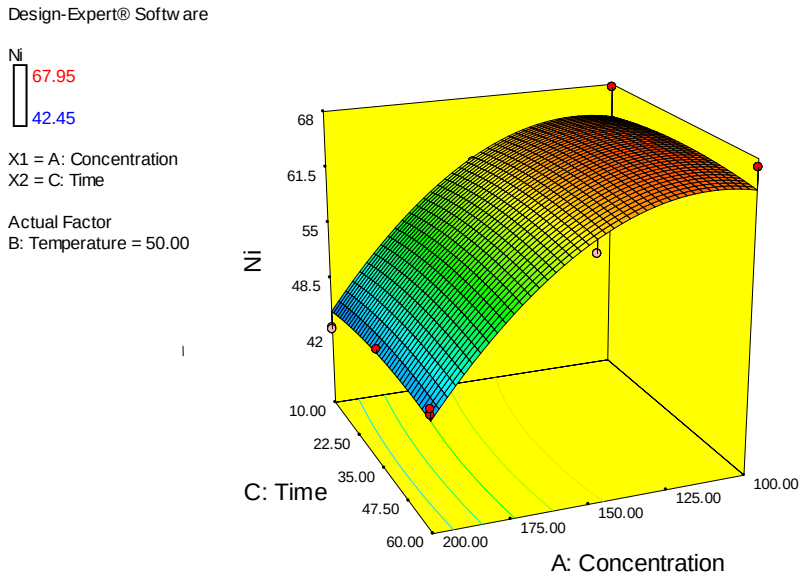

Appendix XXIXa: Contour Response Surface Plot Representing the Effect of Time and Temperature on the Sorption of Ni^{2+} from the Aqueous Medium

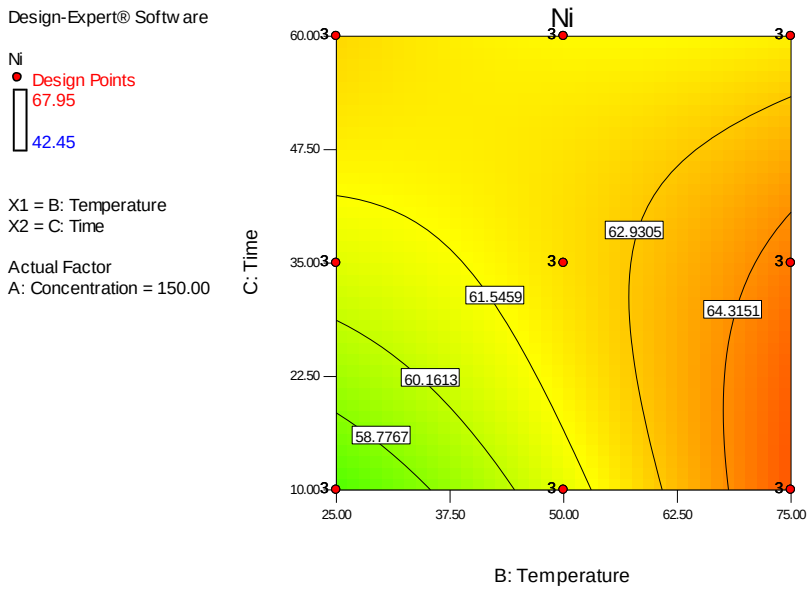

Appendix XXIXb: 3D Response Surface Plot Representing the Effect of Time and Temperature on the Sorption of Ni^{2+} from the Aqueous Medium

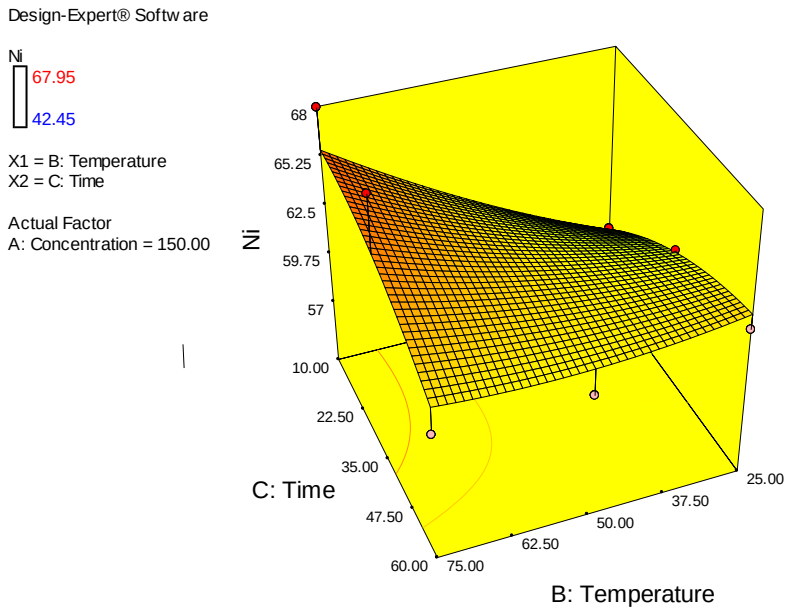

Appendix XXX: Plot of the Interaction between Concentration and Temperature for Ni^{2+} Sorption onto CFK Composite

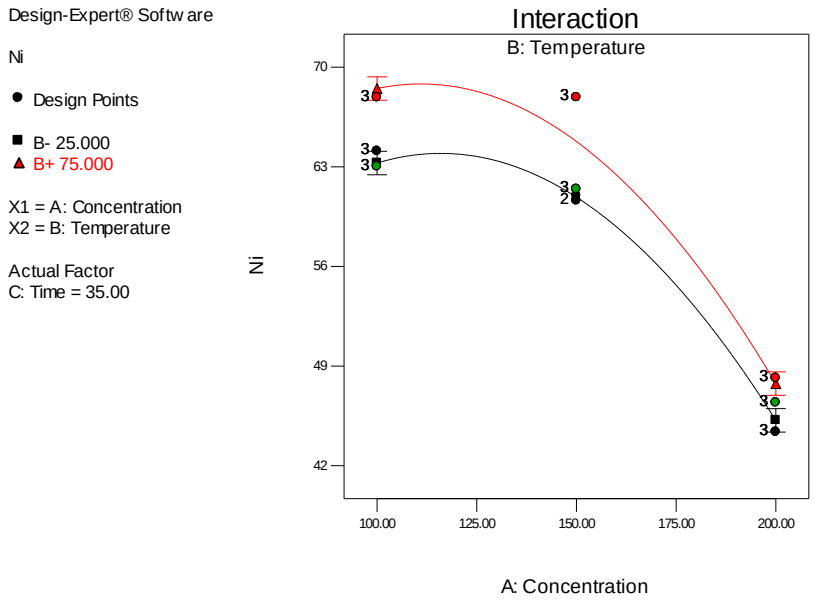

Appendix XXXI: Plot of the Interaction between Concentration and Time for Ni^{2+} Sorption onto CFK Composite

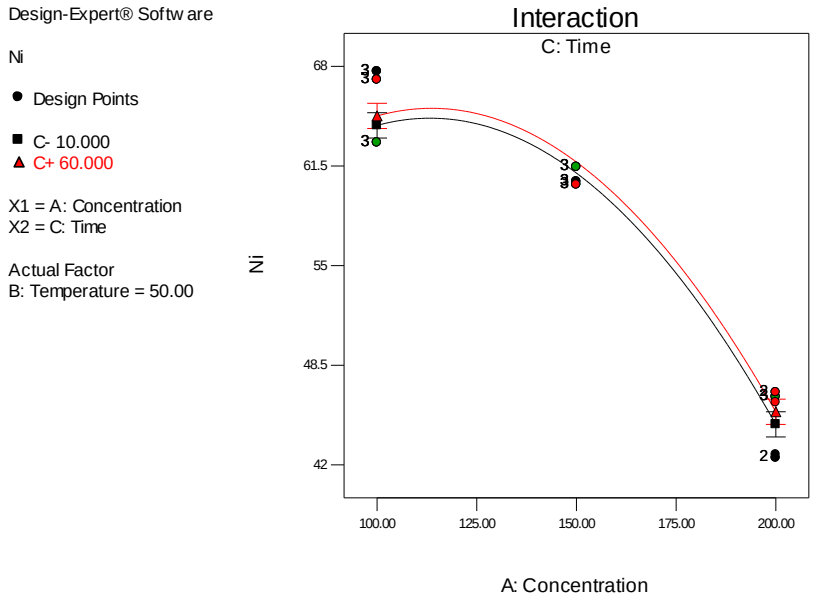

Appendix XXXII: Plot of the Interaction between Time and Temperature for Ni^{2+} Sorption onto CFK Composite

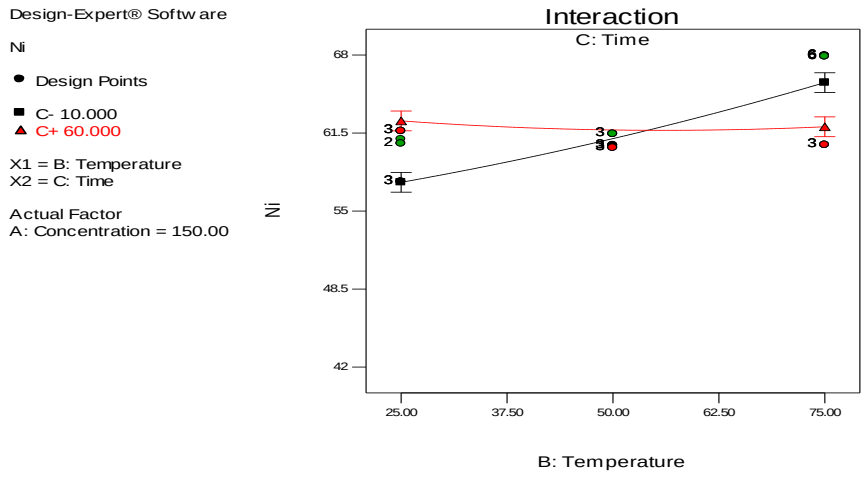

Appendix XXXIII: Cube Plot for Ni^{2+} Sorption onto CFK Composite

Design-Expert® Software

Ni
X1 = A: Concentration
X2 = B: Temperature
X3 = C: Time